

FERMILAB

MAY 10 1978

LIBRARY

Fermilab Proposal No. 581

Scientific Spokesman:

A. Yokosawa, ANL

FTS 972-6311

Commercial (312) 972-6311

CONSTRUCTION OF POLARIZED BEAMS
AND AN ENRICHED ANTIPROTON BEAM FACILITY IN THE
MESON LABORATORY AND EXPERIMENTS USING SUCH A FACILITY

- I. P. Auer, E. Colton, H. Halpern, D. Hill, H. Spinka
G. Theodosiou, D. Underwood, R. Wagner, Y. Watanabe
and A. Yokosawa, Argonne National Laboratory,
Argonne, IL.
- A. Michalowicz, D. Perrett-Gallix, and K. Kuroda,
LAPP, Annecy, France.
- Y. Hemmi, R. Kikuchi, K. Miyake, T. Nakamura,
and N. Tamura*, Kyoto University, Kyoto, Japan.
- G. Shapiro, Lawrence Berkeley Laboratory, University
of California, Berkeley, California.
- H. E. Miettinen, T. A. Mulera, G. S. Mutchler,
G. C. Phillips, and J. B. Roberts, Rice University,
Houston, Texas.
- R. Birsa, F. Bradamante, M. Budini, M. Giorgi, A. Penzo,
P. Schiavon, and A. Vascotto, INFN. Sezione di Trieste,
Trieste, Italy.

January 27, 1978

Revised May 1, 1978

* N. Tamura presently at Argonne National Laboratory.

184 pgs.

ABSTRACT

Lambda and anti-lambda production at Fermilab energies is so abundant that an enriched antiproton, polarized proton and polarized antiproton beams with reasonable intensity can be constructed for the use of counter physics. We particularly emphasize the completion of necessary digging and modification of the target train during the mesopause period.

We propose to construct such a facility and to study the substructure of hadrons through the spin effects at high energy. Physics motivation and proposed experiments are described. We propose measurements of total cross-section difference and of high- x_F low- p_{\perp} inclusive pion production using a polarized beam and a polarized target.

CONTENTS

	Page
I. Introduction	1
II. Enriched Antiprotons, Polarized p and \bar{p} in the Meson Laboratory	4
Polarized Protons from Λ Decay	
Target Train, Sweeping Magnet, Collimator, and Beam Dumping	
Polarized-Beam Transport	
Beam Polarimeter	
Necessary Equipment and Modifications	
III. Description of Proposed Experiments	
<u>Part A</u> Experiments to measure $\Delta\sigma_L^{\text{Tot}}$ in p-p scattering up to	11
340 GeV/c.	
Experimental Setup	
Polarized Beam and Target	
Scintillation-Counter Hodoscopes	
Setup Requirements	
Trigger Requirements and Data Collection	
Trigger Logic and Electronics Requirements	
$\Delta\sigma_L$ Measurement	
Rates and Run Plan	
Systematic Errors	
Apparatus	
<u>Part B</u> Asymmetries in inclusive pion production with a	23
polarized beam and target.	
Physics Interest	

Experimental Technique

Equipment Requirements

Rates, Resolutions, and Run Plan

IV. Summary	36
V. References	37
Appendix I High-p hadron production with a toroidal spectrometer	40
II Other possible experiments using the polarized - beam facility	44
III Trigger logic functions	45
Figures 1 through 15	47-61
Addendum to Proposal	62

I. INTRODUCTION

It has been shown that spin effects are important experimentally and theoretically at high energy. Large polarizations are observed in inclusive Λ^0 production in the neutral-hyperon beam,¹ and in inclusive proton production in the internal-target experiment.² A sizeable asymmetry effect is observed at CERN in π^0 production by 24-GeV/c protons at $x \approx 0$ and high p_{\perp} .³ Unexpected energy dependence in p-p elastic polarization is observed at Fermilab energies (E-61 experiment)^{3,4} and $|t|$ -dependence near the dip region is remarkable.⁴

More importantly, the study of spin effects in the scattering of quarks could be crucial for further development of current theoretical ideas regarding the constituent nature of hadrons.^{7,8} An attempt has been made to obtain information about the spin distribution of quark-partons by using a polarized-electron beam and a polarized-proton target.⁹

At Fermilab we can produce reasonably intense polarized-proton and antiproton beams for counter experiments from the decay of Λ and $\bar{\Lambda}$ respectively with polarization of ~50%,¹⁰ and with the spin direction reversed from spill to spill. This gives an important advantage over experiments with polarized target only. The spin reversal on a short time scale minimizes systematic errors in experiments with polarized beam and hydrogen- or nuclear-target and in experiments with both target and beam polarized.

At ZGS energies the importance of spin effects has been well demonstrated: structures in the total cross-section difference,¹¹ large asymmetries in inclusive scattering;¹⁶ structures in asymmetry measurements at large p_{\perp} ,¹² and the connection to quark-quark scattering.¹³ At Fermilab energies, the polarized beam will be unique and useful in investigating effects of this nature at much higher energies.

The reason for the rise in the total cross section at energies above 150 GeV is not presently understood. This cross section can be described in terms of two s-channel helicity amplitudes, $\phi_1(0)$ and $\phi_3(0)$,¹⁴ as:

$$\sigma^{\text{Tot}} = (2\pi/k) \text{Im}\{\phi_1(0) + \phi_3(0)\},$$

where k is the center-of-mass momentum of the incident beam.

By studying these amplitudes separately, we could learn whether they behave similarly at increasing energy or whether the rise could be ascribed to one of them. The total cross-section difference in longitudinal spin states allows us to do just that:

$$\Delta\sigma_{\text{L}}^{\text{Tot}} = (4\pi/k) \text{Im}\{\phi_1(0) - \phi_3(0)\}.$$

The study of $\Delta\sigma_{\text{L}}^{\text{Tot}}$ at lower energies has proven to be useful in other ways. It has provided evidence for a diproton resonance¹⁵ and for an A_1 -like exchange trajectory. In addition to the measurements of $\phi_1(0)$ and $\phi_3(0)$, it is interesting to investigate $\phi_2(0)$, which can be determined by the total cross-section difference in transverse spin states:

$$\Delta\sigma_{\text{T}}^{\text{Tot}} = (-4\pi/k) \text{Im}\phi_2(0).$$

Measurements of inclusive pion production with a polarized beam, $p^\uparrow p \rightarrow \pi + x$, have revealed large asymmetries in these processes at ZGS energies, especially for large values of $x = p_{\text{L}}^*/p_{\text{max}}^*$.^{16,17} Recent experiments have shown that the particle ratios π^+/π^- and K^+/K^- at high x and low p_{\perp} ¹⁸ are remarkably similar to those at $x = 0$ and high p_{\perp} .¹⁹ These

results have been successfully interpreted in terms of the quark-parton model,²⁰ indicating that high-x meson production gives information about the constituent structure of the initial protons. Both theoretical arguments^{7c,21} and experimental data^{18,22} support the notion that the leading valence quark ($x \approx 1$) in the proton "remembers" the helicity of the proton. Thus, the measurement of asymmetries in the reactions $p \uparrow p \rightarrow \pi^{\pm} + x$ and $p \uparrow p \rightarrow \pi^{\pm} + x$ in the high-x region may be a direct way of probing the spin dependence of the quark-quark interaction. In addition, if sizeable asymmetries were found in the first reaction, then this process could be used for monitoring the beam polarization in other types of experiments.

We show in the Appendix I and II other possible experiments under consideration. A separate proposal is written on high- p_{\perp} asymmetry measurements using calorimeters.

II. ENRICHED ANTIPROTONS, POLARIZED p AND \bar{p}

IN THE MESON LABORATORY

Polarized Protons from Λ Decay

In the rest frame of the Λ^0 , the proton decays with a longitudinal polarization of 64%.²³ Under the transformation from the rest system to the lab system, the spin vector of the proton remains almost fixed. The polarization in the lab system can be in the longitudinal or transverse direction depending on $\theta_{cm} = 0$ or 90° respectively.

The production of polarized beams from Λ^0 decay has already been proposed by several authors.¹⁰ We find that there are many ways to optimize the intensity and polarization of polarized beams.

We propose to construct polarized beams by using the following two schemes. Details of the polarized beam design are given in a report.²⁴ We describe here the outline.

The basic idea is that polarization direction corresponds to decay direction of the protons in the Λ^0 rest frame. If we select this decay direction in the lab frame with some property of the beam line, we have selected the polarization. The best place to make this selection is at the first focus where protons with different decay angle have different focal points; those with $\theta_{cm} = 0$ are centered and those with $\theta_{cm} = 90^\circ$ are furthest from the center.

i) Transverse Scheme

A transversely-polarized beam can be selected at the first focus with a sliding collimator or two moving collimators as shown in Fig. 1. (Better, a vernier magnet may be used to move the beam spot). Polarization direction can be changed to the desired direction by the 4-magnet scheme. Spin reversal is done by either a collimator or a vernier magnet located downstream of the production target. This scheme gives high-intensity beam with variety of momenta.

ii) Longitudinal Scheme

By choosing fast protons from lambda decays, we will obtain protons primarily from forward-decaying events. The resulting proton polarization will be longitudinal. This scheme is for high momentum protons, $> 300 \text{ GeV}/c$ with $400 \text{ GeV}/c$ primary protons. Spin reversal is done by using a set of reversing magnets in such a way that there is no motion of the beam in the beam transport system or at the experiment.²⁴ The scheme uses 8 magnets of 27.4 kG-m field integral each.

iii) Predicted intensities of enriched antiproton and polarized beams are shown in Fig. 2 together with π background.

Table I: Summary of polarized beams

400-GeV/c primary protons, $5 \cdot 10^{12}$ /spill, $1/2$ interaction-length Be target ± 1 mr acceptance, and $\pm 5\%$ momentum bite			
Scheme	Momentum	Intensity/pulse	Spin Reversal/ each spill
Transverse	<280 GeV/c	1.5×10^7	Collimator or Vernier
Longitudinal	>320 GeV/c	5.0×10^6	Eight-magnet scheme at the downstream end of the beam trans- port system

A universal set of spin precession magnets would be eight magnets of at least 27.4 kG-m field integral which fit into roughly 16 m and have 5-inch gaps. The power supplies could be ramped and the magnet polarities switched on a spill-to-spill basis. For most experiments this full set would not be necessary but the minimum set for any experiment is four magnets with 3-inch gaps. The spin-reversing scheme is illustrated in Fig. 3.

Target Train, Sweeping Magnet, Collimator, and Beam Dumping

We need zero-degree production angle, and the three-way split beam presently planned by Meson-lab physicists is well suited to our purpose. A dipole magnet to be used for sweeping is shown in Fig. 4 where the beam positions of M-1, M-2, M-3, and M-6 are also indicated. The sweeping

magnets can be drilled or cut to allow simultaneous use of the M-1, M-6, and M-3 lines with beam splitting in Meson lab. The second of the two sweeping magnets is used to sweep away hadronic shower particles that leak into the collimator opening, so that they will not get into the beam line. Collimators and beam dump are shown in Fig. 5. Collimators used at high intensity should be made of aluminum so that the hadronic shower will be spread out sufficiently to allow adequate heat dissipation. The beam should be dumped far from the coils of the sweeping magnet.

We should be compatible with other uses of the M-2 and M-3 lines in a time sharing manner. Specifically, the high-intensity K^0 experiment in M-3 and a fraction of the primary ($\sim 10^{10}$) being transported directly through our sweeping system and down the M-2 line. A new target train should be constructed during the mesopause.

Polarized-Beam Transport

The decision to plan this beam for the M-3 line which has no bend is made in terms of polarization. A focusing element such as a quadrupole triplet would depolarize a high-divergence beam such as we are proposing. The first order solution is to use another identical element after a focus to compensate and return spins to their original directions. The initial focusing stage must match the final focusing stage. An odd number of foci between the first and last stage is required.

We are constrained to compensate all bends between sets of quadrupoles and further constrained to compensate all momentum dispersions between

quadrupole sets.

The schematic of the beam transport system is shown in Fig. 6. The problems arise because the beam pipe is only 12 inches in diameter and displacements of the beam of roughly a foot are needed both for neutral beam dumping and momentum selection. Alternative methods include i) the use of superconducting magnets and ii) different beam design with more depolarization.

We recommend strongly to make a bigger beam pipe in the region of momentum selection. We need 15-ft. deep, 4-ft. wide, and 600-ft. long (4,000 cubic yards) digging.

Beam Polarimeter

While the polarization of the beam can probably be calculated to better than three per cent, including correlations of polarization with position and angle, a beam polarimeter could greatly reduce the risk of taking data where the beam was not working properly. Details of this subject are discussed extensively in reference 25. Two types of polarimeters which could in principle give an absolute measurement of the beam polarization are:

- (1) Measure the p-p asymmetry, A_{pp} , from elastic scattering in the Coulomb-nuclear interference region with an

N-type polarized beam. ^[10d] Soffer *et al.* ^[27] have calculated A_{pp} to be $\sim 5\%$ at $-t=2 \cdot 10^{-3}$ and almost independent of energy. This calculation assumes the strong flip amplitude $\phi_5=0$ for very small $-t$. (The hadronic polarization $A_{pp} \sim \text{Im}(\phi_1 + \phi_3)\text{Re}\phi_5$ has been observed to be very small in FNAL E-61 at moderate t values. In light of the small value of $\text{Re}(\phi_1 + \phi_3)$ at FNAL energies, we believe that hadronic $A_{pp} \sim \text{Im}\phi_5\text{Re}(\phi_1 + \phi_3)$ will be very small in the Coulomb scattering region.

The rates are quite high in the Coulomb region, and with an $A_{pp} \sim 5\%$, this should be good mechanism beam polarization measurement. The inclusive pion spectrometer (Figure 12) could be used as this polarimeter. The Čerenkov counters and hodoscopes could be used to help discriminate against inelastic events and the hodoscopes spread further apart to allow a measurement of the scattering angle to $\lesssim 1$ mr. The θ_{rms} for multiple Coulomb scattering in the LH_2 is an order of magnitude less, and thus should not jeopardize the measurement. Sample MWPC data would be used for a cleaner measurement off line. Assuming useful $\Delta\phi = \pm 45^\circ$ and $\Delta t \approx .001 \rightarrow .01$, there are 2.5×10^5 events per 200 pulses, giving $\Delta p_{\text{Beam}} = \pm .06$ for $\langle A_{pp} \rangle = .04$.

(2) The process $pA \rightarrow p\pi^0 A$ can be related via the Primakoff effect to low energy $\gamma p \rightarrow \pi^0 p$, which has large polarization asymmetries. The effective γp kinetic energy is typically 500 MeV, yielding asymmetries $\sim 40\%$ at certain scattering angles. (25,26)

Both longitudinal and transverse polarization of the beam can be analyzed using this effect, if the asymmetries in $\vec{\gamma}p \rightarrow \pi^0 p$ and $\vec{\gamma}\vec{p} \rightarrow \pi^0 p$ are known at the appropriate low energies. The inclusive pion spectrometer (Figure 12) with the addition of a hodoscope of γ detectors at the end can be used for this sort of polarimeter.

The total cross section, for Coulomb dissociation, is ~ 20 mb, so the rates are quite adequate. 10^7 protons/pulse incident on a 3mm Pb target gives about 100 events/burst in the region of useful asymmetry region for $M_{p\pi^0} \sim 1300$ Mev, for example, thus giving $\Delta p_B \sim .03$ in about 20 minutes. These measurements require measurement of the $p\pi^0$ lab angles to .03 mR for $\pm 5^\circ$ angular resolution in the equivalent low energy γp c.m. This method should give a more certain measurement but requires a much more elaborate polarimeter.

A third type of polarimeter is discussed in the proposed experiment part B.

NECESSARY EQUIPMENT AND MODIFICATIONS

- i) Modifications to Meson lab: target train and M-3 line (See Ref. 24, p. 46 and p. 47)
- ii) High-field quadrupoles (See Ref. 24, p. 49)
- iii) Spin-precession magnets (See Ref. 24, p. 50)
- iv) We need 4000-cubic yards digging as discussed in the section of Beam Transport. According to the Architectural Service, this can be accomplished within a month with \$45 to \$50 K.

III. DESCRIPTION OF PROPOSED EXPERIMENTS

PART A EXPERIMENTS TO MEASURE $\Delta\sigma_L^{\text{Tot}}$ IN p-p SCATTERING UP TO 340 GeV/c.

We propose to measure the pp total cross-section difference of pure longitudinal spin-states, $\Delta\sigma_L^{\text{Tot}} (\sigma_{\Rightarrow} - \sigma_{\Leftarrow})$, in the polarized beam line at FNAL. Measurements will be made at six different momenta between 100 and 340 GeV/c, where the cross-section rises by about 1 mb unit. (38.5 to 39.5)

This experiment will be a standard transmission experiment with the detectors specially designed for a high-divergence beam.

EXPERIMENTAL SETUP:

The layout of the experimental setup is shown in Fig. 7. A polarized proton beam, in the M-3 beam line, entering from the left, passes through a threshold Cherenkov counter (C_1), set to reject π^+ 's, then through 4 scintillator-hodoscope planes (HX1, HY1, HX2, HY2) and finally interacts with a polarized proton target. The unscattered beam and forward scattered particles pass through 6 scintillator-hodoscopes (HX3, HY3, HX4, HY4, HX5, HY5).

The anticoincidence counters A define the useful beam and the counter-hodoscopes IC help in the identification of inelastic events. The detectors downstream of the target are positioned on rails so that their distances from the target can be adjusted depending on the incident proton momentum. At $p_{\text{lab}} = 200 \text{ GeV}$, $Z_5 = 18 \text{ m}$.

POLARIZED BEAM

Momentum bite: $\Delta p/p = \pm 5 \%$ (rms).
 Angular divergence: $\Delta \theta_b = 1$ mradian (rms).
 Intensity: $I = 5 \cdot 10^6$ protons/spill.
 Degree of Polarization: $P_B = 40 - 50. \%$

POLARIZED TARGET.

It will consist of NH_3 molecules, of which the 3 hydrogen atoms can only be polarized. We list its characteristics:

Free-hydrogen polarization: $P_H = 80 \%$
 Target Density: $\rho_{\text{NH}_3} = .56 \text{ gr/cm}^3$.
 Length: $L_t = 10\text{-}20 \text{ cm.}$
 Diameter: $D_t = 2.5 \text{ cm.}$

SCINTILLATION-COUNTER HODOSCOPES.

Schematic diagrams for the HX1 and HY1 planes are shown in Fig. 8. Each X-and Y-plane (i) consists of an array of N_i scintillation-counters
 $5\text{mm (thick)} \times W_i \text{ mm (wide)}$
 Both planes are placed parallel to each other and the center beam line passes perpendicularly through their centers. Whenever a beam-or forward scattered particle passes through a hodoscope-pair, it is almost always counted by only one X and one Y scintillation-counter. The light from both ends of each counter is fed via two fiberglass lightguides to the corresponding

photomultiplier device.

Some hodoscope characteristics are shown in the following table.

TABLE II: SCINTILLATOR-HODOSCOPIES

i	N_i	Counter Width W_i (mm)	Hodoscope Width $N_i W_i$ (mm)	Target to- Hodoscope Distance* Z_i (m)
1	20	1.0	20	-9.0
2	20	1.5	30	-0.2
3	20	1.5	30	1.0
4	30	1.5	45	9.0
5	45	1.5	68	18.0
* $P_{lab} = 200$ GeV.				

SETUP REQUIREMENTS.

For the design of this setup and hodoscope system, the following considerations were taken into account.

- i) It is possible that spills of opposite proton spins will have different π^+ -contamination. This necessitates the use of a threshold Cherenkov-counter to reject them.
- ii) The counter width size is mainly determined from efficiency and counting rate requirements as well as mechanical construction

feasibility:

$$1 \text{ mm} \leq W \leq 1.5 \text{ mm}$$

iii) It would be desirable to have a beam spot at the target with a diameter slightly smaller than the target diameter ($D_b \leq 2.5 \text{ cm}$).

iv) We require a t-resolution (4-vector momentum transfer):

$$\delta t \simeq (1.5 - 2.5) \cdot 10^{-3} \text{ GeV}^2.$$

For $p_{\text{lab}} = 200 \text{ GeV}$, this corresponds to a polar angle-resolution

$$\delta\theta \simeq (.20 - .26) \text{ mradians.}$$

v) To maintain the same t-resolution, independent of the incident proton momentum, for each scintillator-hodoscope, one must maintain a target-hodoscope distance proportional to p_{lab} .

$$Z_{\text{hod}} \sim p_{\text{lab}}.$$

vi) By requiring the beam divergence to be smaller ($\Delta\theta < 1 \text{ mrad}$) one could move the target further downstream and keep the size of the beam spot at the target the same.

In addition, one can get better t-or θ -resolution by moving the downstream hodoscopes further away from the target without increasing the number of scintillation-counters. Or, one can increase the counter widths and maintain the same angular resolution.

vii) Since our sample of forward scattering events contains a small fraction of inelastics, care must be taken not to introduce biases in our extrapolation to $\Delta\sigma(t = 0)$.

TRIGGER REQUIREMENTS AND DATA COLLECTION

The two pairs of beam hodoscopes (see fig. 7) will be used to define the direction of incident protons.

The beam hodoscope logic will reject ambiguous or multi-particle incident tracks. In addition, the Cherenkov counter upstream (of the beam hodoscopes) will veto charged pions present in the beam. The anticoincidence counters A will be used to insure that only beam particles that potentially pass through the whole length of the target are in the trigger.

The primary function of downstream hodoscopes is to define the angles and positions of the out going particles. The presence of the three pairs of hodoscopes will provide sufficient redundancy to permit the continuous monitoring of the individual hodoscope elements. The comparison of the hodoscope hit patterns upstream and downstream of the target will provide an additional check on the continuity of the beam and scattered particle-tracks through the target.

The electronic hardware will provide sufficient flexibility to either reject multi-particle events entirely, thus selecting elastic or low multiplicity events, or to identify the leading particle track (more precisely the track with the minimum scattering angle.)

To simplify the logic we plan to process the signals generated by the X and Y arrays separately. This method lends itself more naturally to the use of the projected angles θ_x and θ_y and not to the polar angle θ . ($\theta^2 \equiv \theta_x^2 + \theta_y^2$) From the incident and outgoing angles (projected) the scattered angles will

be calculated by hardware. After each event the appropriate scalers associated with the incident and outgoing angles and positions will be incremented. At this stage we use the hardware to combine θ_x , θ_y and increment the scaler corresponding to the polar angle θ . The θ -distributions of opposite incident-proton spin-directions will serve to eliminate elastic scattering background.

These as well as the other scalers will be read into an on-line computer at least once for each spill. In addition, magnet currents, target polarization and hodoscope hit-patterns will periodically be sampled and read into the computer in order to monitor various experimental parameters such as beam profiles and phase space.

We would like to emphasize that since this is a scaler experiment and since beam polarization flips every alternate spin, it is relatively easy to obtain $\Delta\sigma_L$ values on-line.

TRIGGER LOGIC AND ELECTRONICS REQUIREMENTS

To measure a total cross-section, we must count all incident tracks within the live time of the apparatus. A transmitted particle is defined by the following 5 requirements.

T_0 = Neither the incident, nor the most forward track should be a pion.

T_1 = One and only one incident track in each x and y-plane.

T_2 = The incident track must lie within the range of the angular beam-divergence, and pass through the target.

T_3 = Only one outgoing scattering track in H4 or H5 or both.

T_4 = The most forward scattering track must match with the incident track at the target within the spatial resolution of the hodoscope-system.

We scale all beam tracks, outgoing tracks, and their matrix-coincidences. We scale separately coincidences with only 1 hit in H3 and coincidences with multiple hits in H3 and/or hits in IC1 and IC2.

The high rate of about $5 \cdot 10^6$ particles/spill in each hodoscope, poses rather stringent constraints on the electronic logic's time resolution and speed. We estimate that we need approximately a speed of 30 - 100 nsec.

To be able to distinguish particles from different RF-buckets, we need a maximum of 15 nsec in time resolution.

We plan to use standard electronic logic with matrices to perform all the required functions. In Table IIa we list the electronic circuitry to be used for most of these functions.

TABLE IIa:

FUNCTION	ELECTRONIC CIRCUIT
N_i	Digital Adder
$\sum X_i \leq 1$	Analog Linear Add
Minimum (A, B, C, ...)	Matrix + "And"
θ_x^2, θ_y^2	Matrix
Δx	Matrix

In Fig. 9 we sketch the implementation of some of the above functions.

In the appendix we express these requirements in terms of logic functions, to be hardwired in the electronic circuitry.

$\Delta\sigma_L$ MEASUREMENT

The amount of beam passing through the polarized-proton target is attenuated by both the free polarized protons and by the rest of the material in the target. The number of particles, N_i (corrected for efficiency), that is transmitted through the target into the i th solid angle covered by segments of the transmission hodoscope is given by:

$$N_i^{\pm} = N_0^{\pm} \exp \left[-\alpha_i - \frac{1}{A} (\sigma_i \pm P_B P_T \frac{\Delta\sigma_{L,i}}{2}) \right], \quad (1)$$

where \pm refers to the beam and target polarization oriented antiparallel (+) or parallel (-), N_0 is the number of incident beam particles, α_i is an attenuation constant for everything in the target except free hydrogen, σ_i is the integrated differential cross section from the i th solid angle subtended, $A = (N_A \rho_F L)^{-1} = 2320 \text{ mb}$ is the target constant for free hydrogen, N_A is Avogadro's number, $\rho_F = 0.0714 \text{ gm/cm}^3$ is the free-proton density, $L = 10 \text{ cm}$ is the target length, and $P_B = 0.5$ and $P_T = 0.8$ are the magnitude of the beam and target polarizations, respectively.

The partial cross-section difference for each counter, $\Delta\sigma_{L,i}$, is calculated from these numbers by:

$$\tanh \frac{\Delta\sigma_{L,i} P_B P_T}{2A} = - \frac{N_i^+/N_0^+ - N_i^-/N_0^-}{N_i^+/N_0^+ + N_i^-/N_0^-}. \quad (2)$$

Note that the dominant contributions to the attenuation, α_i and σ_i/A , exactly cancel in this expression. The efficiencies also cancel to first order because the beam polarization is flipped on alternate pulses.

RATES AND RUN PLAN

The accuracy of $\Delta\sigma_L$ measurement is expressed by:

$$\Delta(\Delta\sigma_L) \approx (4800/\sqrt{N_0}) \text{mb.}$$

We wish to measure $\Delta\sigma_L$ to $\pm 10 \text{nb}$. We will need $2.0 \cdot 10^{11}$ incident protons per beam momentum. Therefore we will need to take data for 100 hours per beam momentum. (Assume incident beam of $5 \cdot 10^6$ protons/spill). We will also need 100 hours for checking out the geometry of the experiment to reduce systematic errors. We need a total of 600 hours to complete $\Delta\sigma_L$ measurements. We note that for high-momentum data points a polarized beam will be produced by using the longitudinal scheme and for low-momentum points by the transverse scheme.

SYSTEMATIC ERRORS:

Experiments with polarized beams and polarized targets, in which the polarization of each is reversed frequently, have the happy property of cancelling out many kinds of systematic errors. Sources of -- for example, detector inefficiencies, or geometrical misalignments -- which change slowly with respect to the period of polarization reversal, have little effect on the value of the parameters measured by the experiment.

The systematic errors that are correlated with the beam or target polarization can be classified as multiplicative or additive. The multiplicative errors refer to those factors by which the raw asymmetry must be multiplied, or divided, to yield the final result. When the asymmetry is small, and the number of counts are so few that statistical errors dominate,

multiplicative errors may not be important.

Additive errors, which can introduce a spurious asymmetry into the data, are more serious. In the case where both beam and target are polarized, and reversed at independent intervals, each type of polarization can be used to monitor, and to cancel out, additive errors associated with the other polarization.

The following kinds of systematic error are common to most polarization experiments:

- 1) Target polarization measurement (multiplicative error associated with polarized target). The polarization of the target can be measured to an accuracy of $\pm 3\%$. The principal uncertainties lie in the calibration of the nuclear magnetic resonance system, using the (small) thermal equilibrium signal. Other uncertainties are introduced by non-linearities in the measuring system when the polarization becomes very large.
- 2) Beam polarization measurement (multiplicative factor associated with polarized beam). Several schemes have been suggested for measuring the beam polarization. The calculation based on beam kinematics is probably accurate to $\pm 3\%$.
- 3) Change in beam geometry with beam polarization (additive factor associated with beam). We control this source of error by (a) using the 8-magnet spin reversal scheme that maintains constant beam geometry, or doing polarization reversal upstream of the collimator, (b) using the incident beam telescope and matrix

coincidence to define acceptable incident beam direction, (c) comparing asymmetries observed with the two senses of target polarization.

In the total cross-section measurement there is an additional source of systematic error because, in a transmission geometry, the quantity measured is the total cross-section minus the cross-section for elastic scattering into the solid angle unresolvable by the detector (about .1 milrad in this design. The latter cross-section ranges from less than a millibarn up to several millibarns as the beam momentum increases. To estimate the contamination, we can measure the angular dependence of the elastic cross-section in the two spin states using the diagnostic data from these scattering events sampled by the computer.

APPARATUS

- 1) Use of one of the existing Argonne polarized proton targets.
- 2) Threshold Cherenkov upstream to reject incident pions.
- 3) Threshold Cherenkov downstream to reject events in which fast pions are produced.
- 4) Ten scintillator hodoscopes, five horizontal and five vertical whose characteristics are given in Table II.
- 5) Fast hard-wired matrix coincidence logic, with 15 ns time resolution, to perform the following functions for each event triggering the experiment.
 - a) Veto any event in which more than one scintillator has a count in any of the upstream hodoscopes.
 - b) Define trajectories that will intersect the polarized target.
 - c) Measure $(x, y)^{(in)}$ and $(x, y)^{(out)}$ - coordinates and (θ_x, θ_y) angles of these trajectories.
 - d) Calculate $\theta^2 = \theta_x^2 + \theta_y^2$.
 - e) Measure number of hits in each hodoscope. ($N^{(i)}$).
- 6) Fast scalars, gated for live-time (plus some ungated ones) to count:
 - a) Incident protons.
 - b) Events from x- and y-hodoscopes.
 - c) Events from the matrix coincidence logic.
- 7) Monitor telescope.
- 8) On-line computer to perform the following functions:
 - a) Control and measure target polarization.
 - b) Record all scalars and monitors, once per spill.
 - c) Various on-line diagnostics.

Part B: ASYMMETRIES IN INCLUSIVE PION PRODUCTION
 WITH A POLARIZED BEAM AND TARGET

ABSTRACT

We propose to measure asymmetries in inclusive production of high momentum pions in the reactions

- 1) $p \uparrow p \rightarrow \pi^{\pm} + \text{anything}$, using a transversely polarized beam and a liquid hydrogen target, and
- 2) $p \uparrow p \rightarrow \pi^{\pm} + \text{anything}$, using a longitudinally polarized

beam and a longitudinally polarized target.

The measurements would be made using the polarized proton beam proposed by the M-3 Beam Workshop, and a single arm spectrometer consisting of an analyzing magnet, proportional chambers and gas threshold Čerenkov counters. The kinematic range covered by the experiments would be $p_T \leq 1.0$ GeV/c and $x = p_L^*/p_{\text{max}}^* \approx 0.5 \rightarrow 0.9$. If sizeable asymmetries are found in reaction (1), then the proposed apparatus could be used as a beam polarimeter for further experiments: modified versions of the same apparatus could be used as possible polarimeters utilizing electromagnetic effects.

PHYSICS INTEREST

Measurements of inclusive pion production in p-p collisions with a polarized beam, $p\uparrow p \rightarrow \pi^\pm + \text{anything}$, have revealed sizeable asymmetries in these processes at $p_{\text{lab}} = 6$ and 12 GeV/c. [16,17] These asymmetries seem to be energy independent, they increase with both increasing p_T and increasing x ($=p_L^*/p_{\text{max}}^*$) of the scattered pion, and reach large values (30-40%) for $x \geq 0.7$ (Figure 10). The presence of these large effects in inclusive reactions was rather unexpected, since it was thought that contributions from different inelastic channels would tend to cancel out, resulting in small asymmetries. At the present time there is no clear theoretical understanding of the origin of these effects.

In order to study the spin dependence of inclusive pion production at Fermilab energies, we propose to measure asymmetries in the processes

$$p\uparrow p \rightarrow \pi^\pm + \text{anything} \quad (1)$$

$$p\uparrow p\uparrow \rightarrow \pi^\pm + \text{anything} \quad (2)$$

with special emphasis on the high x region. The first experiment would utilize a transversely polarized beam, and thus we would measure the asymmetry

$$A_n(s, p_T, x) = \frac{E \, d^3\sigma_{\uparrow}/dp^3 - E \, d^3\sigma_{\downarrow}/dp^3}{E \, d^3\sigma_{\uparrow}/dp^3 + E \, d^3\sigma_{\downarrow}/dp^3}, \quad (3)$$

where $E \, d^3\sigma/dp^3$ is the invariant cross-section for pion production and \uparrow, \downarrow refer to the transversity of the incoming proton. The second experiment would employ a longitudinally polarized

beam and a longitudinally polarized target, and we would measure

$$A_{\ell\ell}(s, p_T, x) = \frac{E \, d^3\sigma_{++}/dp^3 - E \, d^3\sigma_{+-}/dp^3}{E \, d^3\sigma_{++}/dp^3 + E \, d^3\sigma_{+-}/dp^3} \quad , \quad (4)$$

where the ++ and +- refer to the helicities of the initial protons. Presently there are no data on these parameters at Fermilab energies, and no data at all on $A_{\ell\ell}$. Furthermore, current theoretical models give very little guidance as to what to expect. Hence, it would be particularly valuable to obtain experimental information on these asymmetries, to be tested against further theoretical developments.

However, we believe that the study of these processes may yield direct information about the constituent structure of the proton and about the spin dependence of the constituent-constituent interaction. This possibility arises from the fact that recently there has been considerable success in explaining certain features of high x meson production in p - p collisions in terms of the quark-parton model.^[20] It has been generally thought that the description of low p_T phenomena within the framework of this model is very involved since all the constituents must be included in the considerations simultaneously. This is in marked contrast with high p_T processes, in which the high p_T hadrons or "jets" presumably are fragments of a single quark scattered through a hard collision. However, recent data of Johnson *et al.*^[18] show that the particle ratios π^+/π^- and K^+/K^- at high x and low p_T are remarkably similar to those at $x=0$ and high p_T (Antreasyan *et al.*^[19]), as shown in Figure 11.

This independence of p_T seems to indicate that the relevant variable for describing meson production is the radial scaling variable $x_R = E^*/E_{\max}^*$ [18] and that there may be a connection between high p_T production and low p_T , high x production.

Ochs [28] has noticed that the π^+/π^- ratio vs. x_R closely resembles the $u(x)/d(x)$ ratio, where $u(x)$ and $d(x)$ are the number of up and down quarks of fractional momentum x in a proton as determined by deep inelastic lepton scattering experiments. This observation suggests that the π^+ production cross-sections in p-p collisions are determined by the u and d valence quark distributions in the proton, and in particular that the u quark in a fast π^+ should be one of the original u quarks in the incident proton (similar arguments hold for the d quark in π^- production). Hence, low p_T , high x single pion production gives information about the constituent structure of the initial protons.

In addition, there are theoretical reasons to believe that the leading valence quark ($x \approx 1$) in the proton carries the helicity of the proton. [21,6c] This assumption implies that the u/d ratio approaches 5 as $x \rightarrow 1$, [21] which in turn leads to the π^+/π^- ratio approaching 5 as $x_R \rightarrow 1$, in agreement with the data of Johnson *et al.* There are also data from deep inelastic scattering of longitudinally polarized electrons on longitudinally polarized protons [22] supporting the notion that quarks "remember" the helicity of the proton even at moderate values of x . Thus it may be that the alignment of the spin of the proton and the spin of the leading valence quark is a general phenomenon and this in fact is our main motivation for emphasizing the high x region.

In conclusion, we believe that measurements of the asymmetries of fast pions produced in inclusive processes (1) and (2) may be a very direct way of probing the spin dependence of the quark-quark interaction. These studies may also shed light on the question of whether the high momentum pions result from quark fragmentation through gluon emission^[29] or whether they are produced through the quark recombination process as has been recently suggested.^[20,30] Finally we wish to point out that if sizeable ($>10\%$) asymmetries were found in reaction (1) then this discovery would have an immediate application in that the proposed apparatus could be used as a simple and convenient beam polarimeter for other types of experiments.

EXPERIMENTAL TECHNIQUE

The proposed layout of the experimental apparatus is shown in Figure 12.

The transversely or longitudinally polarized proton beam is incident upon either a 100 cm long liquid hydrogen target or a longitudinally oriented polarized proton target. Since the beam originates from Λ decay, its divergence will be large ($\sim 1\text{ mrad}$). To obtain good resolution in p_T , the angle of each incoming particle is measured by the two x-y hodoscopes H1 and H2. The other hodoscopes H3 and H4 will be used in the trigger. These hodoscopes will have a spatial resolution of 1.5 mm and will be spaced 15 m apart.

The production angles of charged particles emerging from the target are measured in the multiwire proportional chambers

(MWPC) labeled P1 and P2. Their angles, after magnetic analysis, are again measured in MWPCs P3-P5. The MWPCs are standard Rice University proportional chambers with "fast" (40 nsec strobe) readout electronics so that rates 1 MHz/2 mm can be tolerated. For some parts of the experiment, especially "hot" sections can be deadened. Most of the needed MWPCs already exist and, in fact have been tested and utilized in medium and high energy physics experiments. Fast readout electronics are being constructed for all planes.

The analyzing magnet shown is a standard BM109 (24VIII72) or BM105 (18VI72) bending magnet. Such a magnet should be readily available at FNAL or one could be borrowed from Argonne.

For π^- production, particle identification is simple due to the opposite curvature of pions and protons in the field of the BM109. We plan to trigger only on π^- produced to beam left; thus, at P_5 π^- are separated from the beam by >1 m. Simply placing a scintillation counter (labeled C_π) as shown should provide a clean trigger for π^- . The π^- trigger will be tightened further by requiring the two threshold \hat{C} erenkov counters in coincidence. We expect to be able to make reliable estimates of π^- asymmetries on line.

For π^+ production, particle identification is much more difficult, especially at very high values of x . We plan to use the two gas threshold \hat{C} erenkov counters, labeled $\hat{C}1$ and $\hat{C}2$, in coincidence to suppress background from proton induced δ -rays

from the beam and the copious inelastically scattered protons ($p/\pi^+ \approx 10^4$ at $x=.9$). Each counter should discriminate against protons at a level $<10^{-2}$ giving a total suppression of $10^{-4} \rightarrow 10^{-5}$ of spurious proton triggers. We expect singles rates $\sim 10^5/\text{sec}$ for each counter, but multiple coincidence trigger requirements should eliminate this problem. The \hat{C} threshold setting along with the bend of the BM109 should strongly suppress background due to lower x pions ($p_{\text{lab}} < 70 \text{ GeV}/c$). These counters are standard pieces of FNAL equipment such as were used in E-61. It is our understanding that the bodies of the E-61 counters still exist in storage at FNAL, and we would hope to use them after rehabilitating the optics and providing our own photomultiplier tubes.

We plan to trigger the π^+ experiment by detecting deflection of scattered particles using the x-y hodoscopes H1-H4 and a hard-wired coincidence matrix to further suppress spurious beam induced triggers. The hodoscopes have 2 mm spatial resolution and each pair H1-H2, H3-H4 provides a lever arm of approximately 20 m. A deflection in particle trajectory of at least 0.2 mrad will be required to trigger the experiment corresponding to a cutoff $p_T \gtrsim .05 \text{ GeV}/c$. Although this requirement introduces a bias against legitimate events with a very small angle particle, we believe it is necessary for distinguishing very high x , small p_T π^+ from protons, and that in fact, this small p_T cutoff will negligibly bias the physics results. We have had experience

in previous experiments with fine grained hodoscopes and with coincidence matrix electronics. We expect to improve our spatial resolution by a factor of approximately 2 and upgrade the complexity of our matrix electronics. There should be $\approx 10^4$ trigger candidates/burst, so that a clean decision can be made by the matrix electronics with little deadtime.

The trigger for π^+ will therefore consist of deflection through an angle of greater than 0.2 mrad. in coincidence with a count in both Čerenkov counters. For π^- the trigger will consist of the required bend in the BM109, i.e., a count in the C_π counter and the coincidence of $\hat{C}1$ and $\hat{C}2$. This trigger can be further tightened by hodoscope requirements if necessary. For the single spin measurements with a liquid hydrogen target, an appropriate amount of target empty running will be included. From our experience at the ZGS, we expect the target empty background to be $\approx 20\%$.

In the case of a longitudinally polarized beam incident on a longitudinally oriented polarized target, all single spin hadronic asymmetries must vanish due to conservation of parity. Any observed asymmetries must then be due to spin-spin effects involving scattering off of the free protons (only the free protons are polarized) in the target. Thus, the problem in inelastic measurements using a transversely polarized target of contamination due to asymmetries from scattering from carbon and other bound nucleons is avoided for measurements involving longitudinal spin orientations.

Spurious asymmetries due to long term drifts in beam position, spot size, intensity or spill structure will be averaged away by reversal of the sign of the beam polarization on alternate accelerator pulses. Additional signal averaging will be provided during polarized target running by periodic reversal of the spin direction of the target polarization.

This apparatus can be used to extend these measurements to higher values of p_T simply by shifting the downstream elements in the apparatus by one meter transverse to the beam direction. At these higher values of p_T discrimination of π^+ from protons becomes less difficult due to the greater angular separation of the π^+ s from the beam protons.

EQUIPMENT REQUIREMENTS

We will need the following equipment:

1. Use of the M3 polarized proton beam operated in both the transverse and longitudinal modes.
2. A BM109 or BM105 bending magnet and power supply or the arrangement of a loan of such equipment from Argonne.
3. A 100 cm long liquid hydrogen target
4. Two threshold Čerenkov counters of the type used in E-61.
5. Use of one of the existing Argonne polarized proton targets.

The trigger and monitor counters, proportional chambers, cabling, and electronics trailer (which includes a PDP-11 computer, tape drives, discs, fast and slow logic and scalers) will be furnished by Rice. We require only AC power hook-up, beam line controls, and timing signals from accelerator control.

RATES, RESOLUTION, AND RUN PLAN

A summary of the expected rates and run time required to execute the initial parts of the experiment is shown in Table 3. The parameterizations of the inclusive scattering data by Anderson *et al.* [31] and Johnson *et al.*, [18] have been used for these rate estimates. With the initially expected intensity and beam polarization $I_0 = 10^7$ /pulse and $p_B = .4$, we should be able to measure asymmetries for $x = .6 \rightarrow .9$ in bins of .05 in five bins of p_T for $p_T < .5$ with an accuracy of $\Delta A \approx .025$ in the running time indicated. We will also explore the region $.5 \lesssim p_T \lesssim 1.0$, since the π^+ asymmetries here were largest at ZGS energies. We also request a tune up period which may be parasitic with low intensity beam on target; however, rates in the MWPCs and Čerenkov counters should be tested at $I_0 \approx 10^7$ /burst during the final stages of tune up.

The rates expected in a polarized beam-polarized target experiment at low p_T are listed in the last line of the table. We hope to execute this experiment some time after the initial polarized beam turn on, even if single spin asymmetries prove uninteresting.

We expect to use a BM105 or a BM109 shimmed to a 6" gap as the spectrometer magnet, giving a 1.2 GeV/c transverse deflection. The angular resolution of the upstream hodoscopes H1 and H2 determine the resolution $\Delta p_T \approx .03$ GeV/c, and the MWPCs give $\Delta x \approx \pm .02$. Our resolution should enable measurement of the asymmetries in sufficiently small bins to determine their x and p_T dependence. Discrimination against spurious proton triggers and lower energy pions should ensure clean measurements of π^- asymmetries up to $x=.90$, and π^+ asymmetries up to $x=.8 \rightarrow .9$.

We hope to tune and debug the apparatus during initial tune-up of the M3 beam line soon after the Mesopause. We then plan to quickly explore the high x , low p_T region for possible large single spin asymmetries. If these are found, the apparatus could then be used as a relative polarimeter for further beam tune-up. After the polarized beam is in stable operation, we then propose to explore the higher p_T pion production asymmetries. We believe that the measurements with a polarized target are especially compelling, and request an additional 200 hours as an initial run, since averaging out systematic errors may prove time consuming. A summary of running time requests are as follows:

Tune-up (mostly parasitic)	200 hours	
Low p_T : H ₂	100 hours]] 300 hours
Higher p_T scan: H ₂	200 hours]	
Polarized beam-polarized target run, low p_T	200 hours	

The systematic errors incurred with a polarized beam-polarized target measurement will be studied in such measurements soon to be carried out at the ZGS. We hope to attain an accuracy of $\Delta A \sim \pm .03$ in the measurements at Argonne.

If substantial asymmetries ($\sim .2-.3$) are found in one spin measurements, a polarimeter which measures $\Delta P_B/P_B = .05$ in ~ 20 minutes can be effected with the same spectrometer. [25]

TABLE 3 RUNNING TIME ESTIMATES

Reaction	Simultaneously Recorded Range		$I_o(ppp)$	Target	ΔA in 5 bins of p_T for $\Delta x = .05$	Beam Time (hrs) Assume 180 useful pulses/hr on average		TOTAL (Est.)
	p_T	x				π^+	π^-	
$p \uparrow p \rightarrow \pi x$.1 \rightarrow .5	.6 \rightarrow .9	10^7	1 m LH ₂	.01/ p_B	13	70	100 hrs.
$p \uparrow p \rightarrow \pi x$.5 \rightarrow 1.0	.6 \rightarrow .85	10^7	1 m LH ₂	.01/ p_B	25	140	200 hrs.
$p \uparrow p \rightarrow \pi x$.1 \rightarrow .5	.6 \rightarrow .9	10^7	10 cm NH ₃ , 80% polarized, 20% free H	.02/ p_B	20	105	150 hrs

IV. SUMMARY

The construction of a beam for polarized protons and anti-protons will provide a unique facility for study of some of the outstanding problems in hadron physics. In particular, the substructure and interactions of hadrons can be studied through spin effects at high energy.

We are submitting two separate proposals. In this proposal, we include measurements of the pp total cross-section difference in the region where the rise in cross-section is observed, and low- p_{\perp} large-x hadron-production process using a polarized beam and a polarized target. The second proposal concerns measurement of the asymmetry in high- p_{\perp} events.

In this proposal, we request the following machine time:

Part A, $\Delta\sigma_L$ measurements including polarized-beam tuning - 600 hours. This experiment will be a standard transmission experiment with the detectors specially designed for a high-divergence beam.

Part B, Asymmetries in inclusive pion production - 600 hours.

Equipment requirements are

- (i) a BM109 or 105 bending magnet,
- (ii) liquid hydrogen and polarized targets,
- (iii) threshold Cherenkov counters,
- (iv) scintillation-counter hodoscopes, and
- (v) multiwire proportional chambers.

REFERENCES

1. G. Bunce et al., Phys. Rev. Lett. 36, 1113 (1976).
2. M. Corcoran et al., Indiana University preprint IUHEE no. 9.
3. Private communications, L. Dick and K. Kuroda.
4. I. P. Auer et al., Phys. Rev. Lett. 39, 313 (1977).
5. I. P. Auer et al., to be published.
6. Proceedings of the Symposium on Experiments Using Enriched Antiproton, Polarized Proton, and Polarized Antiproton Beams at Fermilab Energies, edited by A. Yokosawa, ANL-HEP-CP-77-45 (1977).
7. For instance, see theoretical talks presented in Ref. 6 by a) C. K. Chen, p. 38; b) E. Fischbach, p. 65; c) R. D. Field, p. 88.
8. F. E. Close and D. Sivers, Phys. Rev. Lett. 39, 1116 (1977).
9. M. J. Alguard et al., Phys. Rev. Lett. 37, 1261 (1976).
10. Earlier work on this subject includes:
 - a) O. E. Overseth, NAL 1969 Summer Study Report, SS-118, Vol. I.
 - b) O. E. Overseth and J. Sandweiss, NAL 1969 Summer Study Report, SS-120, Vol. I.
 - c) P. Dalpiaz, J. A. Jansen, and G. Coignet, CERN/ECFA/72/4, Vol. I, p. 284.
 - d) CERN proposal SPSC/p. 87, July 1977.
11. For instance, see I. P. Auer et al., Phys. Lett. 70B, 475 (1977).
12. J. R. O'Fallon et al., Phys. Rev. Lett. 39, 733 (1977).
13. C. K. Chen, to be published. ANL-HEP-PR-77-76.

14. s-channel helicity amplitudes: $\langle ++|++ \rangle = \phi_1$, $\langle --|++ \rangle = \phi_2$, and $\langle +-|+- \rangle = \phi_3$.
15. H. Hidaka et al., Phys. Lett. 70B, 479 (1977).
16. R. D. Klem et al., Phys. Rev. Lett. 36, 929 (1976).
17. J. B. Roberts, "Measurement of Asymmetries in Inclusive Proton-Proton Scattering," in AIP Conference Proceedings No. 35, M. L. Marshak, Editor, Argonne (1976).
18. J. R. Johnson et al., FERMILAB-Pub-77/98-EXP (October 1977).
19. D. Antreasyan et al., Phys. Rev. Lett. 38, 112 (1977). and 38, 115 (1977).
20. K. P. Das and R. C. Hwa, Phys. Lett. 68B, 549 (1977).
21. G. R. Farrar and D. R. Jackson, Phys. Rev. Lett. 35, 1416 (1975).
22. P. Cooper, Ref. 6, p. 126.
23. J. W. Cronin and O. E. Overseth, Phys. Rev. 129, 1795 (1963);
O. E. Overseth et al., Phys. Rev. Lett. 19, 391 (1967).
24. D. Underwood et al., A Polarized Beam for the M-3 line, December 1977.
25. J. B. Roberts, "Polarimeters: A Summary" (included with the proposal).
26. D. Underwood, ANL-HEP-PR-77-56.
27. E. Leader and J. Soffer, private communication.
28. W. Ochs, Nucl. Phys. B118, 397 (1977).
29. R. D. Field and R. P. Feynman, Phys. Rev. D15, 2590 (1977).
30. D. W. Duke and F. E. Taylor, FERMILAB-Pub-77/95-THY (October 1977).
31. R. L. Anderson et al., Phys. Rev. Lett. 37, 1111 (1976).
32. See. C. Sorensen's talk presented in Ref. 6, p. 210.
33. C. K. Chen, Phys. Rev. D16, 1576 (1977).

34. E. Fischbach and G. W. Look, Phys. Rev. D13, 752 (1976), D16, (1976); L. L. Frankfurt and V. B. Kopeliovich, Nucl. Phys. B103, 360 (1976); J. Missimer, L. Wolfenstein and J. Gunion, Nucl. Phys. B111, 20 (1976); E. M. Henley and F. R. Krejs, Phys. Rev. D11, 605 (1975); L. L. Frankfurt, JETP Lett. 12, 379 (1970); Sov. Phys. JETP 34, 23 (1972); M. Dobovoy, P. Langacker, and M. Suzuki, Phys. Rev. D4, 1474 (1971); N. N. Nikolaev, Sov. J. Nucl. Phys. 17, 62 (1973); K. H. Craig, Nucl. Phys. B109, 156 (1976).
35. T. T. Chou and C. N. Yang, Nucl. Phys. B107, 1 (1976); F. E. Low, Phys. Rev. D12, 163 (1975).

APPENDIX I

HIGH- P_T HADRON PRODUCTION WITH A TOROIDAL SPECTROMETERPHYSICS INTEREST

Hadron production and jet production at high- P_T seem to be two efficient ways for probing quark-quark interactions at short distances. The role of spin-forces in the dynamics of the elementary constituents of the nucleon is emphasized to some extent in the Introduction. We regard this part of physics as one to which very important contributions can come from polarized proton-proton (antiproton) experiments. To this end, we have submitted a separate proposal to study asymmetries of inclusive and jet-like products in high- P_T p-p interactions using large acceptance calorimeters. Here we would like to discuss our interest in the very interesting possibility of using a toroidal spectrometer to study inclusive-charged hadron production at high- P_T .

DETECTOR REQUIREMENTS

The limited luminosity, the low high- P_T inclusive rates, and high low- P_T background due to the sharp fall-off of the cross-section with P_T ($\sim P_T^{-8}$) impose the following stringent requirements on such an experiment:

- (a) Large ϕ -acceptance.
- (b) Maximum possible target length and beam intensity available.
- (c) High signal (high- P_T)/noise (low- P_T) ratio.
- (d) Good momentum resolution.

Up to now, all high- P_T inclusive experiments have had a very limited ϕ -acceptance ($\leq \pi/20$). We have made a preliminary Monte-Carlo study of a toroidal spectrometer design as well as two more conventional large aperture spectrometers.

The results indicate that the toroid

- (a) Is more than 3 orders of magnitude better in signal-to-noise ratio ($2 - 3 \cdot 10^3$ vs. ~ 1).
- (b) Is about 5 times better in ϕ -acceptance (85% vs. 15-20%)
- (c) It can accept simultaneously a large range of $P_T > 2$ GeV and $\chi_F \simeq 0$ inclusives with high acceptance.

DESCRIPTION OF THE SPECTROMETER AND ITS PROPERTIES

Fig. 13 shows some views of our current magnet design. The field inside the toroid has cylindrical symmetry and varies as $\sim 1/r$ (r = radius).

Fig. 14 shows the experimental set up. The beam axis coincides with the toroid axis.

The bending of each particle produced at the target and entering the magnet happens on the production plane containing the beam-toroid axis. The particle trajectory is always perpendicular to the field lines and so the field is fully utilized. The inner cylinder of the toroid of $\simeq 10$ cm radius allows the beam and the forward-going low- P_T products of multiparticle events to pass unaffected by the field. The field can be set so that positive particles bend outwards and negative ones inwards, getting trapped around the beam axis. This and the dependence of the angle of bend on the particle momentum provide this spectrometer with charge and kinematic selectivity in (χ_F, P_T) .

With such a field configuration, the low-energy ($\chi_F \leq 0$, low- P_T) particles can be swept with high efficiency away from the MWPC and DC-planes (Drift-Chamber) shown in Fig. 14. This should allow the detector to tolerate easily the rates from a 20 cm NH_3 target and a beam intensity $> 10^7$ protons/spill in an optimized setup configuration.

TRIGGER

At S_0 , S_1 , S_2 of Fig. 14, three scintillation-counter hodoscopes, finely segmented and azimuthally symmetric, define the production plane of each inclusive product as well as its x_F and P_T -range. Thus, they can provide a very tight, triple coincidence, coplanar trigger, essentially free from non-coplanar background and a suppression in the geometrical acceptance of

$$\frac{\text{signal } (P_T > 2 \text{ GeV})}{\text{noise } (P_T > 0.5 \text{ GeV})} > 10^3 .$$

Fig. 15 shows the shape of these hodoscopes and the wire configuration of MWPC and DC-planes placed after the magnet to find particle tracks and facilitate their kinematic analysis.

The part of the detector corresponding to those particles that are swept away from the beam-toroid axis has the maximum sensitivity.

Therefore, by simply switching the magnet current polarity, one could study π^+ and π^- separately at that part of the detector.

By placing a segmented Cherenkov-counter, shown in Fig. 14, behind the S_2 -hodoscope, a π^+ vs. proton discrimination will be possible. By placing a π^0 detector further downstream, one could trigger simultaneously on π^0 -inclusive production, essentially free from low-energy background.

INCLUSIVE RATES AND TRIGGERS

Inclusive rates for this experiment have been calculated using the data of Antreysan et al⁽¹⁹⁾ as well as $A_N(\text{ppt})$, $A_{LL}(\text{p}^\dagger\text{p}^\dagger)$ errors, listed in Table I along with the conditions assumed.

TABLE I δA_{LL} and δA_N Accuracies at $p_{\text{lab}} = 200 \text{ GeV}/c$.

p_T (GeV)	$E(d^3\sigma/dp^3) (\pi^+ + \dots)$ (cm^2)	$\langle p_{T\text{jet}} \rangle$ (GeV)	$\delta A_{LL}(\text{p}^\dagger\text{p}^\dagger)$	$\delta A_N(\text{ppt})$
3.0	2.1×10^{-32}	3.6	< .01	< .01
4.0	7.3×10^{-34}	4.8	.04	< .01
4.5	1.0×10^{-34}	5.5	.10	.01
5.0	1.5×10^{-35}	6.1	.18	.03

$I = 1.5 \cdot 10^7$ protons/spill, $L_{\text{NH}_3} = 20 \text{ cm}$, 1 month running (700 hours)

$$\Delta\phi/2\pi = .9, \Delta p_T = .5 \text{ GeV}, \Delta x(x \sim 0) = .1$$

CONSTRUCTION FEASIBILITY AND COSTS

Preliminary calculations and discussions with a toroid specialist at ANL* indicate that its building should pose no problems in mechanical construction. For a regular Cu-coil, water cooled magnet, with a central $\int B dl = 20 \text{ kGm}$ and 2.5 meters long, the following estimates have been calculated:

$$\text{Cost} = \$25 - 30 \text{ k.}$$

Time for construction, test and calibration ≈ 5 months. In addition, the highly symmetric characteristics of the device would allow simplicity and high compactness of the detector, thus keeping building, testing, maintenance costs and time consumption low.

Finally, we point out the easiness of access to the detectors and their flexibility to adapt to different experimental conditions.

*Bert Wang, private communication.

APPENDIX II

OTHER POSSIBLE EXPERIMENTS USING THE POLARIZED-PROTON BEAM FACILITY

First, we note that we can measure $\Delta\sigma_T$ with an N-type polarized target and the apparatus described in the text. This would give us an additional clue about the rise in our total cross section.

Taking advantage of the polarized-antiproton beam, we can measure $\Delta\sigma_L$ and $\Delta\sigma_T$ for pp scattering. Theoretical interests are recently discussed by C. Sorensen.³²

In the dilepton-production experiment, $p^\dagger p^\dagger \rightarrow (\mu^+ \mu^-) + x$, we study the mechanism of ψ production at $m_{\mu\mu} \approx 3$ GeV and the Drell-Yan mechanism at higher mass.^{7,8} With a polarized antiproton beam, a reaction $\bar{p}^\dagger p^\dagger \rightarrow (\mu^+ \mu^-) + x$ enables us to observe the spin effect of valence-quark and anti-valence-quark interactions.³³ Another exciting possibility is that one can perform an experiment like $\bar{p}p \rightarrow (\text{Jet}) + x$. Then we can observe valence quark, q_v , to anti-valence quark, \bar{q}_v , interaction, while in pp scattering, we observe $q_v - \bar{q}_s$ (anti-sea quark) interaction.

Total cross section or large- p_\perp inclusive measurements using a longitudinally-polarized beam should be useful in a search for a parity-nonconserving component in the force between nucleons. The predicted asymmetry effect varies from 10^{-2} to 10^{-5} .³⁴

Finally, we note that polarized beams are useful to pursue "old physics" such as elastic-scattering amplitude measurements at small $|t|$.^{32,35}

APPENDIX III

TRIGGER LOGIC FUNCTIONS

$$T0 = \overline{C_1} \cdot \overline{C_2}$$

where C_1, C_2 are the Cherenkov-counter signals set to detect fast pions.

We define

$$X_j^{(i)} (Y_j^{(i)}) = \text{the } j\text{th-scintillator of the } HX_i (HY_i) \text{ hodoscope.}$$

Then, the above 4 requirements read as follows:

$$T1 = (\sum_{j=1}^{N_1} X_j^{(1)} = 1) \cdot (\sum_{j=1}^{N_2} X_j^{(2)} = 1) \cdot (\sum_{j=1}^{N_1} Y_j^{(1)} = 1) \cdot (\sum_{j=1}^{N_2} Y_j^{(2)} = 1)$$

where N_i = number of scintillation-counters of H_i -hodoscope.

$$\text{Define } \Delta X^{in} = X_{j2}^{(2)} - X_{j1}^{(1)}$$

$$\Delta Y^{in} = Y_{k2}^{(2)} - Y_{k1}^{(1)}$$

$$T2 = \overline{A} \cdot (|\Delta X^{in}| \leq M^{in}) \cdot (|\Delta Y^{in}| \leq M^{in})$$

where $M^{in} \approx 10$,

a parameter defined by the beam-hodoscopes and target setup.

$$T3 = (\sum_{j=1}^{N_4} X_j^{(4)} \leq 1) \cdot (\sum_{j=1}^{N_4} Y_j^{(4)} \leq 1) \cdot (\sum_{j=1}^{N_5} X_j^{(5)} \leq 1) \cdot (\sum_{j=1}^{N_5} Y_j^{(5)} \leq 1)$$

For every hit $(X_j^{(5)}, Y_j^{(5)})$ in H5

$$\text{Find } \Delta X_{25j}^{out} = X_j^{(2)} - X_j^{(5)}$$

$$\Delta Y_{25j}^{out} = Y_j^{(2)} - Y_j^{(5)}$$

Then, find

$$\theta_{x25} = (|2 \cdot \Delta X^{in} - \Delta X_{25j}^{out}|)$$

$$\theta_{y25} = (|2 \cdot \Delta Y^{in} - \Delta Y_{25j}^{out}|).$$

For every hit in $(X_j^{(4)}, Y_j^{(4)})$ in $H4$, find

$$\Delta X_{24j}^{\text{out}} = X^{(2)} - X_j^{(4)}$$

$$\Delta Y_{24j}^{\text{out}} = Y^{(2)} - Y_j^{(4)}$$

Then, find

$$\theta_{x24} = (| 2 \cdot \Delta X^{\text{in}} - \Delta X_{24j}^{\text{out}} |)$$

$$\theta_{y24} = (| 2 \cdot \Delta Y^{\text{in}} - \Delta Y_{24j}^{\text{out}} |) \quad .$$

$$T4 = (| \theta_{x25} - \theta_{x24} | \leq MD) \cdot (| \theta_{y25} - \theta_{y24} | \leq MD)$$

where $MD \simeq 3$ mm, which is the spatial resolution upper limit of the scintillator-hodoscope system.

Finally, the transmitted particle is defined by

$$T = T_0 \cdot T_1 \cdot T_2 \cdot T_3 \cdot T_4 \quad .$$

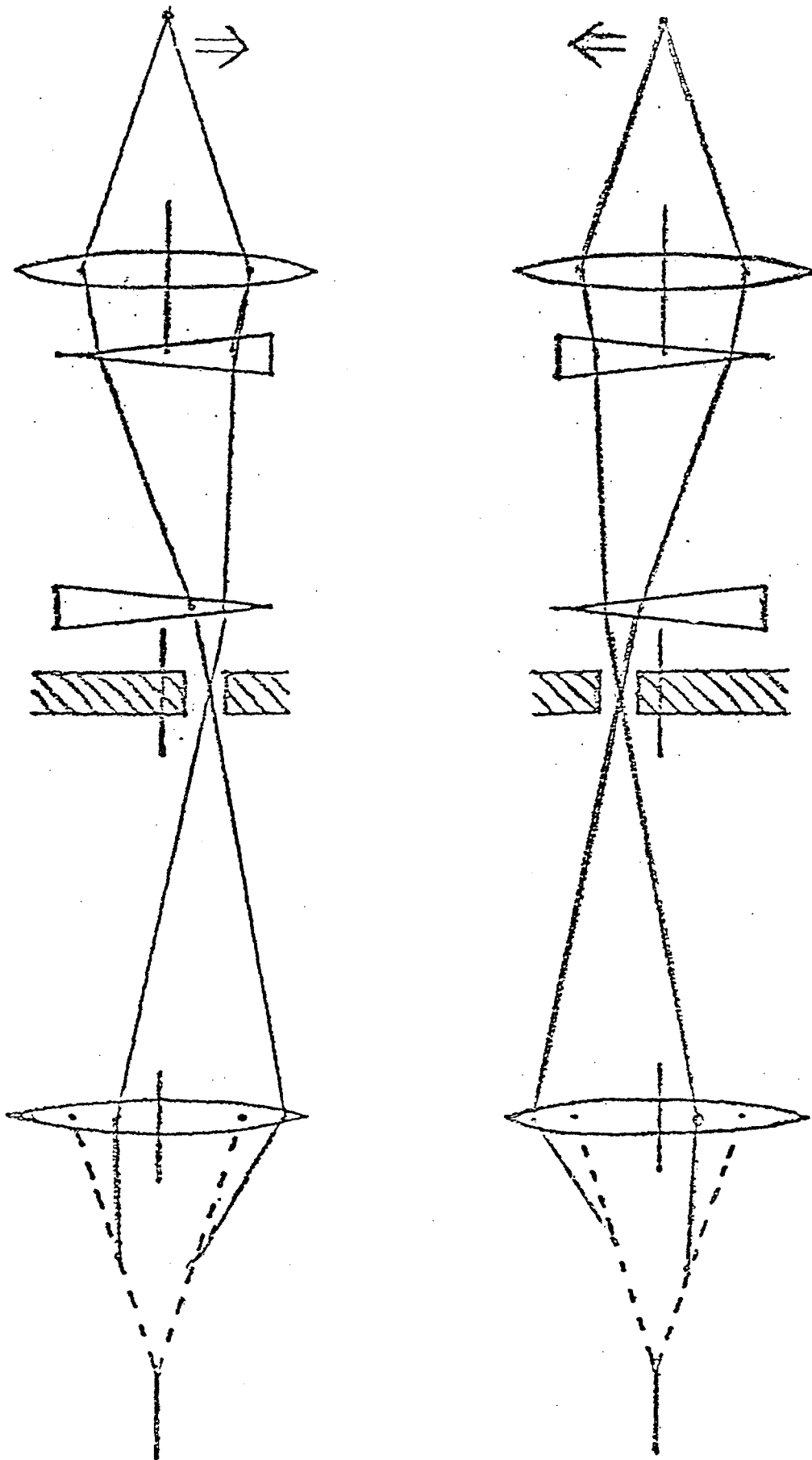


Fig. 1

Two-vernier polarization reversal. An improved version would have one or two verniers upstream of a fixed collimator.

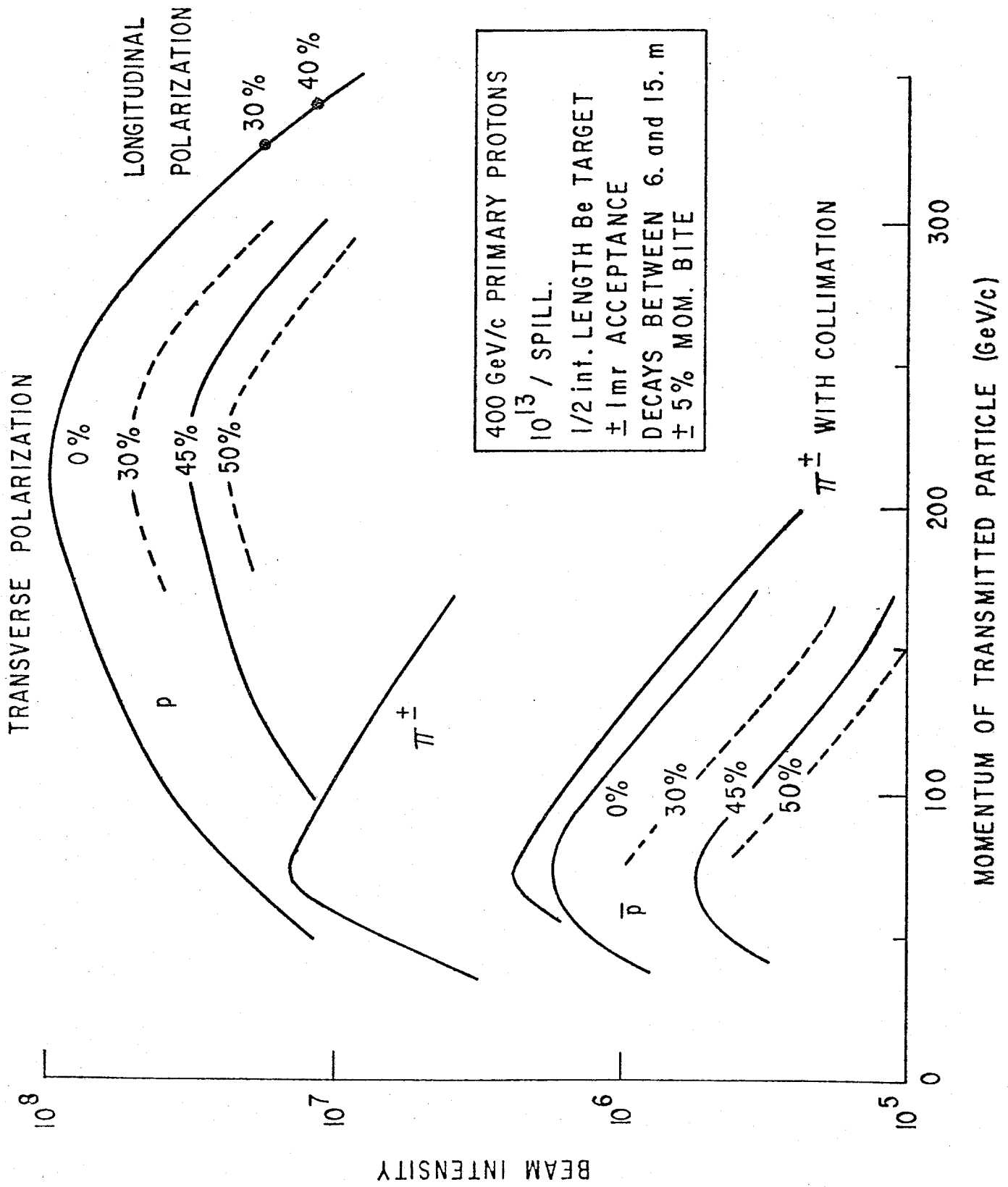
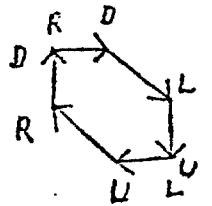
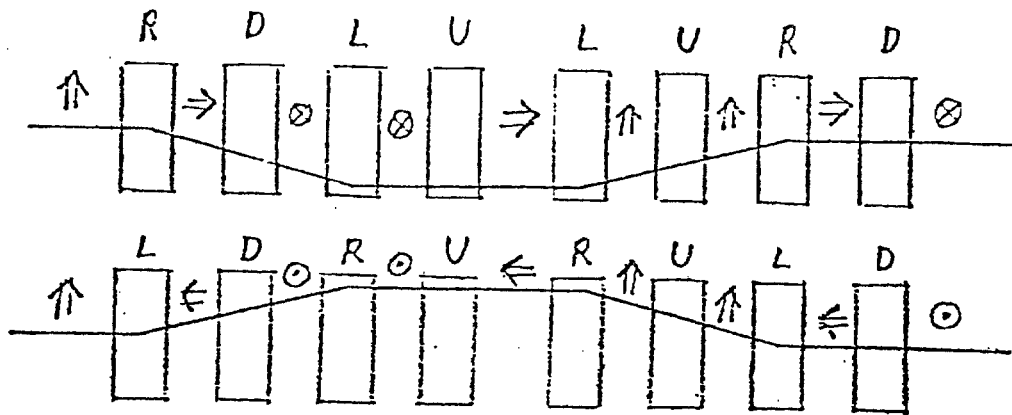
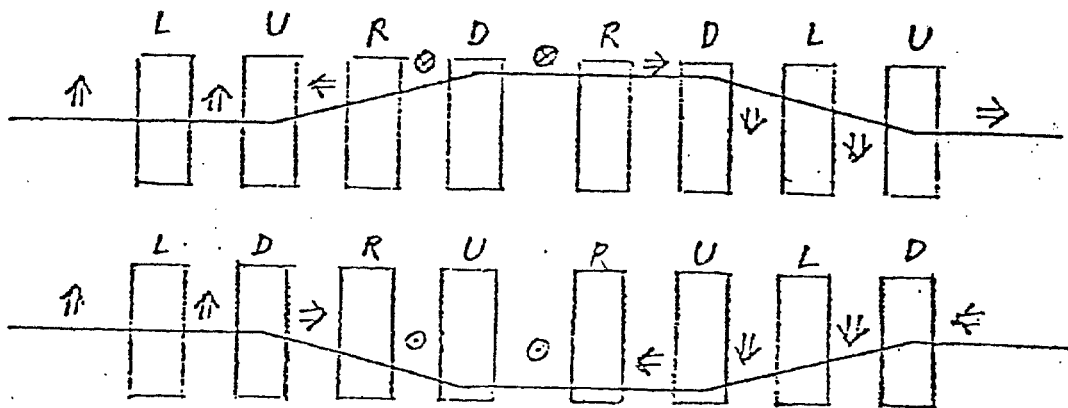


FIG. 2 Estimated polarized proton and antiproton beam intensities.

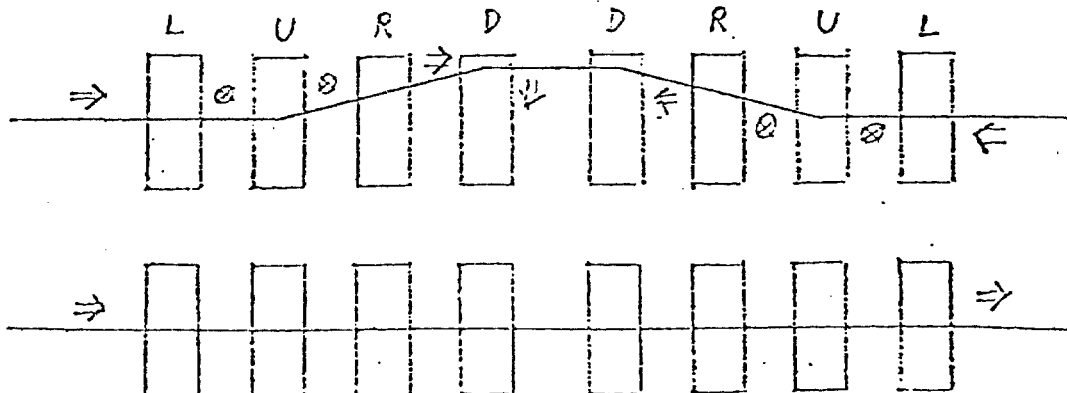
SPIN FLIPPING WITH NO NET BEAM MOTION
 (Transverse) (Reverse 4 of 8 Magnets) (No verniers)



Transverse in - Transverse out

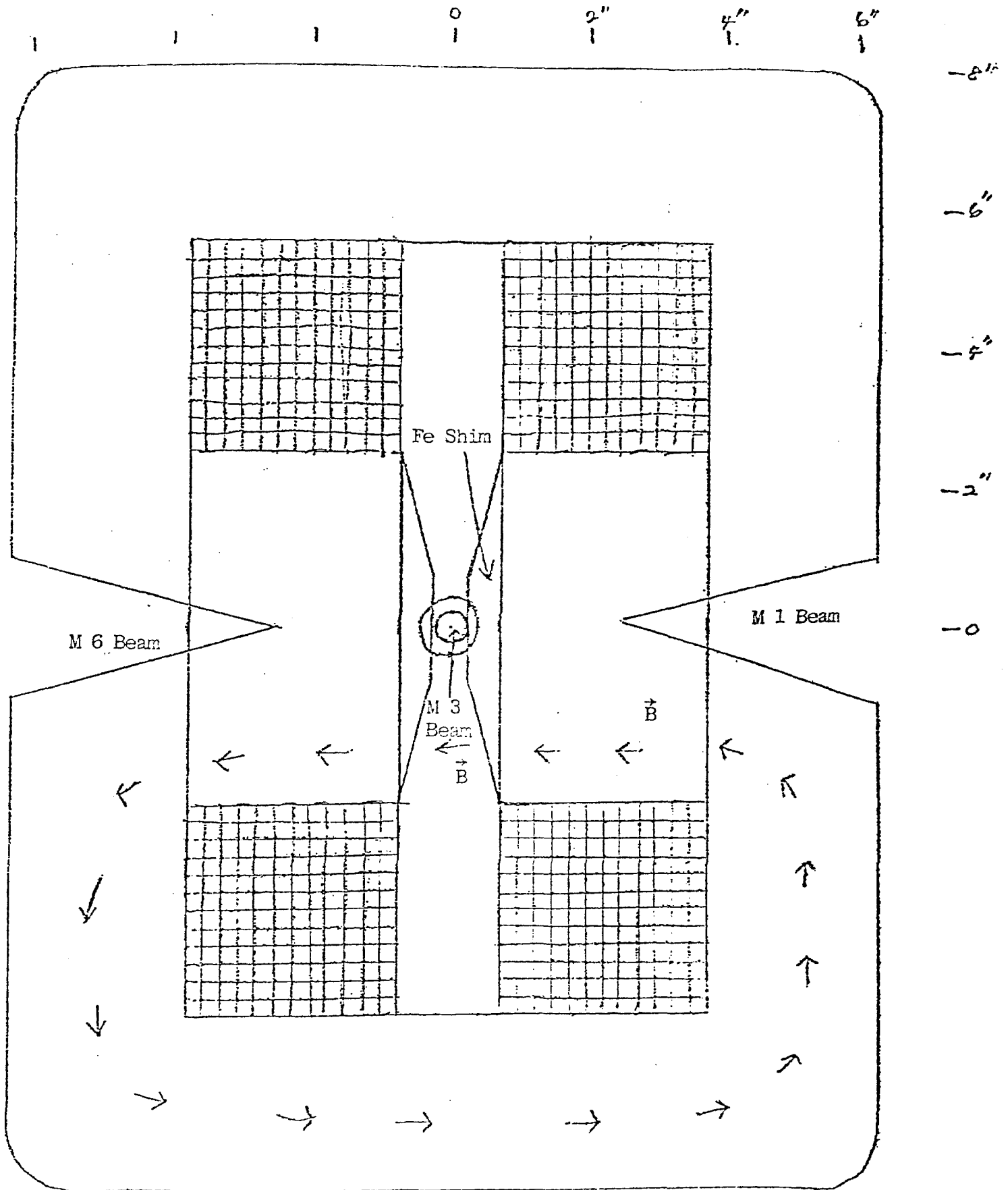


Transverse in - Longitudinal out



Longitudinal in - Longitudinal out

Fig. 3



Modified 5-1.5-1

EPB Dipole for sweeping

Fig. 4

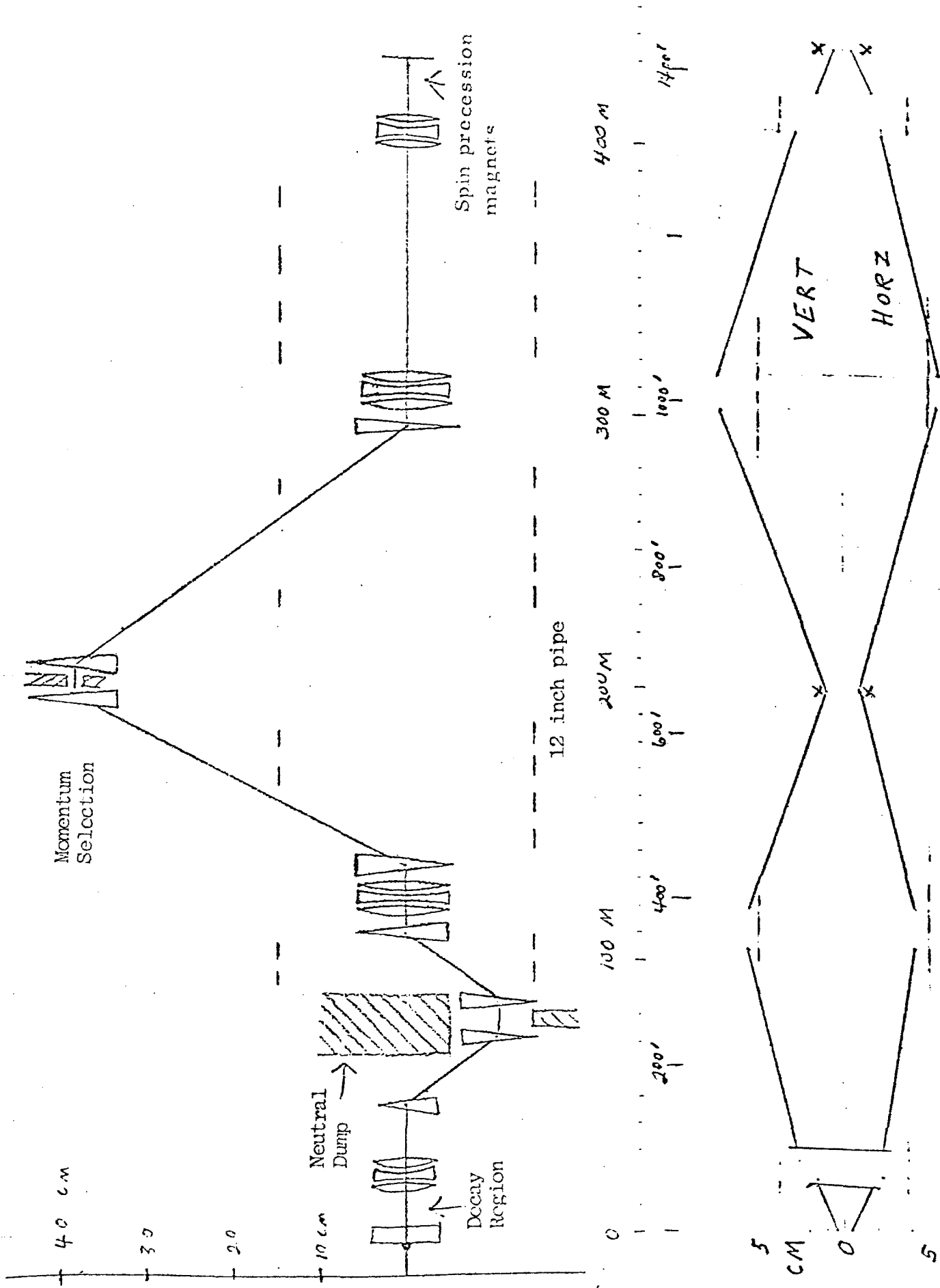


Fig. 6 Beam envelopes. The crosses (x) show the effect of a $\pm 5\%$ momentum bite.

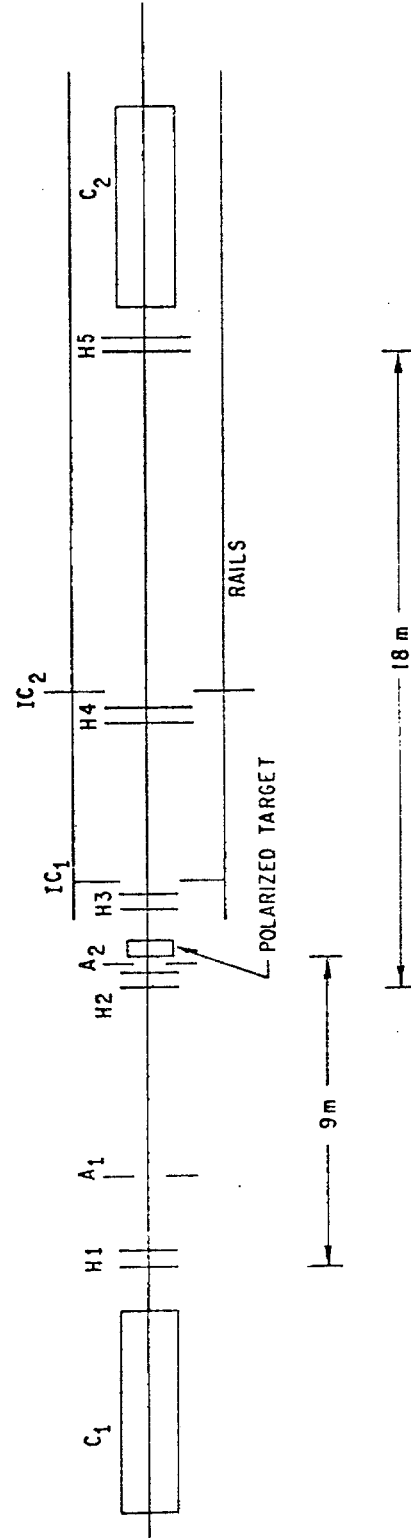


FIG. 7 Layout of total cross-section difference ($\Delta\sigma_L^{\text{tot}}$) experiment at $p_{\text{lab}} = 200 \text{ GeV}/c$.

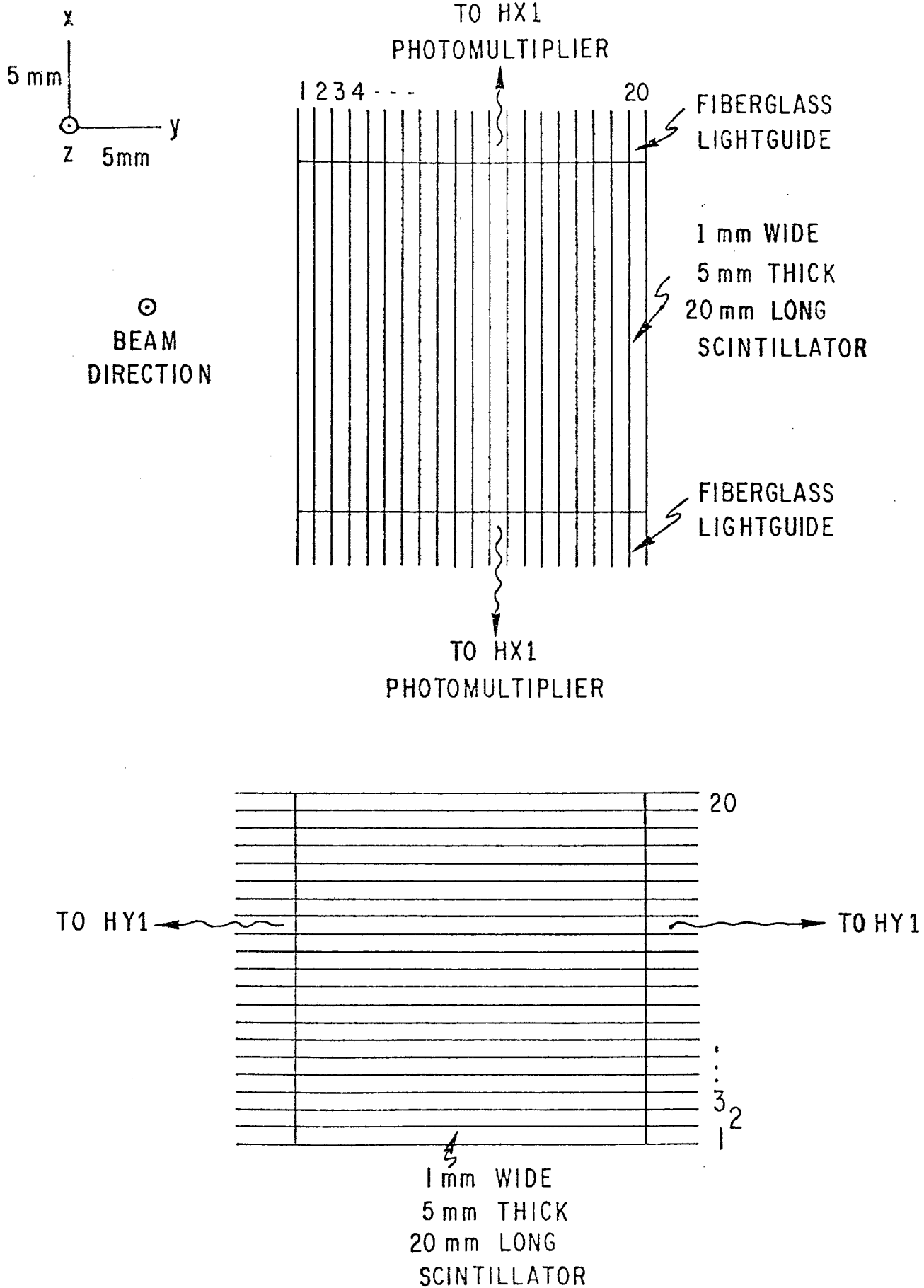


FIG.8 Scintillation-counter hodoscope layout.

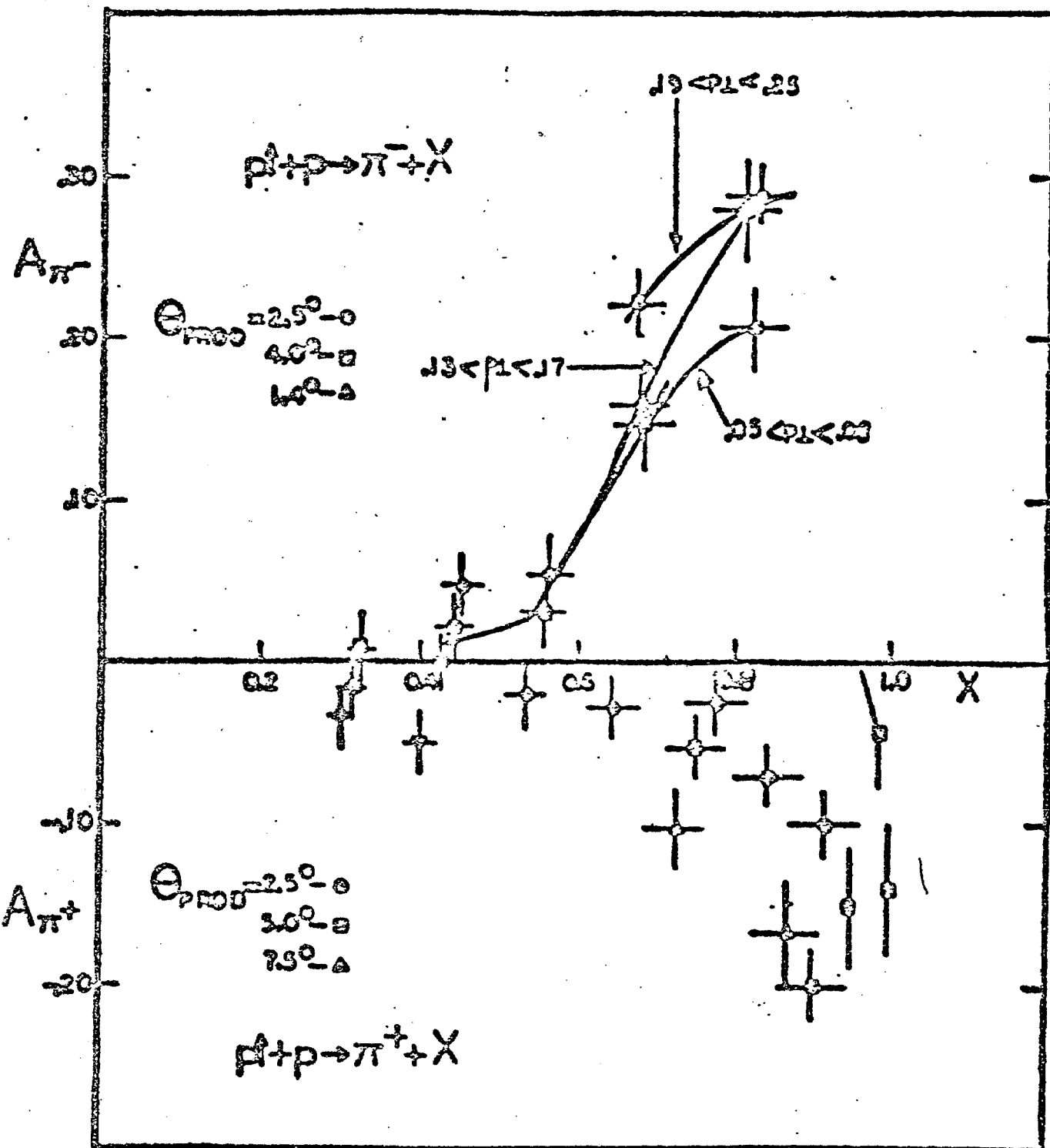


Figure 10: The asymmetry A in $p + p \rightarrow \pi^\pm + \text{anything}$ plotted against $x = p_L^*/p_{\max}^*$ at $p_{\text{lab}} = 6 \text{ GeV/c}$. Lines of approximately constant p_T are drawn for the π^- data.

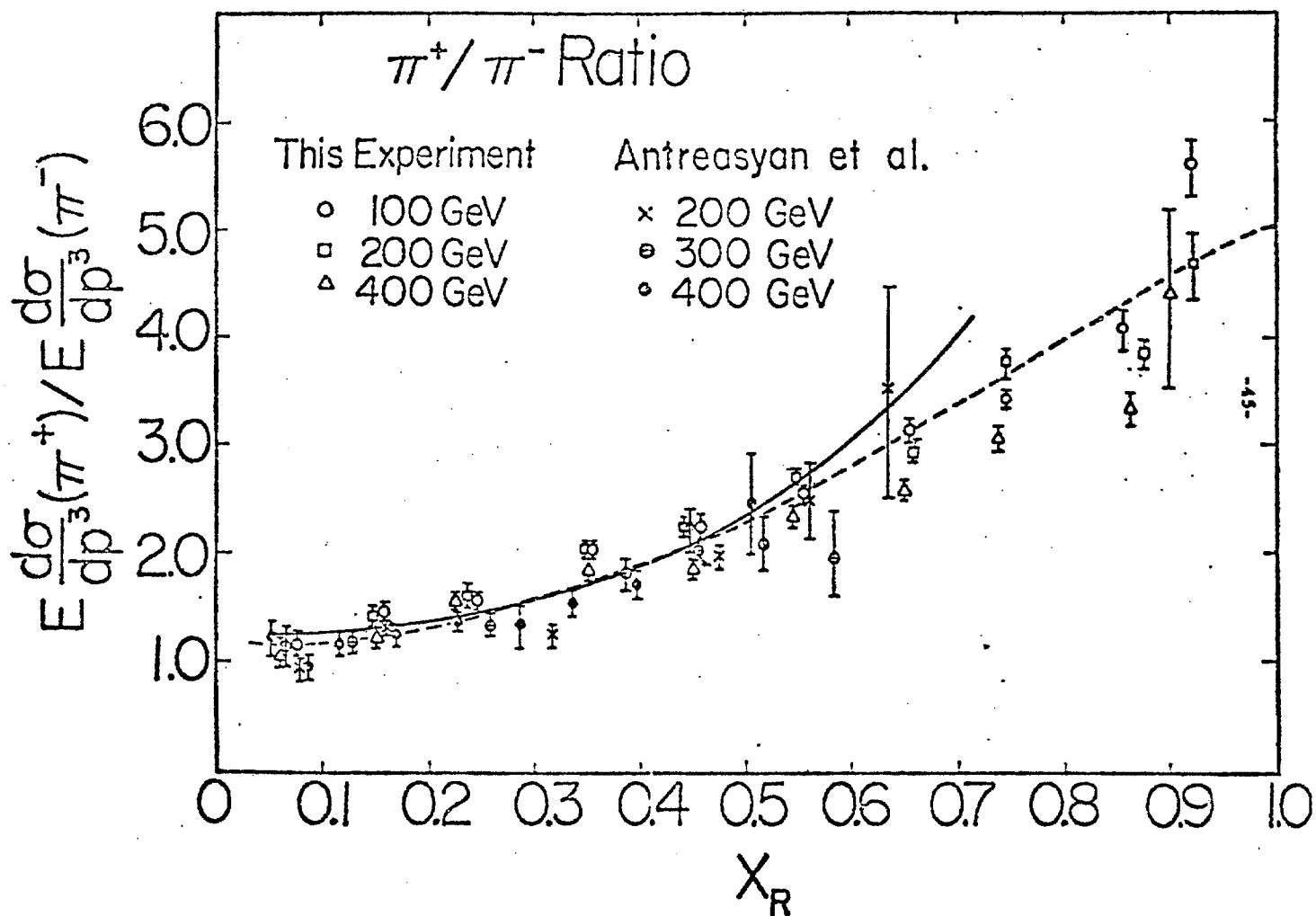


Figure 11: The π^+/π^- ratio plotted against the radial scaling variable $x_R = E^*/E_{\text{max}}^*$. The data are from Refs. [18] (Johnson *et al.*) and [19] (Antreasyan *et al.*). The smooth line is a prediction of Field and Feynman (Ref. [29]) and the dotted line is a prediction of Das and Hwa (Ref. [20]).

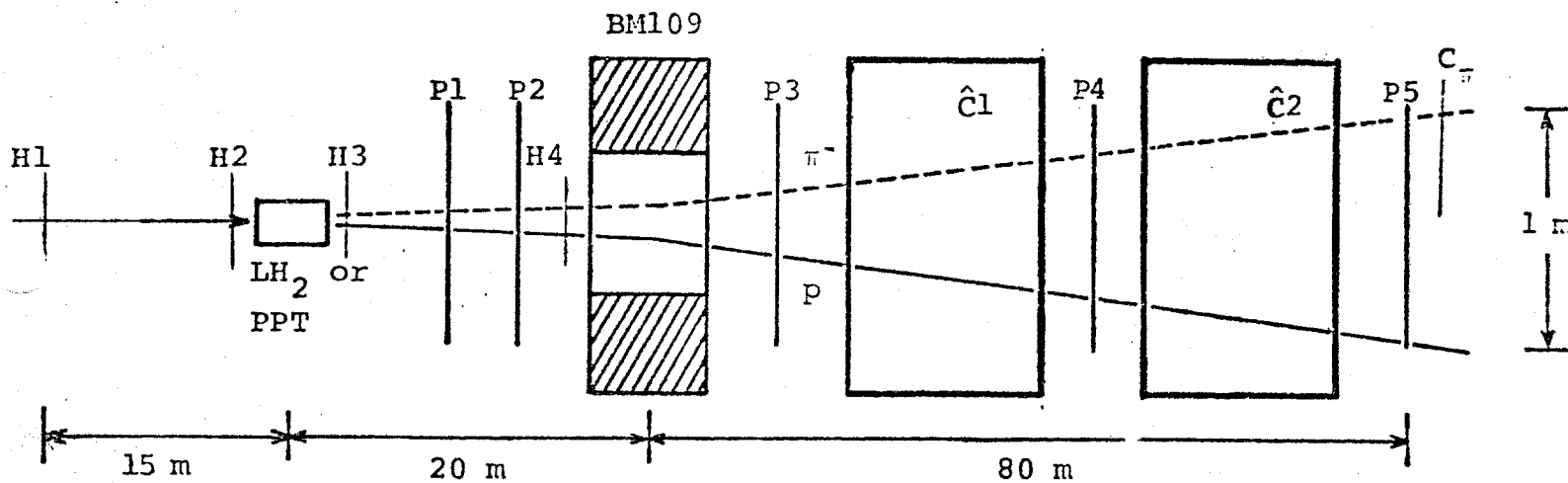


Figure 12: Proposed layout of the apparatus. H1-H4 are x-y hodoscopes, P1-P5 are multiwire proportional chambers, $\hat{C}1$ and $\hat{C}2$ are gas threshold Cerenkov counters and C_π is a scintillation counter.

ELEMENTS NOT TO SCALE

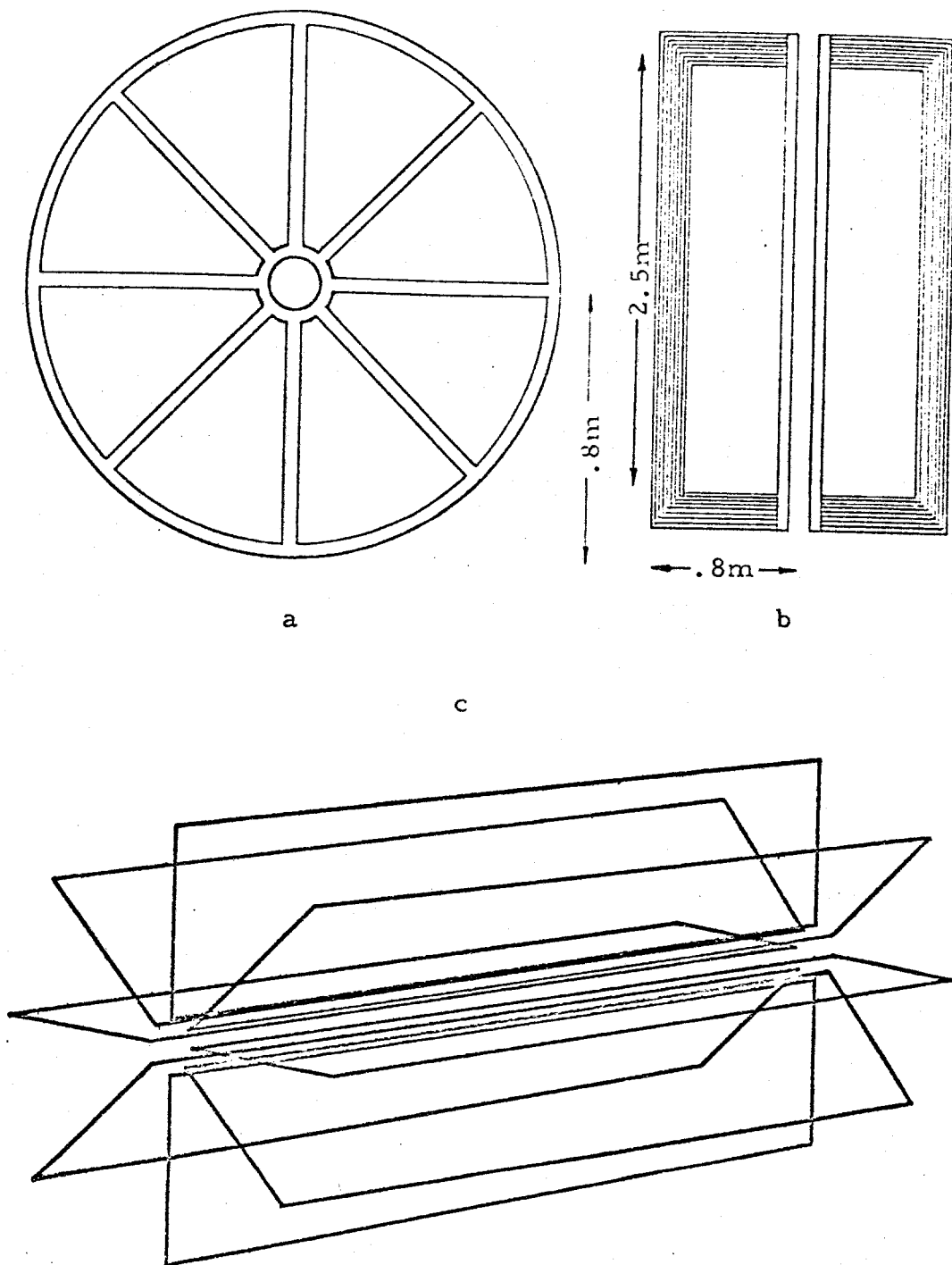


FIG.13 Toroidal-magnet design:

- a. Face-view of an 8-coils support-system with inner and outer rings,
- b. Plane-view of two coils,
- c. Overall view of the 8-coils arrangement.

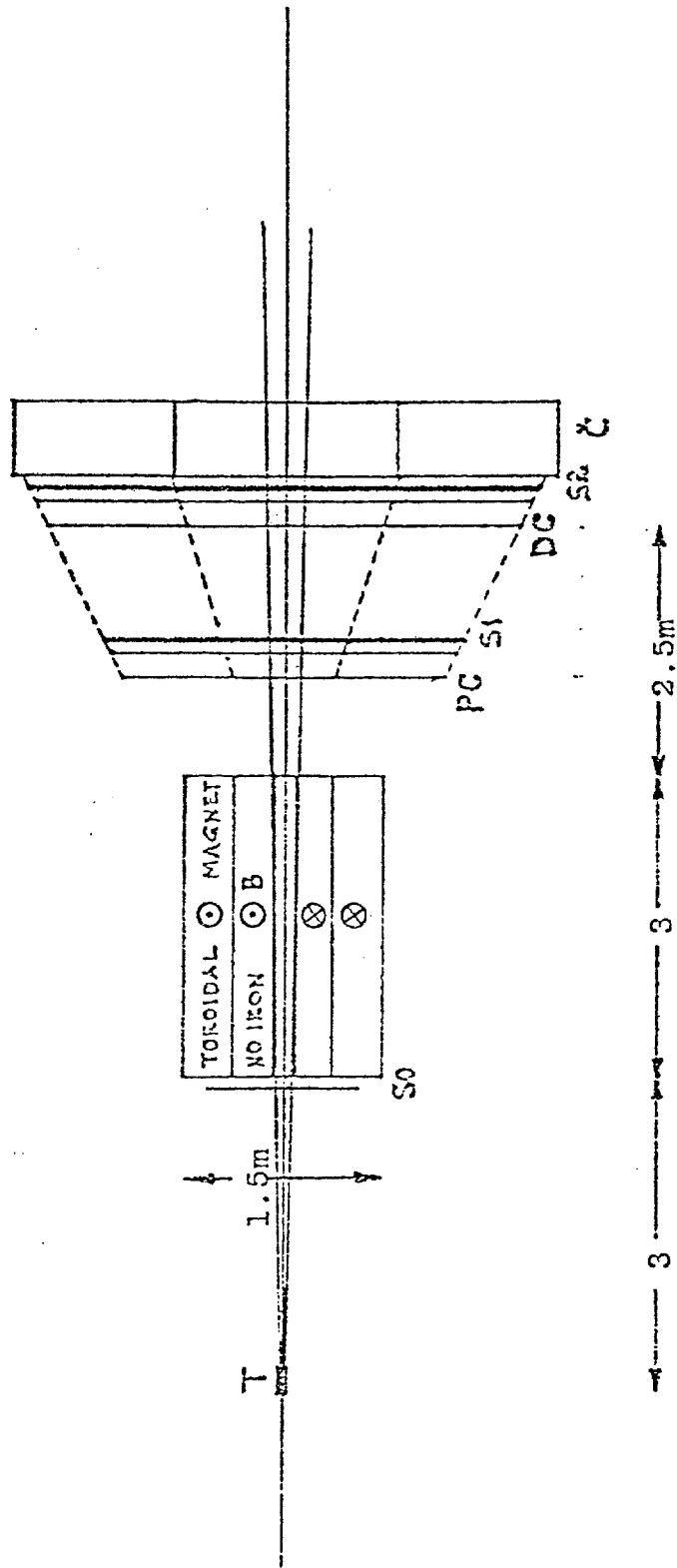


Fig. 14 Toroidal spectrometer setup for high- p_T inclusives ($pp \rightarrow \pi^\pm + \dots$)

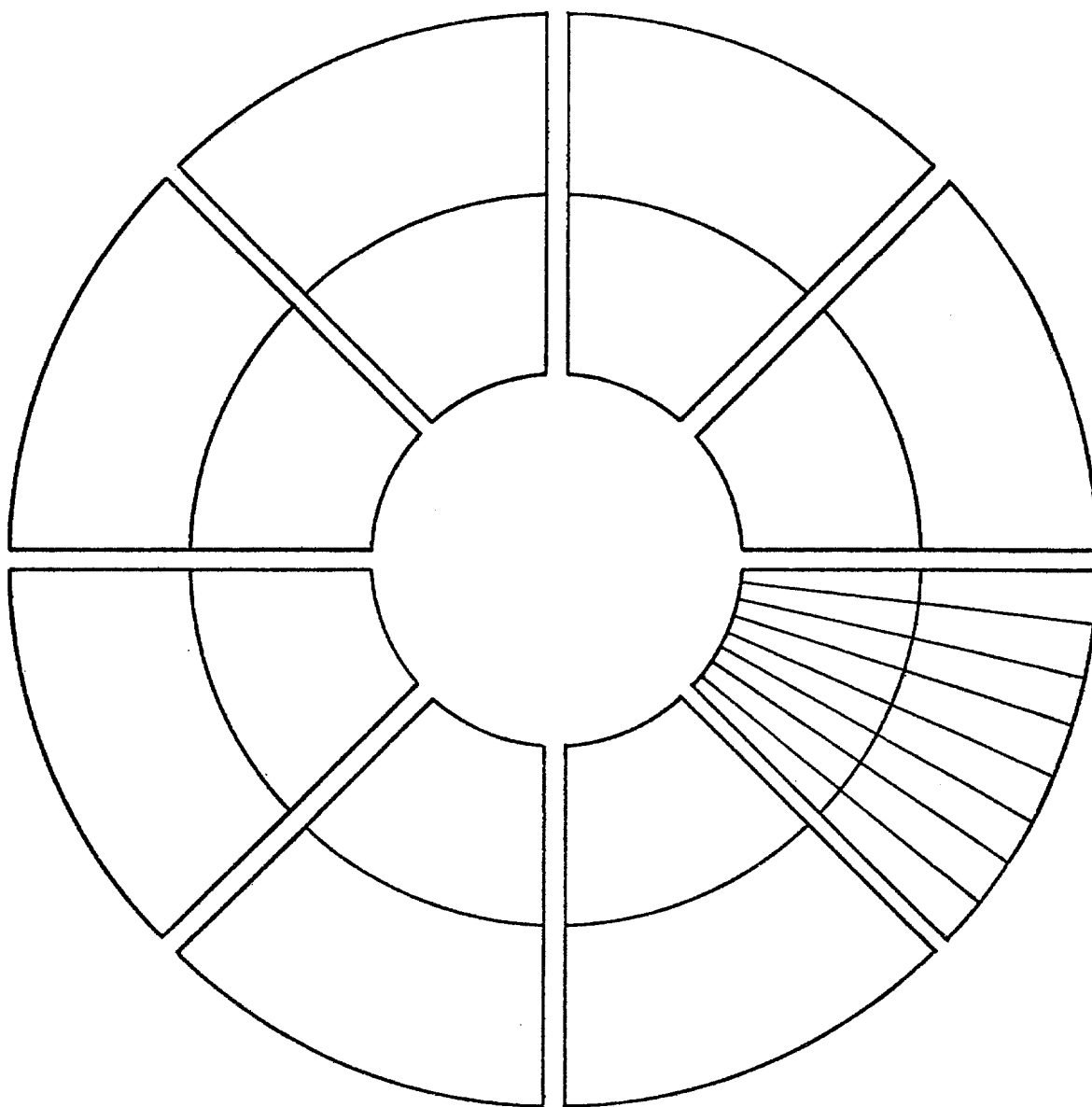


FIG.15 Shape-sketch of the scintillation-counter hodoscopes(S_0, S_1, S_2)

ON THE POSSIBILITY OF USING A POLARIZED PROTON BEAM
AT FNAL FOR ASYMMETRY MEASUREMENTS IN PROTON-PROTON
ELASTIC SCATTERING AT VERY SMALL $/t/$ VALUES AND IN
INCLUSIVE Λ^0 , K^0 , π^0 PRODUCTION.

ADDENDUM TO PROPOSAL 581.

1. INTRODUCTION.

Our Proposal #581 contains a detailed discussion on the construction of a polarized proton beam at FNAL and its use for:

- i) measurements of the pp total cross-section difference ΔG_L^{Tot} in definite initial longitudinal spin states,
- ii) measurements of asymmetries in inclusive π^\pm production.

In this note we consider the possibility of exploiting the proposed facility for performing asymmetry measurements in pp elastic scattering at very small $/t/$ values and in inclusive production of unstable neutral particles (Λ^0, K^0, π^0).

These experiments seem compatible with the set-up proposed for i) and ii); however they involve different degrees of complexity and should be considered as three separate items:

- a) The polarization measurement in pp elastic scattering at small angles can be performed by using the hodoscope set-up and the forward spectrometer foreseen for experiments i) and ii), with some additional equipment to improve the resolution in the scattering angle and, possibly, to implement the measurement of the recoil energy.
- b) The asymmetry measurements in inclusive production of $\Lambda^0(K^0)$ can be performed using the set-up for experiment ii) with the addition of a multiplicity-selective trigger system for tagging V_s^0 within a specified decay path.
- c) The measurement of the asymmetry in π^0 inclusive production can be done with an assembly of lead-glass photon detectors and hodoscopes placed in front of the forward spectrometer magnet used for the π^\pm inclusive experiment, without in-

terfering with the corresponding solid angle of detection.

Experiments a) and b) involve the use of a relatively simple additional equipment, while experiment c) requires considerable technical and financial effort: it could, however, run simultaneously with the charged pion production experiment without interference, while the compatibility with i) and ii) of the low $/t/$ elastic scattering and $\Lambda^0(K^0)$ production measurements has to be verified in detail both from the point of view of simultaneous running and trigger configuration.

2. POLARIZATION AT SMALL $/t/$ VALUES ($10^{-3} \leq /t/ \leq 10^{-1} \text{ GeV}^2$).

The classical method using a polarized target for the measurement of the polarization parameter in p - p elastic scattering is not suitable at very small $/t/$ values, owing to the missing information from the slow recoil (either stopping in the target or being trapped by the polarized-target-holding magnetic field). A measurement relying on the forward scattered particle detection only, would be seriously contaminated by the background due to Coulomb scattering from the complex nuclei in the target and the Fermi motion of bound nucleons.

Making use of the polarized proton beam and a liquid hydrogen target, such a measurement could be performed in cleaner experimental conditions, by determining with high precision the scattering angle; the use of a recoil-sensitive target can also be envisaged.

With this experiment, the p-p amplitude structure, that can be obtained at $t=0$ from the spin dependence of total cross-section measurements, can be further studied at small $/t/$ values. ⁽²⁾

In the region $/t/ \leq 5 \times 10^{-2} \text{ GeV}^2$, where purely hadronic spin flip amplitudes are negligible, sizeable polarization can be produced in p-p elastic scattering by interference of the hadronic non flip amplitude with an electromagnetic flip one (due to the charge-magnetic moment interaction of the two protons). Such effect can be accurately calculated with a minimum of theoretical assumptions⁽³⁾ (Fig.1) and its measurement might be used also to check the beam polarization as evaluated via a Monte Carlo computation.

A better understanding of the role of electromagnetic helicity flip effects outside the interference region, which can be relevant in the interpretation of the measured polarization at intermediate $/t/$ -values,⁽⁴⁾ should come from a complete measurements in the region $10^{-3} \leq /t/ \leq 10^{-1} \text{ GeV}^2$.

Scattering events in the angular range of interest can be selected by using a high resolution telescope of proportional chambers and hodoscopes connected to a fast processor system⁽⁵⁾ which rejects "transmitted" tracks, with the result of reducing the effective beam divergence to the angular resolution of the chamber telescope. The principle of operation of such a system is sketched in Fig.2, for an incident momentum of 300 GeV/c.

The details of the experimental set-up are shown in Fig.3 and the size and resolution of the detectors are given in Table 1. Vacuum pipes or He bags are used to minimize the multiple scattering contribution to the overall angular resolution (~ 0.03 mrad at 300 GeV/c). Chambers PC5 and PC6 are used to select particles originating from the target with momenta close to the beam momentum.

The proportional chambers are strobed by a trigger requiring one and only one particle in hodoscopes H1-3 and no signal from the anticoincidence counters A1-4.

From the measured scattering angle θ and the momentum p , the momentum transfer could be determined with a precision

$$\Delta t/t \sim (\Delta p_0/p_0) + (\Delta p/p) + 2(\Delta \theta/\theta) \quad (1)$$

At 300 GeV/c beam momentum, with $\Delta p_0/p_0 \sim \pm 0.05$, $\Delta p/p \sim \pm 0.02$ and $\Delta \theta \sim 0.03$ mrad⁽⁺⁾

$$\Delta t/t \sim 0.07 + 0.02xt^{-1/2} \quad (2)$$

With a 50 cm long liquid hydrogen target (giving a multiple scattering contribution of less than 0.01 mrad to the scattering angle error) and a beam polarization $P_b \sim 50\%$, the expected precision in the measured polarization is typically $\Delta P \sim 0.5\%$ at $t = 0.003 \pm 0.001$ GeV² for a total number of incident polarized protons $N_p = 4 \times 10^9$, in the hypothesis of a background-to-signal ratio $B/S \leq 1$.

The possibility of frequent polarization flipping without change in the beam direction, should eliminate most of the systematic errors.

An important improvement in removing residual asymmetries as well as in t -resolution and in selectivity for elastic events can be obtained by using a recoil-sensitive scintillating target and correlating the scattering angle with the recoil kinetic energy T , as measured by pulse height (and shape) in the scintillator, according to

$$T = p^2 \theta^2 / 2m \quad (3)$$

The advantages of this method should compensate for

(+) With a telescope of proportional chambers of 1 mm pitch, arranged in pairs of parallel wire planes, staggered by 0.5 mm and placed at a distance of ~ 20 m.

the presence of background from carbon nuclei in the scintillator, which, on the basis of condition (3), could be distinguished from the true elastic events on free protons.

A prototype of this target is now under test, to determine the recoil energy resolution and the rate capability.

If satisfactory this detector could also be used as a polarimeter to monitor the beam: operating in association with a set of three fine-grained hodoscopes, a 4 cm. long scintillating target could be tuned to select elastic pp events in a convenient t range (for instance $5 \cdot 10^{-3} - 2 \cdot 10^{-2} \text{ GeV}^2$) and to provide automatically a measurement of the left-right asymmetry: by this method a precision

$\frac{\Delta p_L}{p_L} \approx \pm 10\%$ can be obtained with $3 \cdot 10^9$ polarized protons for $P_b \sim 50\%$.

Ideal locations for such a polarimeter would be either some straight section of the beam, where the polarization is transverse (at all energies) or a position down-stream the whole set-up, with some magnet to keep the non-interacting beam polarization transverse to its direction.

3. ASYMMETRY MEASUREMENTS IN $p+p \rightarrow \begin{cases} \Lambda^0 \\ K^0 \\ \pi^0 \end{cases} + \text{Anything.}$

Important spin dependence has been found in these reactions at ANL, CERN, and FNAL⁽⁶⁾; these processes can be further studied by taking advantage of the proposed polarized beam facility, in order to understand the relevance of constituent scattering mechanisms, particularly at high p_T .⁽⁷⁾

The investigation can be extended also to the study of these reactions with both beam and target protons polarized; in particular the polarization - analyzing properties of the $\Lambda^0 \rightarrow p\pi$ decay make the process $p_{\uparrow}^+ p_{\uparrow(t)} \rightarrow \Lambda_{(t)}^0 X^{++}$ a suitable reaction also for the study of higher - order spin tensors.

3.1. The $p+p \rightarrow \Lambda^0(K^0) + X^{++}$ process.

The set-up proposed for the study of inclusive π^\pm production seems compatible also for the $\Lambda^0(K^0)$ inclusive production measurements and probably a limited sample of inclusive Λ^0 could even be obtained as a by-product of the former experiment (by looking for the associated high energy protons).

A multiplicity-selective trigger with Cerenkov counters, FC1 and FC2, made of lucite foils, and proportional chambers, FCH1-3, can be used according to the scheme of Fig.4: the multiplicities of fast charged particles, measured with these detectors at the beginning (N_1) and at the end (N_2) of the accepted $\Lambda^0(K^0)$ decay path, are analyzed according to the conditions $N_2 \geq N_1 + 2$ and $N_3 \geq 2$ in a fast processor.

The trigger can be completed by a coincidence with the gas threshold Čerenkov counters \check{C}_1 and \check{C}_2 , tuned to discriminate pions from protons up to 100 GeV/c for a beam momentum of 300 GeV/c (more than 90% of the π^- from the Λ^0 decay have momenta smaller than 100 GeV/c).

For the layout presented in Fig.12 of Proposal #581 the geometrical efficiency of the apparatus for Λ^0 has been calculated; using a parametrization of the measured production cross-section⁽⁸⁾, the expected statistical error in the asymmetry ΔA has been evaluated under the following experimental conditions: integrated number of polarized protons $N_p = 10^{12}$, 1 m long hydrogen target, 50% beam polarization, background-to-signal ratio $B/S=1$, $\Delta x = \pm 0.02$ and $\Delta p_T^2 = \pm 0.1 \text{ GeV}^2/c^2$.

The results (Fig.5) are given in form of acceptance curves in the phase space $x - p_T^2$ for different values of the estimated error $\Delta A = 0.01, 0.05, 0.1$; an accuracy between

0.01 and 0.05 is possible in the range $0.3 \leq x \leq 0.9$ and $0 \leq p_T \leq 1. \text{ GeV/c}$.

The acceptance for this experiment can be extended to larger values of p_T ($\geq 2 \text{ GeV/c}$), by using a SCM 105 magnet (14'x82'x47', 1.5 Tm bending power) in place of BM 109.

3.2. The $p+p \rightarrow \pi^0 + X^{++}$ process.

This reaction can be measured simultaneously with π^\pm production experiment by installing two identical lead - glass γ -detectors on both sides of the polarized proton beam at the front of magnet BM 109 (see Fig.12 of Proposal 581).

In order to detect π^0 s produced in the central region with $\Delta x = \pm 0.05$ it is necessary to cover an angular region in the laboratory from 55 to 110 mrad which guarantees full acceptance for π^0 s with $p_T \approx 2 \text{ GeV/c}$. The required angular resolution to separate the two γ -rays from π^0 s with p_T up to 3 GeV/c (corresponding to $\sim 40 \text{ GeV/c}$ in the lab. system) is of about 7 mrad.

At a distance of approximately 12 m from the target (Fig. 6), taking $\Delta\phi/2\pi \approx 0.25$, each detector would consist of about 50 counters with lead-glass cells of dimensions $10 \times 10 \times 30 \text{ cm}^3$.

Under the assumption of about 40% efficiency for the detection of two γ -rays by two separate cells and using measured π^0 production cross-sections⁽⁹⁾ the rates presented in Table 2 are obtained for a beam intensity of 10^7 /pulse and a liquid hydrogen target 1 m long, with $\Delta x = 0.1$ and $\Delta p_T^2 = 0.1 (\text{GeV/c})^2$. The last column presents the statistical error on the asymmetry for the running time foreseen for the π^\pm experiment (300 hours).

CONCLUSIONS:

The measurements discussed in this note match the experimental apparatus described in Proposal 581 and have a large degree of compatibility with the experiments proposed; they can extend the range of results on spin effects that can be obtained with the proposed polarized beam facility at Fermilab.

The measurement of the polarization in p-p elastic scattering at small $/t/$ has some priority, owing to the possibility of obtaining also a calibration of the beam polarization.

In the case of measurements with both beam and target protons polarized, the statistical error will be about 20 times larger than those above presented, due to the small number of free protons contained in the target and the low effective polarization. However, even with a statistical error of some percent at p_T close to 1 GeV/c, useful indications on higher-order spin correlations could be obtained.

REFERENCES.

- (1) I.P.Auer et al. (ANL, LAPP, LBL, Rice University and Trieste), Construction of polarized beams and an enriched antiproton beam facility in the Meson Laboratory and experiments using such a facility, Fermilab Proposal 581 (January 27, 1978)
- (2) C.Bourrely et al., Nucl. Phys. B77, 386 (1974).
W.Grein and P.Kroll, Dispersion theoretic analysis of the proton-proton helicity amplitudes at $t=0$, University of Wuppertal preprint WUB 77-6 (September 1977).
- (3) N.H.Buttimore et al., Spin-dependent phenomena induced by electromagnetic-hadronic interference at high energies, Westfield College preprint (May 1977).
- (4) C.Bourrely and J.Soffer, Note on the size of the Coulomb-nuclear interference polarization in hadronic reactions at high energy and large momentum transfer, Centre de Physique Theorique note 77/P.899, Marseille 1977.
- (5) A.A.Derevshehikov et al., Nucl. Instr. Meth. 108, 381 (1973)
- (6) CERN-LAPP-Oxford Collaboration, Memorandum to EEC, CERN/PSC/76-15, PSC/M8.
G.Bunce et al., Phys. Rev. Lett. 36, 1113 (1976)
- (7) C.K.Chen, The significance of high energy spin effects in constituents pictures, ANL/HEP/CP 77-46.
R.D.Field, Some remarks about large p_T spin effects, in Symposium on experiments using enriched antiproton, polarized proton and polarized antiproton beams at Fermilab energies (Ed.: A.Yokosawa) Argonne, June 10, 1977, ANL/HEP/CP 77-45.
- (8) T.Devlin et al., Nucl. Phys. 123, 1 (1977)
K.Heller et al., Phys. Rev. D 16, 2737 (1977)
P.Skubic, University of Michigan preprint UM/HE/77-32 (1977)
- (9) D.C.Carey et al., Phys. Rev. D 14, 1196 (1976)

Table 1

Detectors	Dimensions, $x \times y$ (mm ²)	Number of planes	Pitch (mm)	Total number of wires	Number of PM
PC1	50 × 50	2x,2y	1	200	
PC2	50 × 50	2x,2y	1	200	
PC3	50 × 50	2x,2y	1	200	
PC4	100 × 100	2x,2y	1	400	
PC5	500 × 500	x,y	2	500	
PC6	500 × 500	x,y	2	500	
H1	50 × 50	x,y	2		50
H2	26 × 26	x,y	2		26
H3	100 × 100	x,y	2		100

Table 2

$p_{\perp}^2 ((\text{GeV}/c)^2)$	$f (\text{mb}/\text{GeV}^2/c^3)$	n/pulse	$\Delta A (\%)$
1	2.8×10^{-1}	42	0.15
2	4.9×10^{-2}	7.4	0.35
4	4.2×10^{-3}	0.6	1.2
6	7.0×10^{-4}	0.1	2.9
8	1.6×10^{-4}	0.02	6.2
9	8.9×10^{-5}	0.01	8.2

FIGURE CAPTIONS:

- Fig.1 - Polarization in small-angle elastic scattering p-p at 300 GeV/c.
- Fig.2 - Selection of small-angle p-p scattering events:
 a) schematic set-up,
 b) angular distribution at 300 GeV/c,
 c) rejection-efficiency vs. scattering angle.
- Fig.3 - Set-up for the polarization measurement in the small-angle p-p elastic scattering at 300 GeV/c.
- Fig.4 - Trigger for $\Lambda^0(K^0)$ inclusive production.
- Fig.5 - $x-p_T^2$ plots for the expected accuracy in the asymmetry of inclusive Λ^0 production on protons by 300 GeV/c polarized protons; BM 109 used in the set-up of fig. 12, ref.(1).
- Fig.6 - Set-up for the asymmetry measurement in π^0 inclusive production on protons by 300 GeV/c polarized protons; schematic layout of the detector.

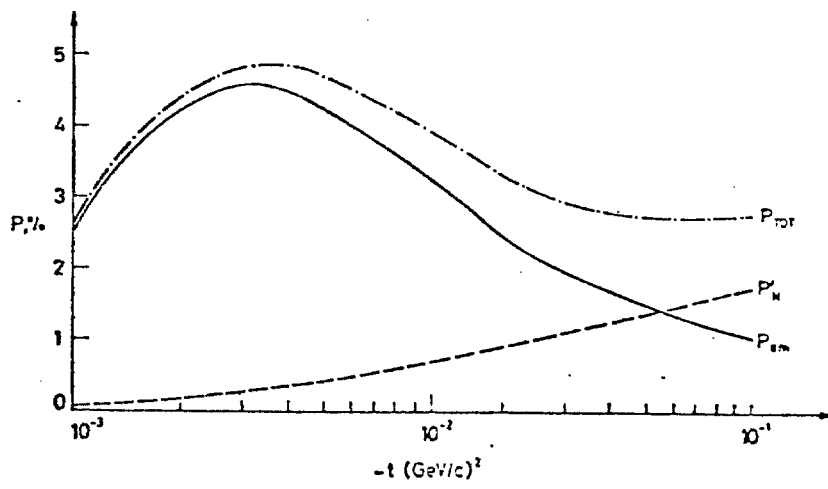
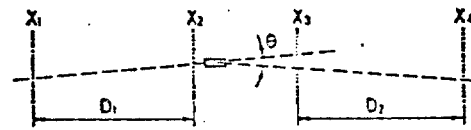


Fig.1



$$\theta = C_1 X_1 + C_2 X_2 + C_3 X_3 + C_4 X_4 + C_5$$

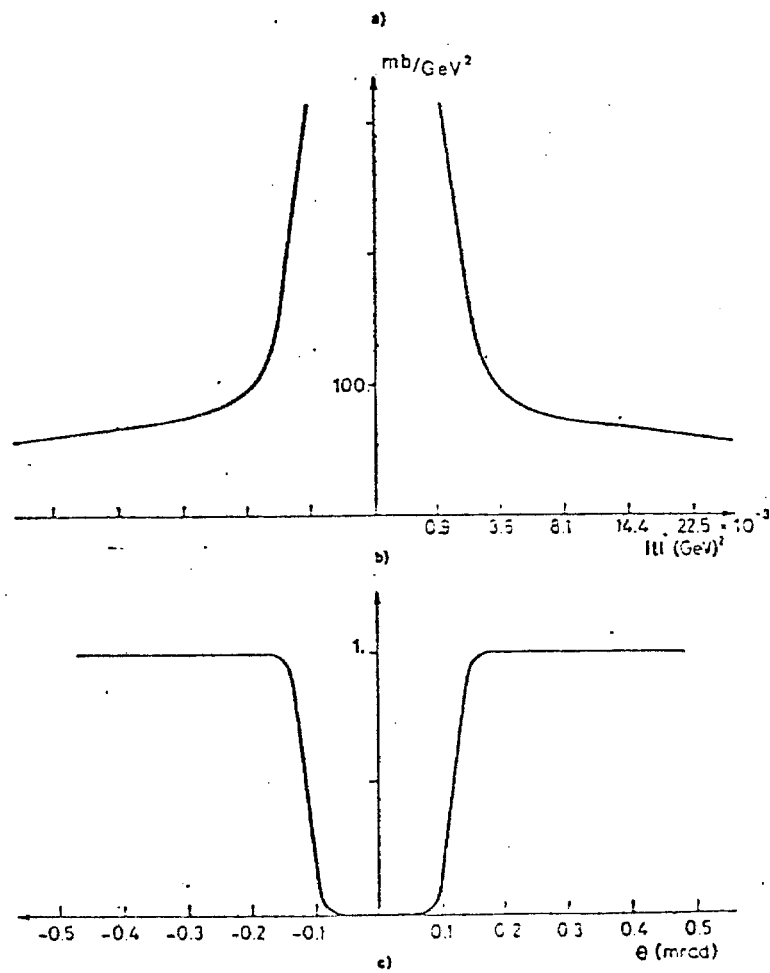


Fig.2

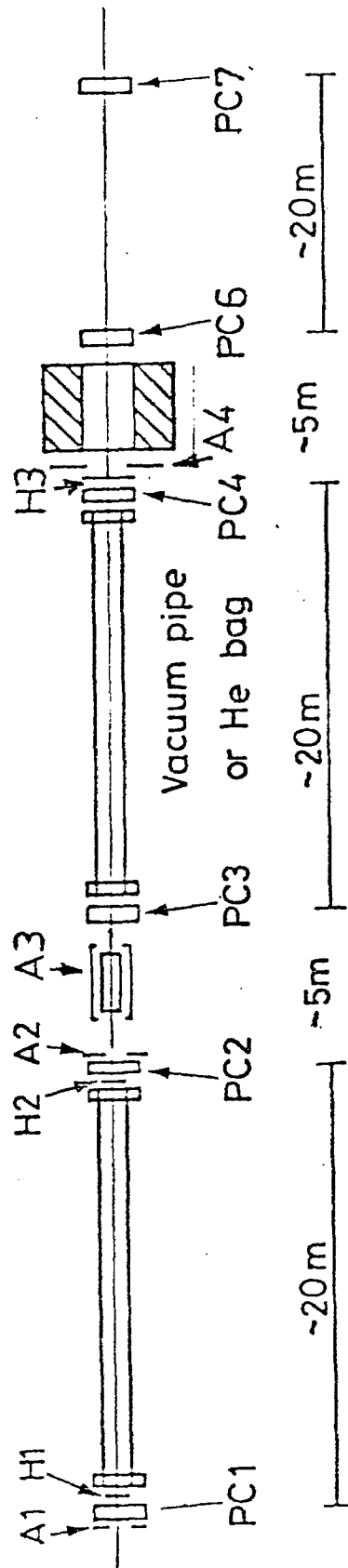


Fig. 3

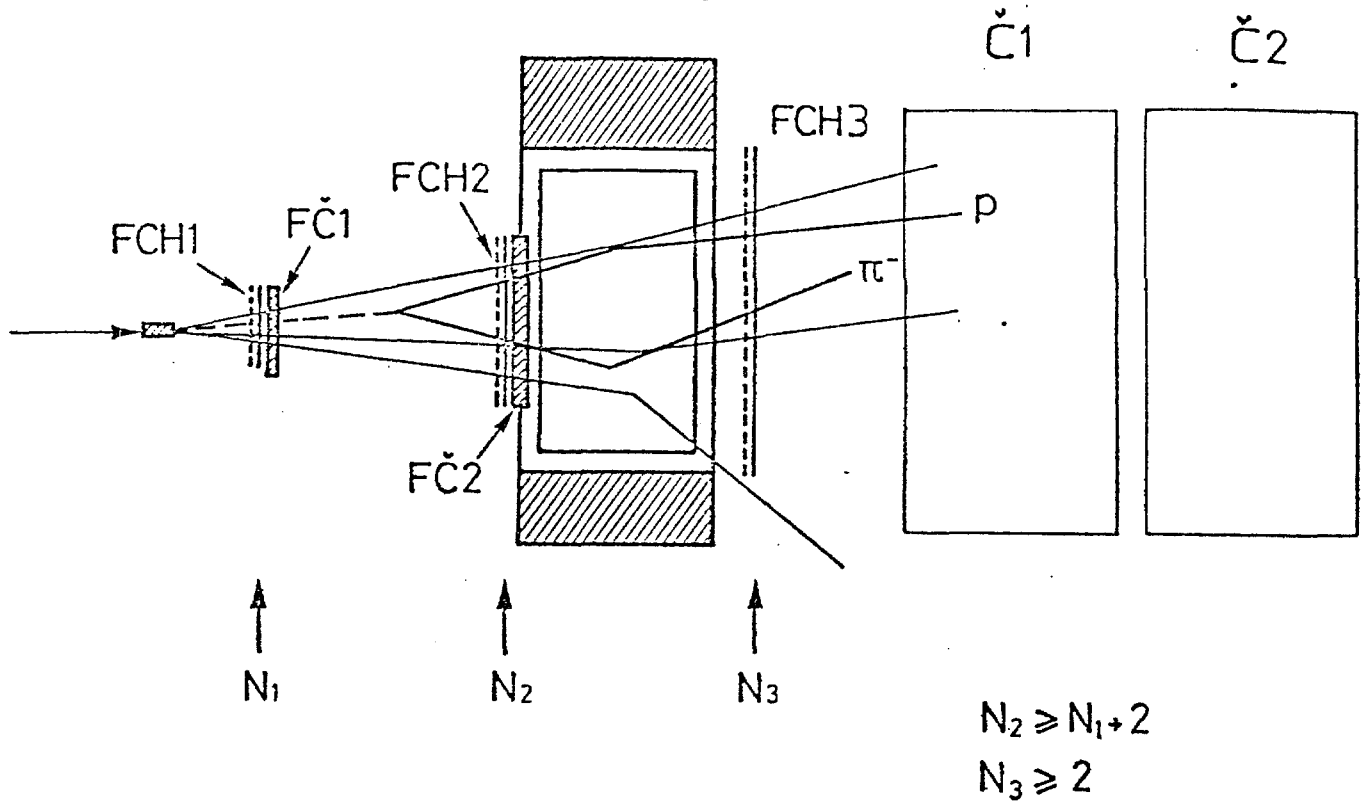


Fig.4

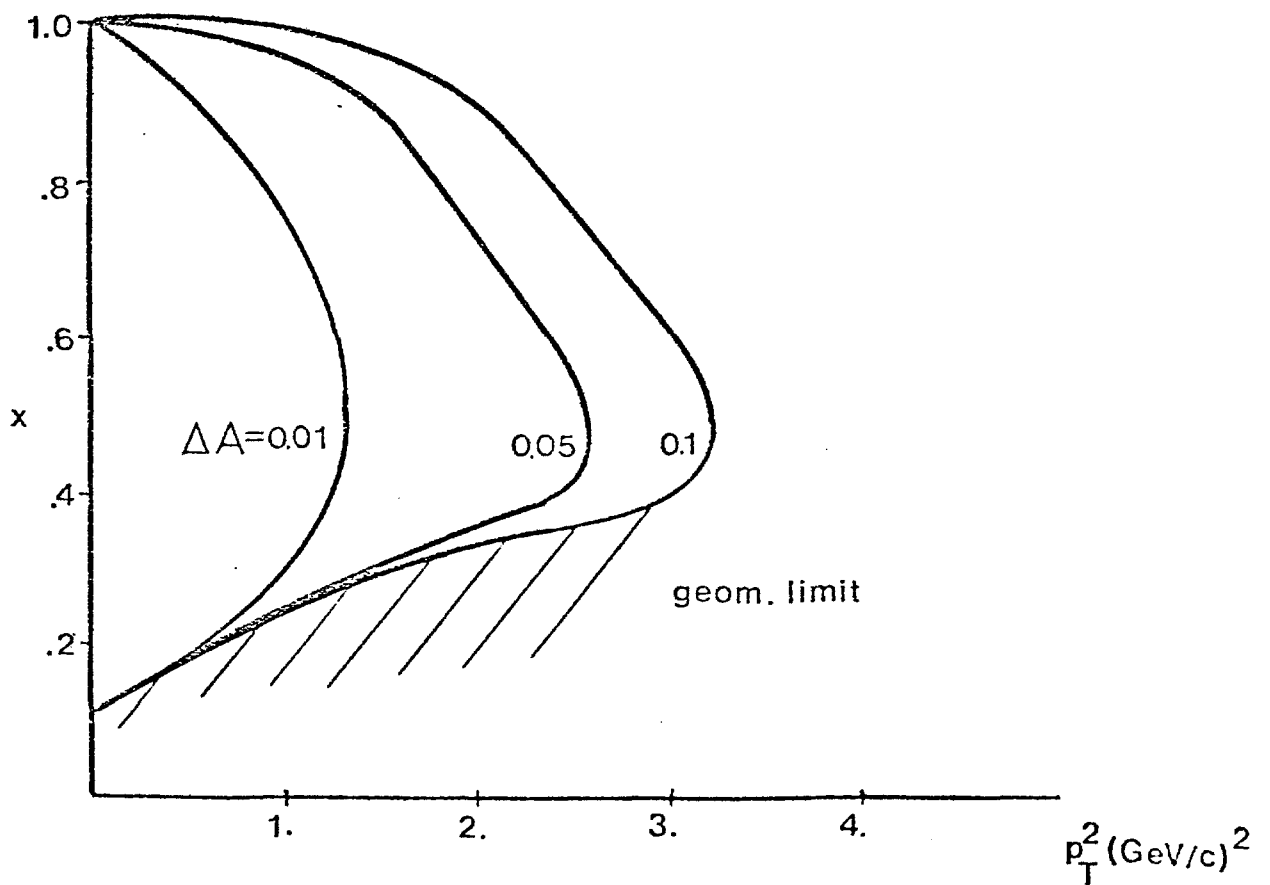
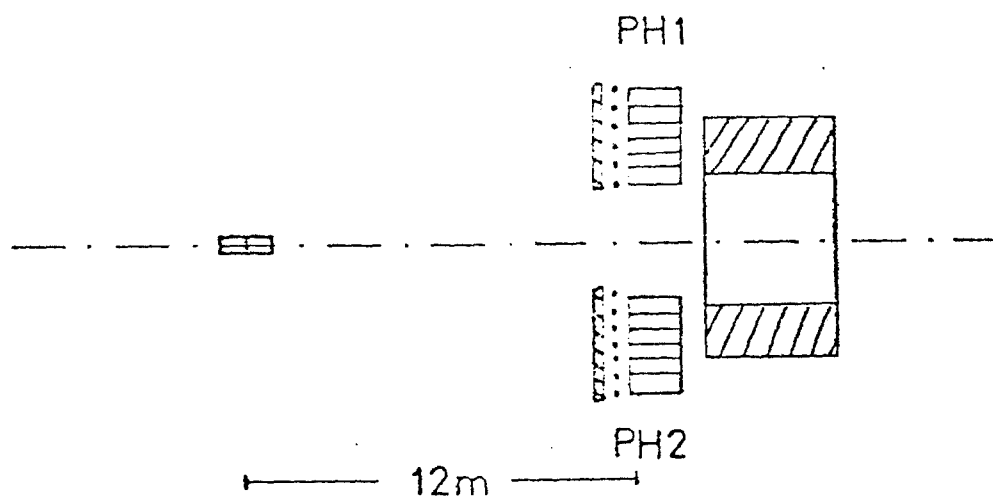
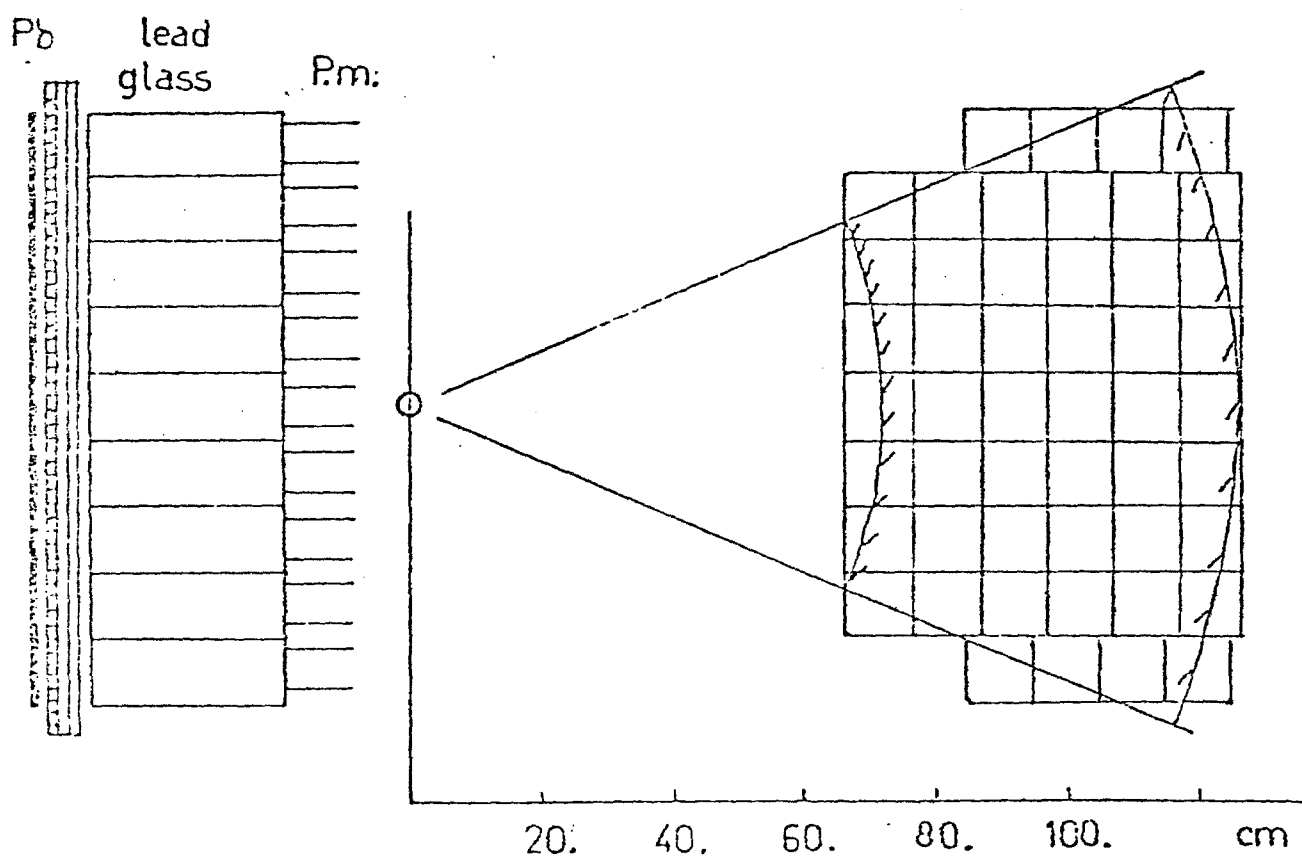


Fig.5



a)



b)

Fig.6

28 September 1979

SECOND ADDENDUM TO PROPOSAL 581**FERMILAB**

OCT 10 1979

LIBRARYConstruction of the Polarized-Beam Facility in the
Meson Laboratory and Experiments Using Such a Facility

- I. P. Auer, E. Colton, R. Ditzler, D. Hill, H. Spinka,
G. Theodosiou, K. Toshioka, D. Underwood, R. Wagner
and A. Yokosawa, Argonne National Laboratory, Argonne, IL.
- Y. Hemmi, R. Kikuchi, K. Miyake, T. Nakamura, and
N. Tamura*, Kyoto University, Kyoto, Japan.
- K. Kuroda, A. Michalowicz, and D. Perret-Gallix, LAPP,
Annecy, France.
- G. Shapiro, Lawrence Berkeley Laboratory, University of
California, Berkeley, California.
- H. E. Miettinen, T. A. Mulera, G. S. Mutchler, G. C. Phillips,
and J. B. Roberts, Rice University, Houston, Texas.
- R. Birsá, F. Bradamante, M. Giorgi, A. Penzo, P. Schiavon,
and A. Villari, INFN. Sezione di Trieste, Trieste, Italy.

We discuss the proposal to construct the polarized-beam facility as a joint project of Fermilab and Argonne National Laboratory. We include a brief description of the physics with the polarized beam which summarizes our previous addendum submitted January 25, 1979.

* N. Tamura is presently at Argonne National Laboratory.

I. BRIEF PHYSICS SUMMARY

The experiments we have proposed in P-581 and Addendum (January 25, 1979) are directed toward studying spin effects in quark-quark scattering. There is a rich field of future experiments to measure the spin distribution functions for sea quarks and gluons that could be pursued after the initial measurements.

Specifically we have proposed to

- 1) Measure pion production at large x and small p_{\perp} in order to gain information on low- p_{\perp} quark scattering, and in order to develop fast beam polarimeter,
- 2) Measure the total cross section in pure spin states in order to determine the amplitudes involved in the rising total cross section, and
- 3) Measure π^0 inclusive production (and eventually jet production as proposed in P-582) in order to study the basic interactions, in particular to see to what extent the spin structure of interactions resembles single vector gluon exchange between spin 1/2 quarks in various kinematic regions.

Future experiments could include the following:

- 1) Studies of inclusive production using a polarized beam and nuclear target would provide information about the space-time structure of interactions.

- 2) Inclusive Lambda production where the incoming beam is polarized and the lambda is analyzed could be used for determining gluon spin distribution functions.
- 3) Di-muon production with a longitudinally polarized proton beam on a longitudinally polarized target could be used to measure the spin distribution functions for sea quarks.
- 4) Di-muon production with a transversely polarized beam and an unpolarized target could be used to determine gluon spin distribution functions.

Finally it should be noted that many unexpected phenomena have been revealed in experiments with polarized beams such as large spin effects at large p_{\perp} and in total cross sections measured at Argonne.

Compatibility With Other Experiments

When not used for polarized protons, the beamline and experimental area could be used for experiments requiring protons or pions.

Tevatron Option

Operation of the polarized beam with the Tevatron would enable us to extend our studies over a largerrange in \sqrt{s} and p_{\perp} as shown in Fig. 2. Predicted intensities with 400- and 1000-GeV/c targetting are shown in Fig. 3. There is a large increase in the flux of polarized \bar{p} 's and high-momentum protons from 1000-GeV/c operation. If the beam were reconfigured and lengthened by 50% (long beam in Fig. 3), then experiments would be possible up to 750 GeV/c.

II. DESCRIPTION OF THE PROPOSED PLAN

In the recent workshop on TEV program at meson area (August 13-14, 1979), we discussed the construction of a polarized proton (or antiproton) beam in the M2 line. The optimum location of the polarized-beam line within the M2 area is still under study, but the cost estimates are being made for the simplest beam design suggested by mesonlab staff.

The proposed beam line as shown in Fig. 1 would provide polarized protons up to 400 GeV/c, although the target box would be built to accommodate 1000 GeV/c. The beam transport system utilizing existing dipoles would use about 2 MW of power. Total liquid He use for the beam line including the snake would be less than 40 ℓ /hour.

The plan is for Argonne to take responsibility for the technical components including:

- i) Beam instrumentation
- ii) Construction of superconducting quadrupoles and helium distribution system; photograph of prototype quad is attached
- iii) Regapping shims, rework, rigging etc. for BM-105 magnets and supplies

Fermilab would assume the main responsibility for the beam line and experimental area including:

- i) Civil construction including buildings
- ii) Power distribution
- iii) Water distribution
- iv) Construction and installation of target box and shielding
- v) Vacuum system

Existing materials and equipment either at Fermilab or Argonne would be utilized whenever possible. The most expensive equipment in this category is the BM-105 magnets and power supplies. As a letter from DOE to Dr. W. E. Wallenmeyer dated September 13, 1979 indicates, the units identified for the polarized beam are to be held in reserve at ANL pending clarification of the status of this project. The original 1963 purchase price was approximately \$1.3M. Sufficient steel is on hand to provide the target-box shielding. It is currently being used in E-613. Adequate concrete shielding also exists.

Detailed cost estimates will be available for the November PAC meeting. We are also making an estimate of the additional expense if we place the beam line in a proposed M2 West (M2') branch.

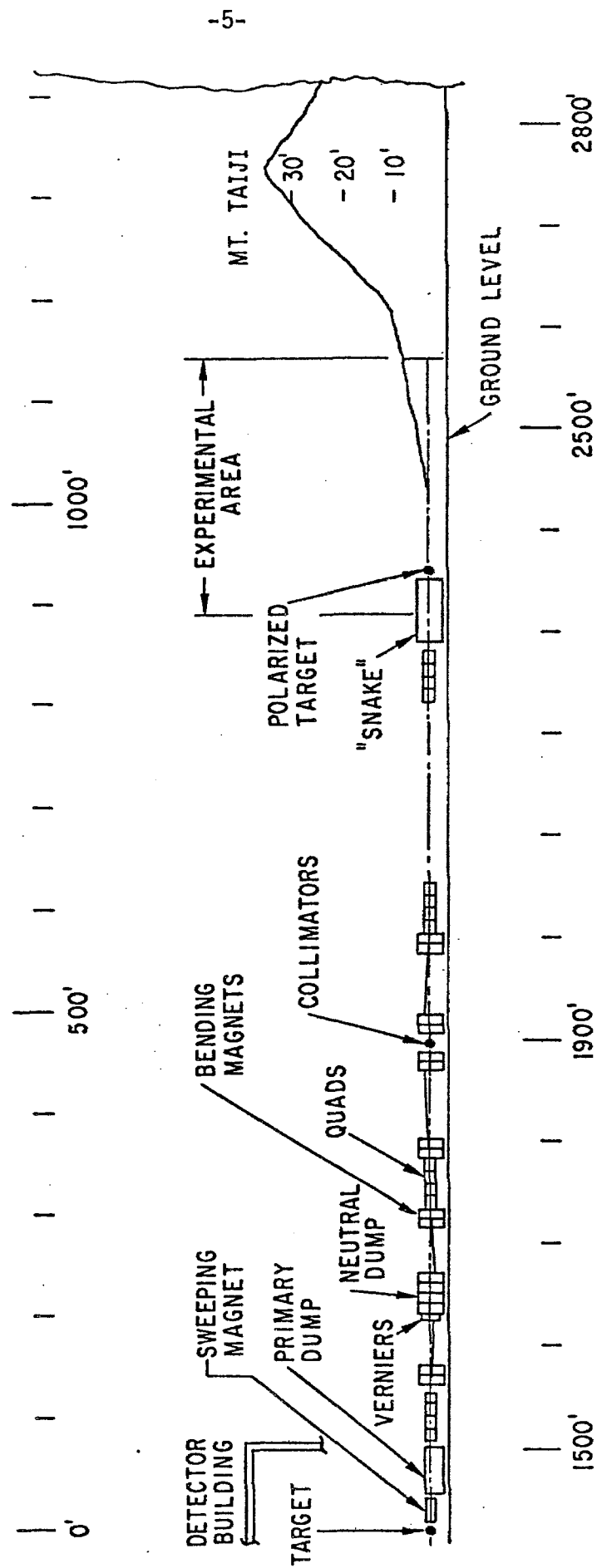


Fig. 1 The overall view of the proposed polarized-beam line.

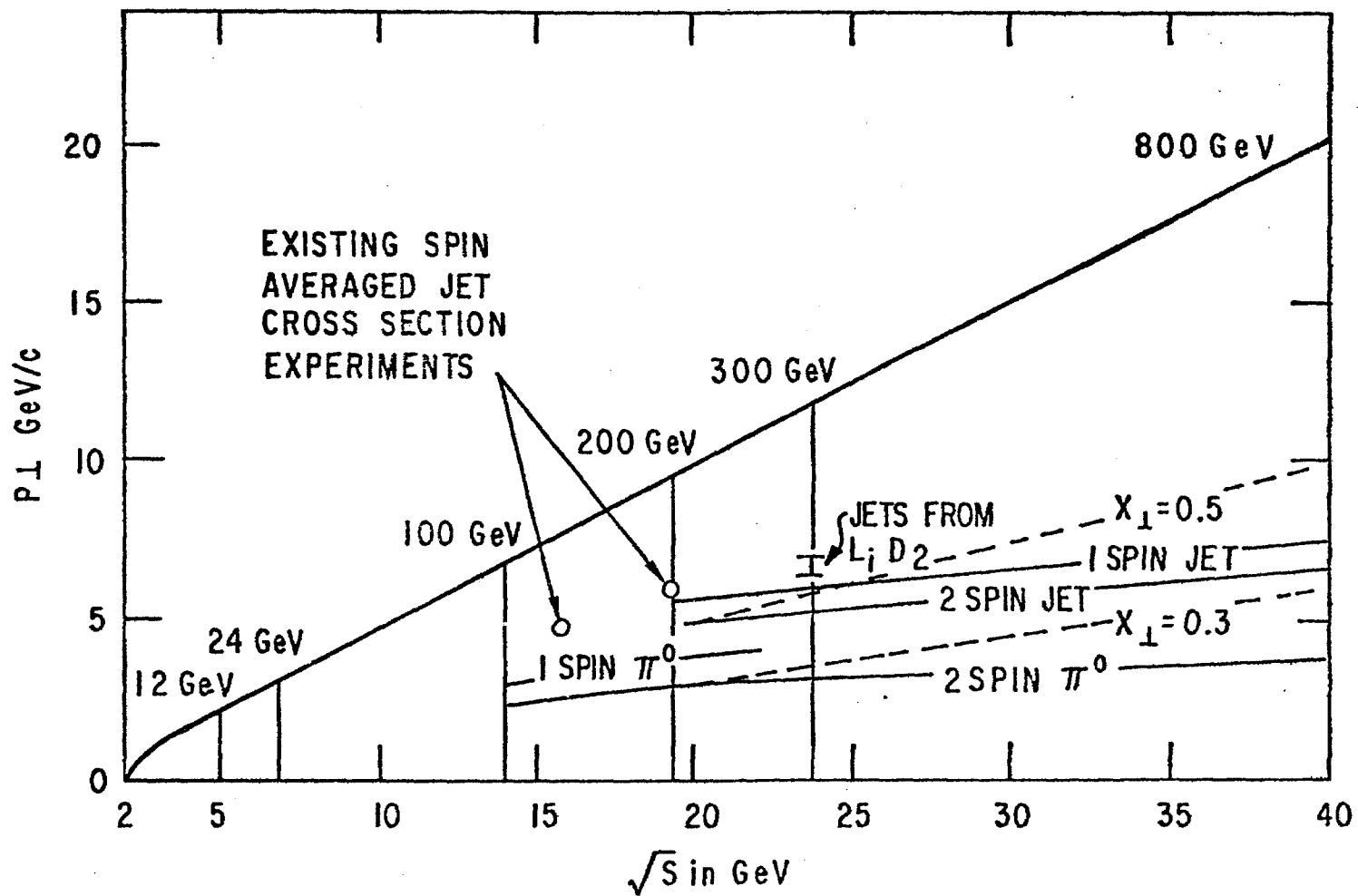


Fig. 2 Maximum p_T attainable in indicated experiments. Kinematic limits for various polarized-beam energies are indicated by upper solid line.

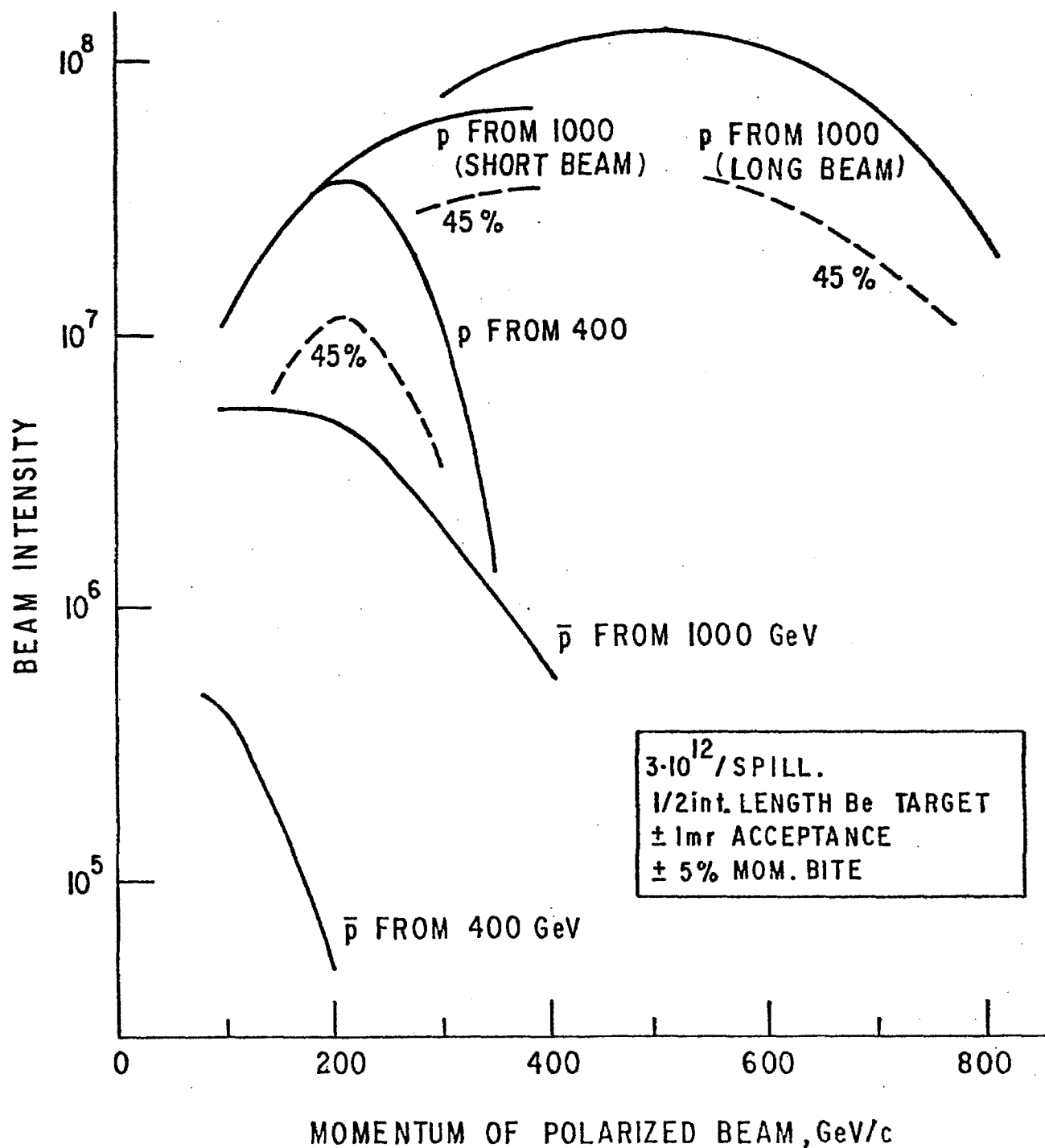
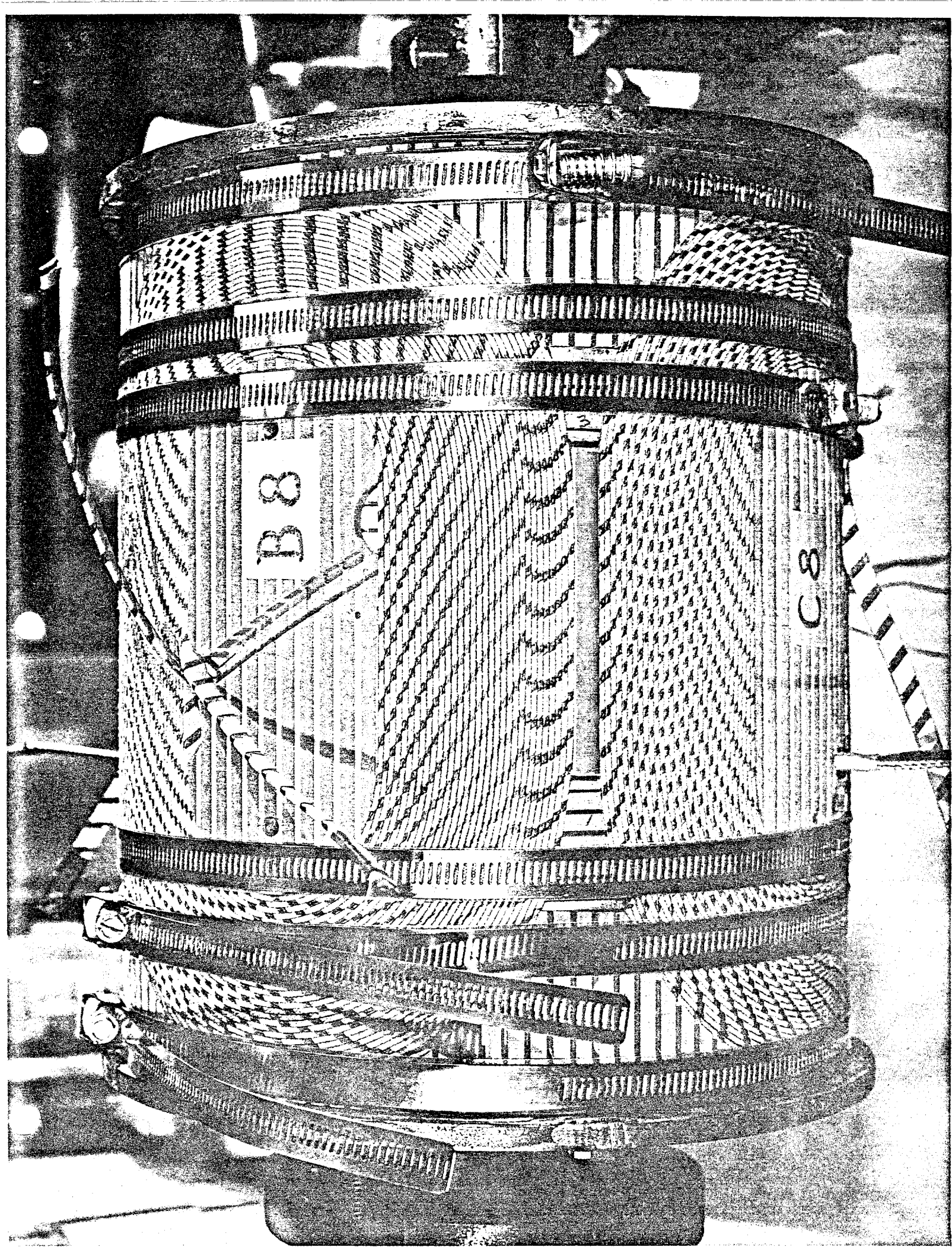


Fig. 3 Predicted intensities with 400-and 1000-GeV/c targetting.



ADDENDUM TO PROPOSAL 581

CONSTRUCTION OF A POLARIZED BEAM FACILITY
IN THE MESON LABORATORY AND EXPERIMENTS USING SUCH A FACILITY

- I. P. Auer, E. Colton, R. Ditzler, D. Hill, H. Spinka
G. Theodosiou, K. Toshioka, D. Underwood, R. Wagner
and A. Yokosawa, Argonne National Laboratory,
Argonne, IL.
- A. Michalowicz, D. Perrett-Gallix, and K. Kuroda,
LAPP, Annecy, France.
- Y. Hemmi, R. Kikuchi, K. Miyake, T. Nakamura,
and N. Tamura*, Kyoto University, Kyoto, Japan.
- G. Shapiro, Lawrence Berkeley Laboratory, University
of California, Berkeley, California.
- H. E. Miettinen, T. A. Mulera, G. S. Mutchler,
G. C. Phillips, and J. B. Roberts, Rice University,
Houston, Texas
- R. Birsa, F. Bradamante, M. Budini, M. Giorgi, A. Penzo,
P. Schiavon, and A. Vascotto, INFN. Sezione di Trieste,
Trieste, Italy.

* N. Tamura presently at Argonne National Laboratory.

CONTENTS

	Page
I. Physics Goals	1
II. Main Features of Polarized Beam	6
III. Description of Proposed Experiments	
<u>Phase 1</u> High p_{\perp} Physics	8
<u>Phase 2</u> $\Delta\sigma_L^{\text{Tot}}$ Measurements	15
<u>Phase 3</u> Hadron Production at Large x	16
References	17
Figures 1 through 5	19-23
Appendix I	24
Appendix Figures 1 and 2	27-28

(ii)

SUMMARY

This document updates several sections of proposal 581 (revised May 1, 1978). We present the latest beam design and give a new list of proposed measurements, placing an emphasis on high p_{\perp} physics.

The running time requested is:

Beam tuning and determination of beam polarization	200 hours
Phase 1 High p_{\perp} physics	1000 hours
Phase 2 $\Delta\sigma_L^{\text{Tot}}$ measurements	220 hours
Phase 3 Hadron production at large x	250 hours

I. PHYSICS GOALS

In our proposals 581 and 582, we have discussed various experiments that could be performed using a polarized beam. In this addendum, we propose a simple study of spin effects which could be most crucial in understanding the interactions of the constituents of hadrons.

i) High p_{\perp} Physics

A recent SLAC experiment¹ measuring deep inelastic scattering of longitudinally polarized electrons on longitudinally polarized protons reports an asymmetry of $.60 \pm .10$ for $0.3 \leq x_F \leq 0.5$. Comparison of this result with the Bjorken sum rule and models of proton spin structure implies that proton spin is communicated to the constituent quarks. Thus, spin dependence in quark-quark collisions can be inferred from the measurements of spin dependence in proton-proton collisions.

At Fermilab and the CERN-ISR there is currently an extensive ongoing program to study high $-P_{\perp}$ physics. The motivation for this program is quite straightforward - by going to large $-P_{\perp}$ one hopes to observe fundamental short-distance interactions between hadronic constituents. There exists a hope that these interactions can be understood in the framework of a perturbation theory based on quantum chromodynamics (QCD). This current belief needs to be systematically tested by quantitative experiments.

The QCD phenomenology is defined in terms of the interactions of spin- $\frac{1}{2}$ quarks and spin-1 gluons and specific calculations show several spin-related effects,² magnitude and sign of which depend on the basic assumptions of the theory.

As a first-round experiment, we therefore propose to measure the asymmetry in large $-p_{\perp} \pi^0$ production from proton-proton collisions using a polarized beam both with and without a polarized target. The study can be continued using a high $-p_{\perp}$ jet-event detector as described in proposal 582.

Single-Spin Asymmetries

Predictions of asymmetries in large $-p_{\perp}$ hadron production in p-p scattering are available from QCD calculations as well as constituent interchange models. The experimental measurement of inclusive one-spin asymmetries provides a test for the hard-scattering model.^{3,4} If large single-spin effects are observed, the interaction cannot be represented by a 1st-order QCD process.

There is also an experimental interest in making the measurement. A sizeable asymmetry effect is observed at CERN in π^0 production by 24-GeV/c protons at $x \sim 0$ and high p_{\perp} .⁵ Large polarization (on the order of $\sim 30\%$) is also observed in inclusive Λ^0 production at p_{\perp} of 1 to 2 GeV/c by the interaction of 20- to 400-GeV/c protons on an unpolarized target.⁶

A-dependence

The single-spin measurements using p-p collisions can be extended to a study of the A-dependence of large $-p_{\perp}$ asymmetries using polarized beams on nuclear targets. For high s , the inclusive single hadron-production cross section¹⁰⁻¹² has an anomalous A-dependence.

If we write

$$\sigma_{inc} = I_i(p_{\perp}) A^{\alpha_i(p_{\perp})} ,$$

where i refers to a kind of outgoing hadrons, then $p_{\perp} = 0$, $\alpha_i \approx 0.7$ as expected due to nuclear shielding effects. However, the α value rises monotonically up to $p_{\perp} \approx 4$ to 5 GeV/c, where α_i values of 1.13 to 1.26 are found depending on the kind of outgoing hadrons. If the proton scattering on the nuclear targets were incoherent, one would expect $\alpha_i = 1.0$ and the polarization would vanish. The experimental data seem to indicate some kind of constructive coherent scattering. In this case the polarization measurement at large p_{\perp} may be important in clarifying this issue and understanding the space-time structure of hadronic interactions.

Two-Spin Asymmetries

Important two-spin asymmetries are predicted by QCD perturbation theory. Measurements of spin-spin asymmetries are therefore regarded as a test of the relevance of the QCD picture in large- p_{\perp} reactions. Using the SLAC results which indicate that the quarks are polarized inside a polarized nucleon, various theorists have phenomenologically estimated the spin-spin asymmetries at large P_T . Babcock, Monsay and Sivers³

have calculated the asymmetry A_{LL} using a hard-scattering model based on perturbative QCD, and positive asymmetries are predicted for inclusive π^0 production. Cheng and Fischbach⁷ predicted $A_{LL} \approx 0.12$ at $x_{\perp} = 0.3$ in agreement with an independent calculation of J. Ranft and G. Ranft.⁸ The asymmetry A_{NN} is predicted to be much smaller than A_{LL} .⁹

ii) Total-Cross Section Measurements With Polarized Beams and Targets

At ZGS energies, structures in the total cross-section difference in pure spin states in pp and pn system were found to be unexpectedly large at low energies.¹³ We propose to make similar measurements at Fermilab energies.

The most interesting energy region is where the rise in the total cross section takes place. This cross section can be described in terms of two s-channel helicity amplitudes, $\phi_1(0)$ and $\phi_3(0)$ ¹⁴, as

$$\sigma^{\text{Tot}} = (2\pi/k) \text{Im}[\phi_1(0) + \phi_3(0)] ,$$

where k is the center-of-mass momentum of the incident beam. The difference between total cross sections for parallel and anti-parallel in longitudinal spin states is given by

$$\Delta\sigma_L^{\text{Tot}} = (4\pi/k) \text{Im}[\phi_1(0) - \phi_3(0)] .$$

Thus a measurement of $\Delta\sigma_L^{\text{Tot}}$ combined with σ^{Tot} allows the separation of $\text{Im}\phi_1$ and $\text{Im}\phi_3$, and also the energy variation of the two amplitudes.

The study of $\Delta\sigma_L^{\text{Tot}}$ at 1 to 3 GeV/c has provided evidence for diproton resonances.¹⁵ The 6- and 12-GeV/c data gave evidence for an A_1 -like exchange trajectory.

In addition to the measurements of $\phi_1(0)$ and $\phi_3(0)$, it is interesting to measure $\phi_2(0)$, which comes from the difference between total cross sections for transverse spin states:

$$\Delta\sigma_T^{\text{Tot}} = -(4\pi/k) \text{Im}\phi_2(0) \quad .$$

iii) Hadron Production at Large X

Measurements of inclusive pion production in p-p collisions with a polarized beam, ($p \uparrow p \rightarrow \pi^\pm + \text{anything}$), have revealed sizeable asymmetries in these processes at $p_{\text{lab}} = 6$ and $12 \text{ GeV}/c$.¹⁶ These asymmetries seem to be energy independent, they increase with both increasing p_\perp and increasing x ($=p_L^*/p_{\text{max}}^*$) of the scattered pion, and reach large values (30-40%) for $x \gtrsim 0.7$. If sizeable asymmetries were found at the high energies, then this inclusive process could be used for monitoring the beam polarization for other experiments.

The result is qualitatively similar to the polarization in backward $\pi^\pm p$ elastic scattering, and thus can be explained with a baryon exchange mechanism. Other experiments have shown that the particle ratios π^+/π^- and K^+/K^- at high x and low p_\perp are remarkably similar to those at $x=0$ and high p_\perp .^{17,18} As stressed by Miettinen the result at high x can be interpreted in terms of the quark-parton model, and in particular can be understood from the constituent structure of the initial protons. If these ideas are correct, then the measurement of asymmetries in the reactions $p \uparrow p \rightarrow \pi^\pm + X$ and $p \uparrow p \rightarrow \pi^\pm + X$ in the high $-x$ region may be a direct way of probing the spin dependence of the coherent interaction of quarks.

II. MAIN FEATURES OF THE POLARIZED BEAM

The details of the polarized beam design are given in the design report of Underwood et al.²¹ and were also discussed in our original proposal 581. In this section we concentrate on the recent developments. The beam was originally considered as a modification of the M3 line. Following the last PAC presentation (April, 1978) mesonlab staff suggested targeting in the detector building and using the M2 beam line. A possible alternate would be a M2 branch. With the main part of the beam downstream of the detector building, there are fewer restrictions on the beam design and the target box construction is simplified. The costs would also be lower. The overall view of the proposed beam line is shown in Fig. 1. Improvements in the polarized beam design and power requirements are described in Appendix 1.

The main features of the present design are:

- i) Predicted intensities of enriched antiproton and polarized proton beams are shown in Fig. 2. Somewhat higher intensities than shown in Fig. 2 could be obtained by optimizing the target length at each momentum. For a 280-GeV/c polarized beam (400-GeV/c primary protons, $3 \cdot 10^{12}$ /spill, $\frac{1}{2}$ interaction-length Be target ± 1 mr acceptance, and $\pm 5\%$ momentum bite), we estimate an intensity of $\sim 10^7$ /pulse with polarization of 40-50%.

- ii) The polarization of the beam will alternate each spill providing a means of eliminating major systematic effects.
- iii) The experimental area, 40' x 100', will be located at the foot of Mt. Taiji.
- iv) The target box should be able to handle $5 \cdot 10^{12}$ protons/pulse striking a production target.
- v) Most of the bending magnets (16 BM105s), magnet bases, and their power supplies could be brought from Argonne.
- vi) We need to construct 16 superconducting quadrupoles (4" bore), and a logical place to build would be at Argonne.

Beam Tuning and Determination of Beam Polarization with a Polarimeter

We have considered the number and location of the beam diagnostic monitors needed to ensure that the beam is correctly tuned. A polarimeter has been designed to measure the p-p asymmetry from elastic scattering in the Coulomb-nuclear interference region (see pages 8 and 64, proposal 581). The polarimeter consists of a single-arm spectrometer for the determination of the angle and momentum of forward scattered particles, and a recoil-sensitive scintillating target. A prototype of this scintillating target has been successfully tested to meet the criteria of the recoil-energy resolutions and the rate capability.

We estimate that 200 hours with a beam intensity of a 10^6 /pulse will be needed to tune the beam and measure the polarization.

III. DESCRIPTION OF PROPOSED EXPERIMENTS

PHASE 1 HIGH p_{\perp} PHYSICS

We propose to measure the asymmetry in large $-p_{\perp}$ reactions from the collisions of polarized protons with and without a polarized target.

$$p^{\uparrow}p \text{ (or A)} \rightarrow \text{single hadron} + X \text{ (} A_N \text{ measurement)}$$

$$p^{\rightarrow}p^{\rightarrow} \rightarrow \text{single hadron} + X \text{ (} A_{LL} \text{ measurement)}$$

We are interested in both single π^0 and π^{\pm} production, but initially we will concentrate on the π^0 -production experiment since we can obtain a good sample of large p_{\perp} events with a simple detector. The γ rays from the π^0 decay will be detected and measured in a standard lead-glass hodoscope. The proposed layout for A_N measurement is shown in Fig. 3.

We first plan to measure the spin asymmetry with only the beam polarized normal to the scattering plane:

$$A_N = E(d^3_{\sigma^{\uparrow}}/dp^3 - d^3_{\sigma^{\downarrow}}/dp^3)/E(d^3_{\sigma^{\uparrow}}/dp^3 + d^3_{\sigma^{\downarrow}}/dp^3)$$

for these processes $p^{\uparrow}p \text{ (or A)} \rightarrow \text{single } \pi^0 + X$.

When both the beam and target are polarized in LL direction (L: longitudinal direction), we will be able to study spin-spin dependence of the constituent scattering processes. We measure

$$\begin{aligned} A_{LL}(s, p_{\perp}, x) &= E(d^3_{\sigma^{\rightarrow}}/dp^3 - d^3_{\sigma^{\leftarrow}}/dp^3)/E(d^3_{\sigma^{\rightarrow}}/dp^3 + d^3_{\sigma^{\leftarrow}}/dp^3) \\ &= E(d^3_{\sigma^{++}}/dp^3 - d^3_{\sigma^{+-}}/dp^3)/E(d^3_{\sigma^{++}}/dp^3 + d^3_{\sigma^{+-}}/dp^3), \end{aligned}$$

where the arrows indicate the beam and target relative spin directions, while + and - refer to helicity states.

Beam

The beam characteristics are described in p. 7. Because of the simplicity in beam construction, we utilize a polarized beam with the transverse scheme (p. 5, proposal 581) for our initial measurements although this won't allow us to go beyond 280 GeV/c.

γ Detectors

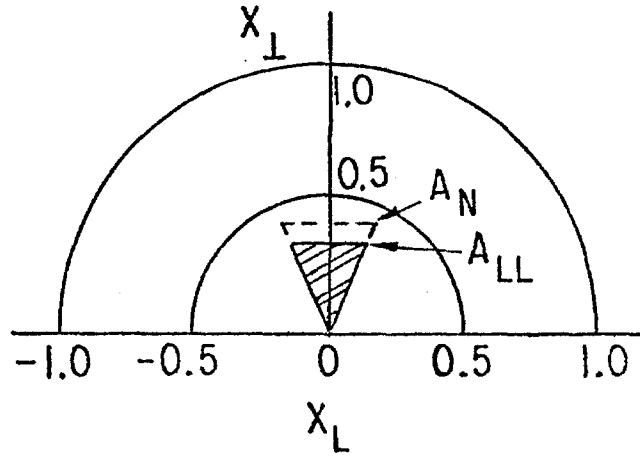
We will install two γ -detectors, one on each side of the polarized-proton beam. The distance between the target and the γ -detectors is approximately 6m.

The experimental setup shown in Fig. 3 uses γ -detectors presently available from this collaboration who have used them in various previous π^0 experiments. The γ -detectors are lead-glass hodoscopes of 28 radiation length (1 radiation length = 2.6 cm), and each hodoscope consists of 150 counters. Depending on the time scale of the experiment we could add additional detectors in order to cover a large solid angle.

For the A_{LL} measurements, we will add electromagnetic shower calorimeter modules (lead-scintillator sandwiches used in E-395 experiment, Pennsylvania - Wisconsin collaboration) of 20 radiation length in order to gain more solid angle (see Fig. 4).

The overall arrangement of available γ -detectors is determined in order to optimize the acceptance of high $-p_{\perp}$ events. We will detect π^0 's produced in the central region with $\Delta y = \pm 0.6$ ($\Delta x = \pm 0.2$).

The angular acceptance in the laboratory system is roughly 50 to 140 mrad in θ , and $\pm 40^\circ$ in ϕ on each side of the beam (see Fig. 4). At 280-GeV/c beam momentum, the acceptance in the center-of-mass frame looks roughly as follows:



We expect an energy resolution of

$$\Delta E/E = 0.12/\sqrt{E}(\text{in GeV}) \quad (\text{FWHM}) \quad .$$

For $E \approx 50$ GeV, the energy resolution would be $\sim 2\%$. The resolution of the spectrometer is as follows:

	Target length (cm)	δx	$\delta p_{\perp}/p_{\perp}$ (at $p_{\perp} = 4$ GeV/c)
A_N measurement	100	$2.2 \cdot 10^{-2}$	$6.2 \cdot 10^{-2}$
A_{LL} measurement	25	$1.4 \cdot 10^{-2}$	$2.1 \cdot 10^{-2}$

Multiwire proportional chambers upstream of the γ -detectors will be used to monitor charged particles.

Triggers

The trigger is a weighted sum of pulse heights from the lead-glass hodoscope exceeding some threshold set for a certain p_{\perp} . This is a standard technique used in experiments 260 and 395.

Polarized Target

The target will be a polarized butylalcohol target for the spin-spin asymmetry measurement. Target density will be 0.61 g/cm^3 and its length 25 cm. Assuming no shadowing, the polarization per nucleon will be 12%. The material in the target corresponds to that of a 0.6-meter LH_2 target. We are currently considering polarized Li^6D or Li^7H target, which will yield higher polarization than the butylalcohol.

Rates

Using the π^0 -production cross-section measured by Carey et al.,²² and assuming a beam intensity of $10^7/\text{pulse}$, we get the rates presented in Table I. Table I indicates the accuracy to which we will be able to measure the asymmetry A_N for polarized beam only, and A_{LL} for beam and target protons, both longitudinally polarized. We assume the following:

$$\Delta p_{\perp} = 0.25 \text{ GeV/c (binning of data)}$$

$$\Delta Y (\text{lab}) \approx 1.2$$

$$\rho_{\text{LH}_2} = 0.071 \text{ g/cm}^3$$

$$\text{Length of LH}_2 = 100 \text{ cm}$$

$$\text{Polarized target: } 25 \text{ cm} \times 0.61 \text{ g/cm}^3 = 15 \text{ g/cm}^2$$

Beam polarization: $P_B = 0.45$

Effective target polarization: $P_T = .12$

$8.0 \cdot 10^4$ pulses (200 hours) for A_N

$2.0 \cdot 10^5$ pulses (500 hours) for A_{LL}

The accuracies in asymmetry measurements are calculated as: $\Delta A_N = 1/(P_B \cdot N)$ and $\Delta A_{LL} = 1/(P_B \cdot P_T \cdot N)$, where N is the total number of events. We estimate the systematic errors will be less than 0.2%.

Table I

$\Delta A_N, \Delta A_{LL}$ Accuracies in Asymmetry Measurements, In Percent

<u>P_{\perp} (GeV/c)</u>	<u>$E(d^3\sigma/dp^3)$ $pp \rightarrow \pi^0 x$</u>	<u>$\Delta A_N(LH_2)$</u>	<u>$\Delta A_N(Be, Ti, W)$</u>	<u>ΔA_{LL}</u>
2.0	$4 \cdot 10^{-30}$	< 0.2%	< 0.2%	< 0.2%
3.0	$7 \cdot 10^{-32}$	0.4%	0.4%	1%
4.0	$2 \cdot 10^{-33}$	2%	2%	7%

The value of A_N is predicted to be zero. Predictions for A_{LL} are shown with these error bars in Fig. 5. It is clear that even this simple experiment can distinguish between two currently attractive models.

Systematic Errors

Experiments with polarized beams and polarized targets, in which the polarization of each is reversed frequently, have the happy property of cancelling out many kinds of systematic errors caused by the detector performance. We discuss here the systematic errors that are correlated with the polarized beam or target.

In A_N measurements, a fake asymmetry due to the effect of beam phase-space variation becomes negligible because of detectors on both sides of the polarized beam.

In A_{LL} measurements, due to the effects of beam phase-space variation and target mass variation, a small fake asymmetry is possible. However, the fake asymmetry can be simply eliminated by using two target polarizations and averaging the data.

Running Time

System check out and calibration	100 hours
Single-spin asymmetry ($p \uparrow p \rightarrow \pi^0 X$) at 280 GeV/c	200 hours
Spin-spin asymmetry ($p \uparrow p \rightarrow \pi^0 X$) at 280 GeV/c	500 hours
Single-spin asymmetry ($p \uparrow A \rightarrow \pi^0 X$) at 280 GeV/c for three different A's (Be, Ti, and W)	<u>200 hours</u>
TOTAL	1000 hours

The natural follow-up measurements will be a study of the energy dependence of A_N and A_{LL} .

Equipment Requirements

We will need the following equipment:

1. Use of the polarized beam operated in the transverse mode with spin rotation magnets to get longitudinal polarization.
2. A BM-109 or BM-105 bending magnet.

3. A 100-cm long liquid hydrogen target.
4. A threshold Čerenkov counter of the type used in E-61,
if necessary.
5. Use of one of the existing Argonne polarized proton targets.
6. Minimal fast logics, CAMAC units, etc. from PREP.
7. On-line computer, magnetic-tape units, etc. for data taking.

PHASE 2: $\Delta\sigma_L^{\text{Tot}}$ MEASUREMENTS

We propose to measure the pp total cross-section difference of pure longitudinal spin-states, $\Delta\sigma_L^{\text{Tot}} (\sigma_{\rightarrow\rightarrow} - \sigma_{\rightarrow\leftarrow})$, in the polarized beam line. Measurements will be made at three different momenta between 100 and 280 GeV/c, where the cross-section rises by about 1 mb unit (38.5 to 39.5). Initially we propose to measure up to 280 GeV/c.

This experiment will be a standard transmission experiment with the detectors specifically designed for a higher divergence beam. A description of the experiment is given in p. 11-22, proposal 581.

Rates and Run Plans

We wish to measure $\Delta\sigma_L$ to $\pm 50\mu\text{b}$ at 100, 200 and 280 GeV/c. We will need $\sim 10^{10}$ incident protons per momentum. Therefore we will need to take data for 40 hours per beam momentum. (Assume incident beam of 2×10^6 protons/spill.) We will also need 100 hours for checking out the geometry of the experiment to reduce systematic errors. We need a total of 220 hours to complete the initial survey of $\Delta\sigma_L$ measurements.

PHASE 3: HADRON PRODUCTION AT LARGE x

We propose to measure asymmetries in the processes

$$p \uparrow p \rightarrow \pi^- + \text{anything} \quad (1)$$

$$p \uparrow p \uparrow \rightarrow \pi^- + \text{anything} \quad (2)$$

with special emphasis on the large x region. The first experiment would determine the parameter $A_N(s, p_\perp, x)$ and the second $A_{LL}(s, p_\perp, x)$.

The measurements would be made using a single arm spectrometer consisting of an analyzing magnet, proportional chambers, and gas threshold Čerenkov counters. The kinematic range covered by the experiments would be $p_\perp \leq 1.0$ GeV/c and $x = p_L^*/p_{\text{max}}^* \simeq 0.5$ to 0.9. Measurements of reaction (1) could be carried out at the initial stages, when the beam polarization is to be determined. If sizeable asymmetries are found, then the proposed apparatus could be used as a beam polarimeter for further experiments.

A description of the experiment is given in pgs. 23-26 and in pgs. 62-77, proposal 581.

Running time estimates are as follows:

Reaction	Simultaneously Recorded Range		$I_0(\text{ppp})$	Target	ΔA in 3 bins of p_\perp for $\Delta x = 0.05$	Beam Time (hrs)
	p_\perp	x				
$p \uparrow p \rightarrow \pi^- x$.1 \rightarrow .5	.6 \rightarrow .9	3×10^6	1-m LH ₂	.01/ P_B	100
$p \uparrow p \uparrow \rightarrow \pi^- x$.1 \rightarrow .5	.6 \rightarrow .9	3×10^6	polarized	.02/ P_B	150

REFERENCES

1. M. J. Alguard et al., Phys. Rev. Lett. 41, 70 (1978).
2. D. Sivers, S. J. Brodsky, and R. Blakenbecker, Phys. Reports 23C, 1 (1976).
3. J. B. Babcock, E. Monsay and D. Sivers, Phys. Rev. Lett. 40, 1161 (1978); Phys. Rev. D (Feb. 1979) and earlier references therein.
4. C. Bournely and J. Soffer, Phys. Lett.
5. Private communication, L. Dick and K. Kuroda.
6. G. Bunce et al., Phys. Rev. Lett. 36, 1113 (1976).
K. Heller et al., Phys. Rev. Lett. 41, 607 (1978).
7. H. Cheng and E. Fischbach, Purdue University preprint, August 1978.
8. J. Ranft and G. Ranft, Paper #487, submitted to the 1978 Tokyo Conference.
9. K. Hidaka, E. Monsay and D. Sivers, submitted to Phys. Lett.
10. L. K. Lubert et al., Phys. Rev. Lett. 38, 670 (1977).
11. J. W. Cronin et al., Phys. Rev. 11D, 3105 (1975).
12. R. L. McCarthy et al., Phys. Rev. Lett. 40, 213 (1978).
13. For instance, see I. P. Auer et al., Phys. Rev. Lett. 41, 354 (1978);
E. K. Biegert et al., Phys. Lett. 73B, 235 (1978).
14. s-channel helicity amplitudes: $\langle ++|++ \rangle = \phi_1$, $\langle --|++ \rangle = \phi_2$, and $\langle +-|+- \rangle = \phi_3$.
15. I. P. Auer et al., Phys. Rev. Lett. 41, 1436 (1978), and earlier references therein.
16. R. D. Klem et al., Phys. Rev. Lett. 36, 929 (1976);
J. B. Roberts, "Measurement of Asymmetries in Inclusive Proton-Proton Scattering," in AIP Conference Proceedings No. 35,
M. L. Marshak, Editor, Argonne (1976).

17. J. R. Johnson et al., Phys. Rev. D17, 1292 (1978).
18. D. Antreasyan et al., Phys. Rev. Lett. 38, 112 (1977) and 38, 115 (1977).
19. R. D. Field, Proceedings of the Symposium on Experiments Using Enriched Antiproton, Polarized Proton, and Polarized Antiproton Beams at Fermilab Energies, edited by A. Yokosawa, ANL-HEP-CP-77-45 (1977), p. 88.
20. G. R. Farrar and D. R. Jackson, Phys. Rev. Lett. 35, 1416 (1975).
21. D. Underwood et al., A Polarized Beam for the M3 Line, ANL-HEP-PR-78-05 (1978).
22. D. C. Carey et al., Phys. Rev. D14, 1196 (1976); F. W. Büsler et al., Phys. Lett. 46B, 471 (1973).

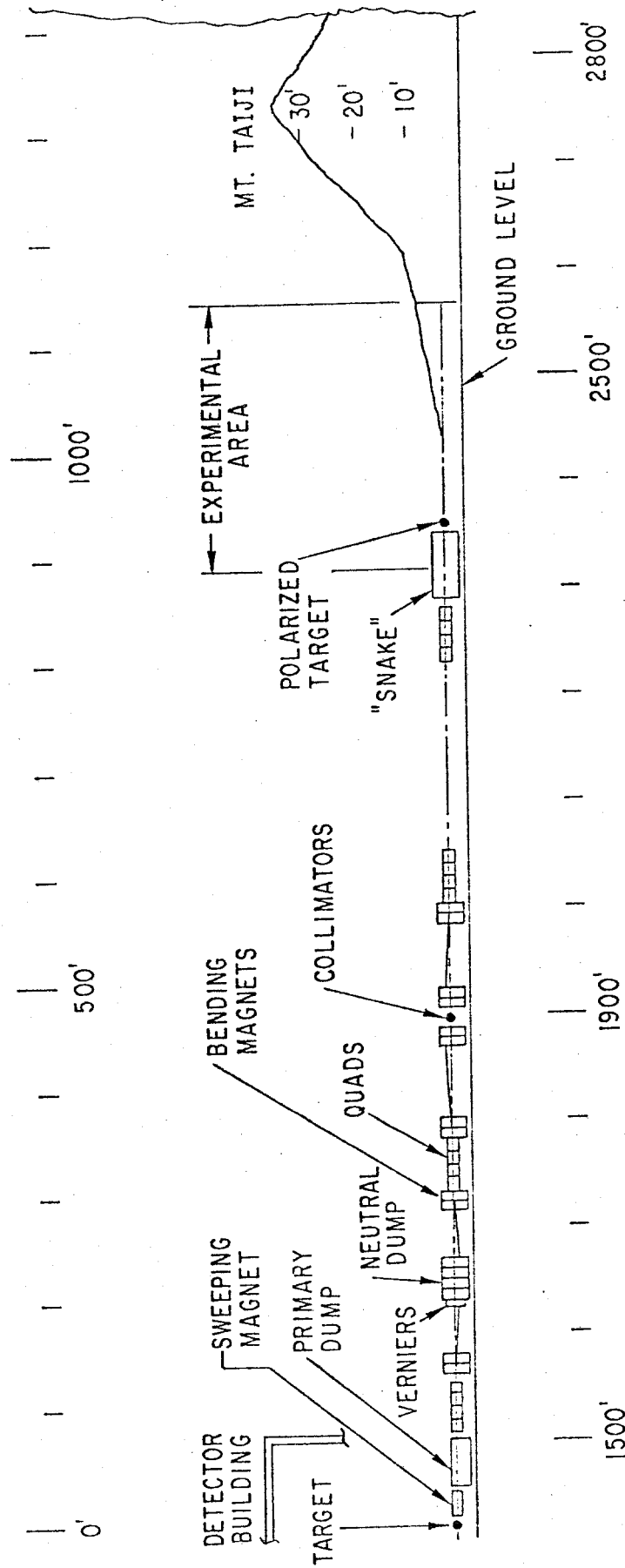


Fig. 1 The overall view of the proposed polarized-beam line.

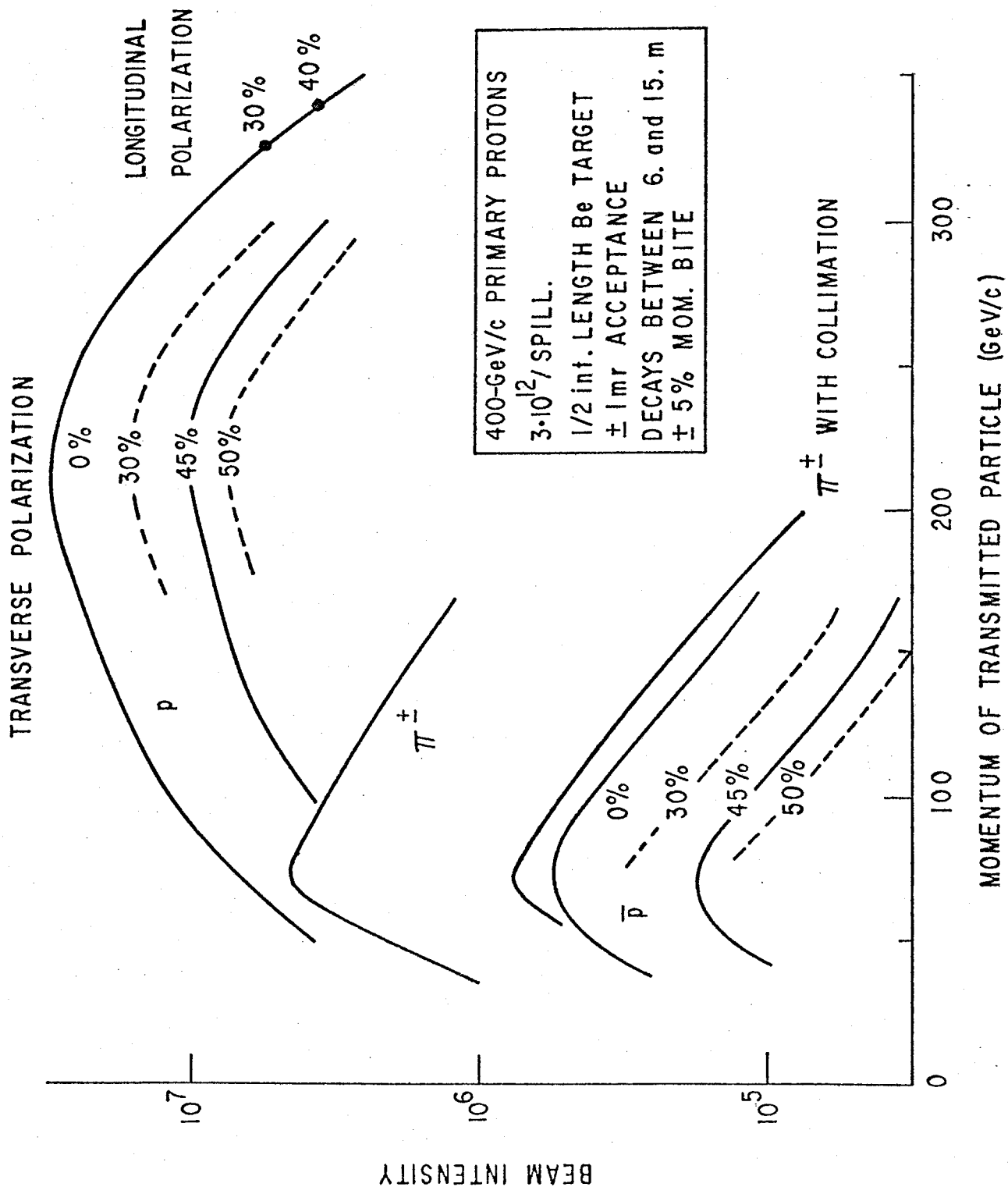


Fig. 2 Estimated polarized proton and antiproton beam-intensities.

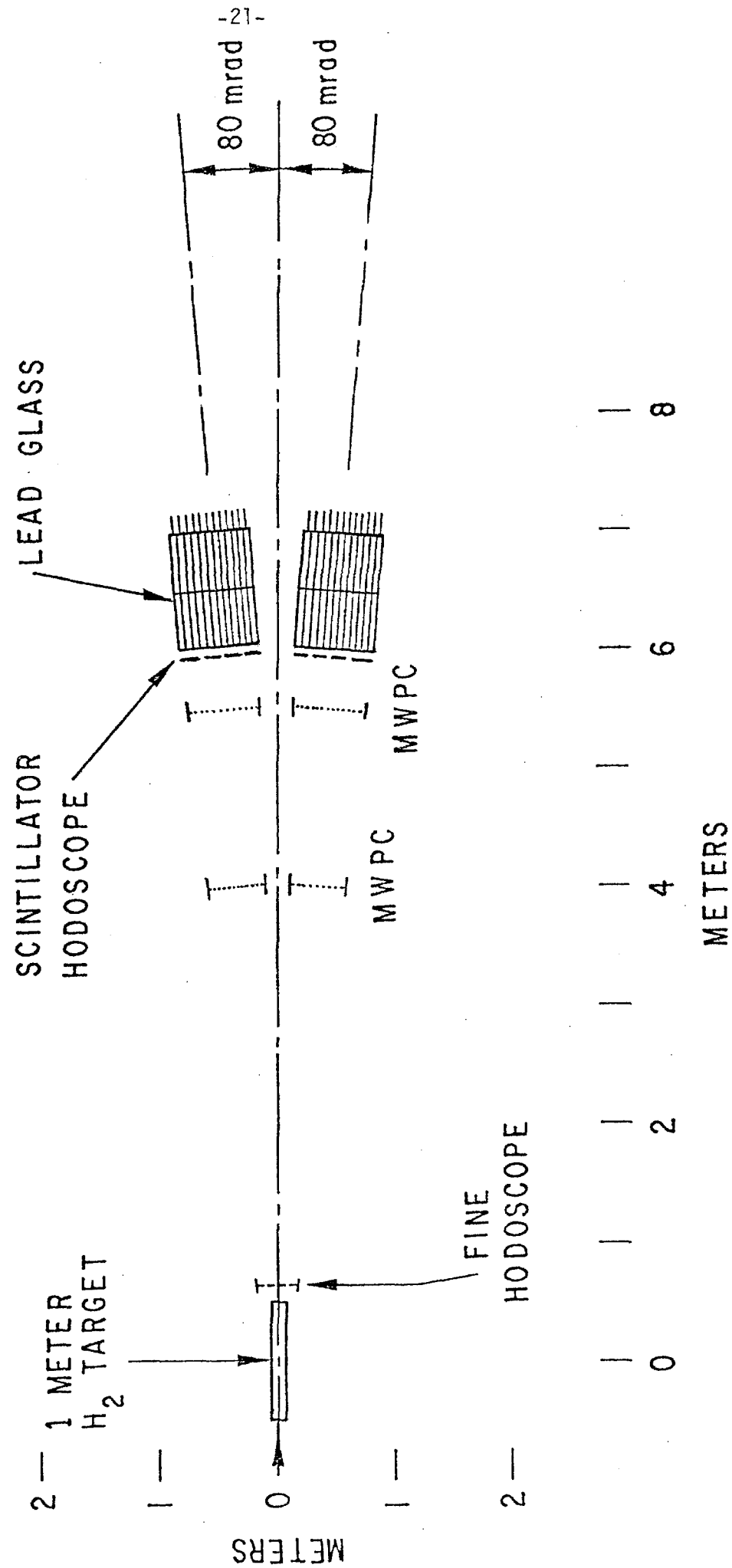


Fig. 3 The proposed layout for A_N measurement.

π^0 - Detector: Downstream View

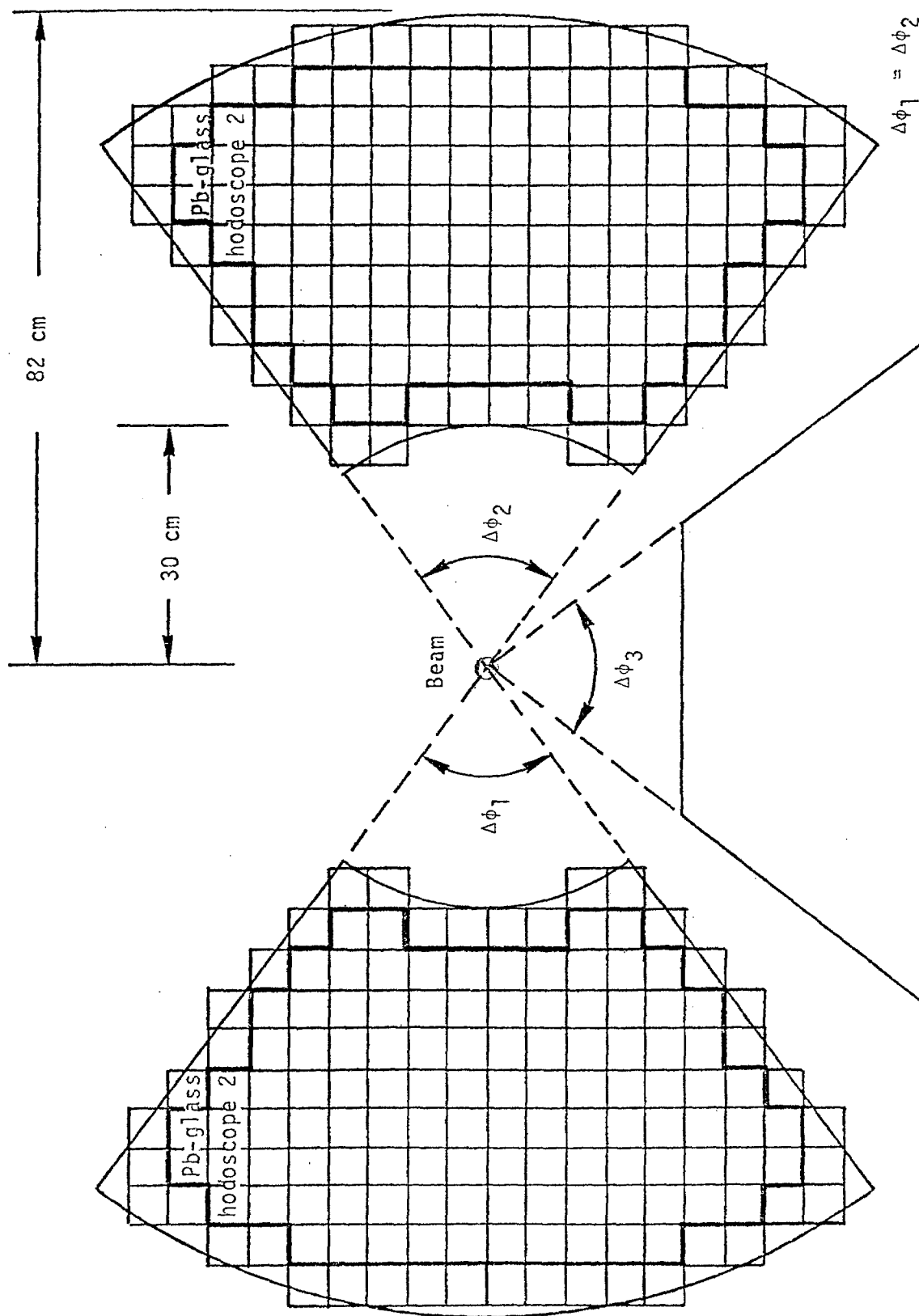


Fig. 4 Lead-glass hodoscopes and shower calorimeter modules.

Pennsylvania - Wisconsin π^0 Calorimeter

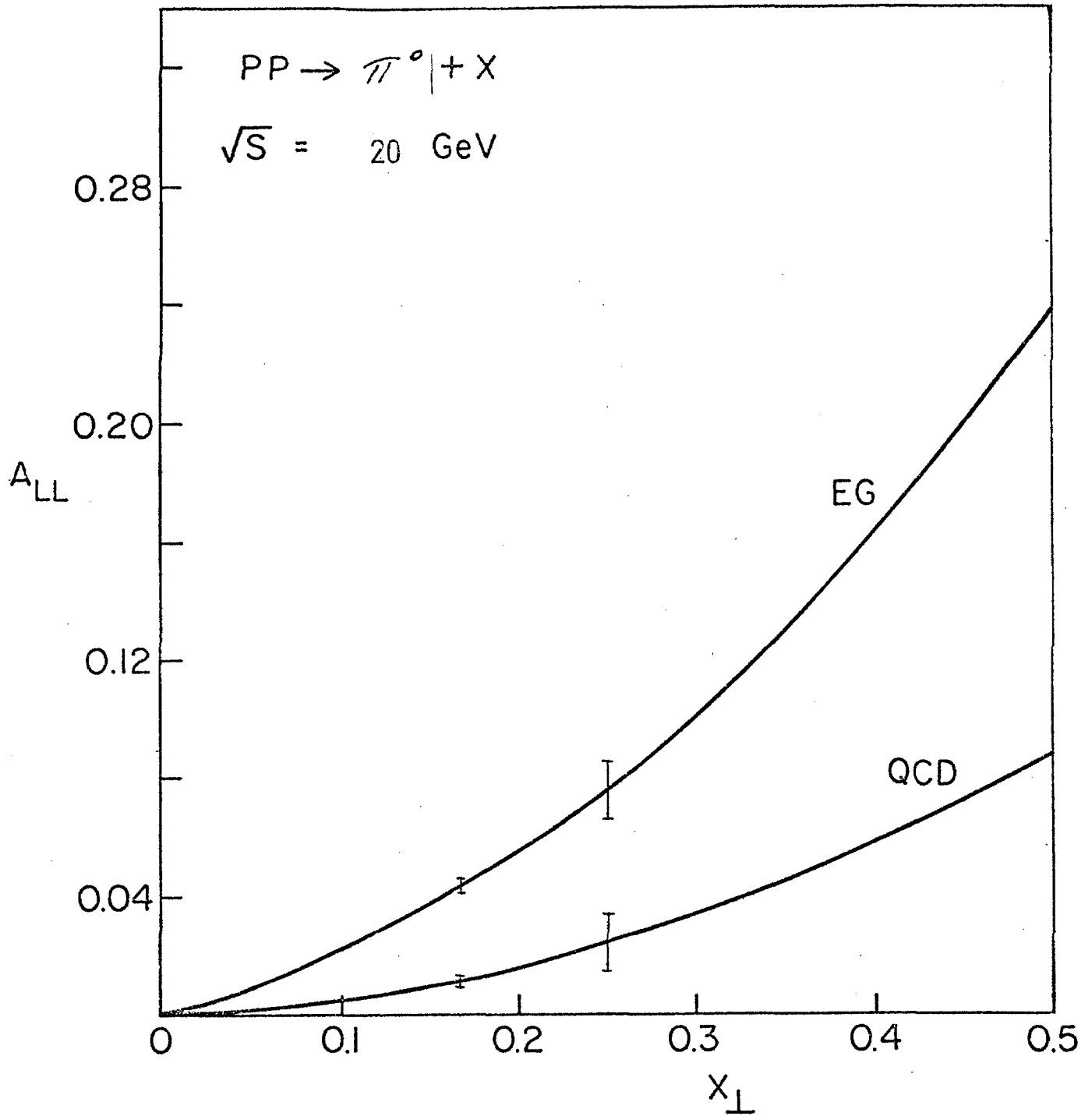


Fig. 5 Predictions of Ref. 7 for A_{LL} based on effective gluon model (EG) and quantum chromodynamics (QCD), shown with expected experimental error bars. Future use of a polarized Li^6D target and/or jet detector could allow measurements with small statistical errors at even higher x_{\perp} .

APPENDIX I TO P581 UPDATE

IMPROVEMENTS IN THE POLARIZED BEAM DESIGN

The basic beam design remains the same as described in P581 of 1978 and the design for the M3 line of Jan. 11, 1978. During the past year we have made further studies of the beam which confirm the polarization properties as shown in Fig. 1. Also, new opportunities for optimizing the beam in terms of chromatic aberration and power consumption have arisen as a result of the decision to put the beam transport downstream of the detector building.

We are now proposing the following configuration:

1. The target box containing the target, sweeping to produce a neutral beam, and primary dump would be inside the meson detector building where it could be serviced by the crane. Targeting of a high intensity beam in the detector building was accomplished for E439 and we have been assured by the laboratory that it will also be done for an approved beam dump experiment in the M2 line.

Radiation shielding would consist of 3 feet of steel for the box and approximately an additional $1\frac{1}{2}$ feet of steel and 9 feet of concrete on the sides and top for 3×10^{12} primary protons.

2. For polarization selection we require that the primary beam be relatively narrow (1 to $1\frac{1}{2}$ mm) at the Λ^0 production target but it could be larger in the vertical direction.
3. Eight large aperture dipoles of about 2 GeV/c kick are required in the beam transport. Existing conventional magnets could be used in a way that would make only modest power demands. Each bend would be accomplished with two BM 105 (18-VI-72) magnets shimmed down to $3\frac{1}{4}$ " gap and run in series at 1500 amperes instead of the 3000 amperes usually required for full field. Measurements of such magnets are shown in Fig. 2. Such a configuration is well matched to existing 150V 1500A power supplies.
4. Sixteen large aperture - high field quadrupoles are needed for the four focusing triplets. These would be low current (300 amperes) superconducting quadrupoles similar to a 9 cm bore - 1m long prototype at Argonne National Laboratory. The beam line quadrupoles would have a 10 cm bore and could be 3m long for 800 GeV/c. Helium consumption would be low so that local dewars could be used instead of a large He transport system. The prototype works well and attains gradients of 80 T/M.
5. Most experiments would be done with the beam operating in transverse mode in order to have variable momentum, get higher intensity, and eliminate the power requirements of a pulsed reversing snake. Vertically or longitudinally polarized beam

will be obtained in this mode by using a short superconducting snake which need not be reversible. Magnets of the type required for such a snake presently exist in a superconducting beam line at the Argonne ZGS.

Total power consumption of the beam line would be less than 2 MW with the shimmed BM 105's and superconducting snake.

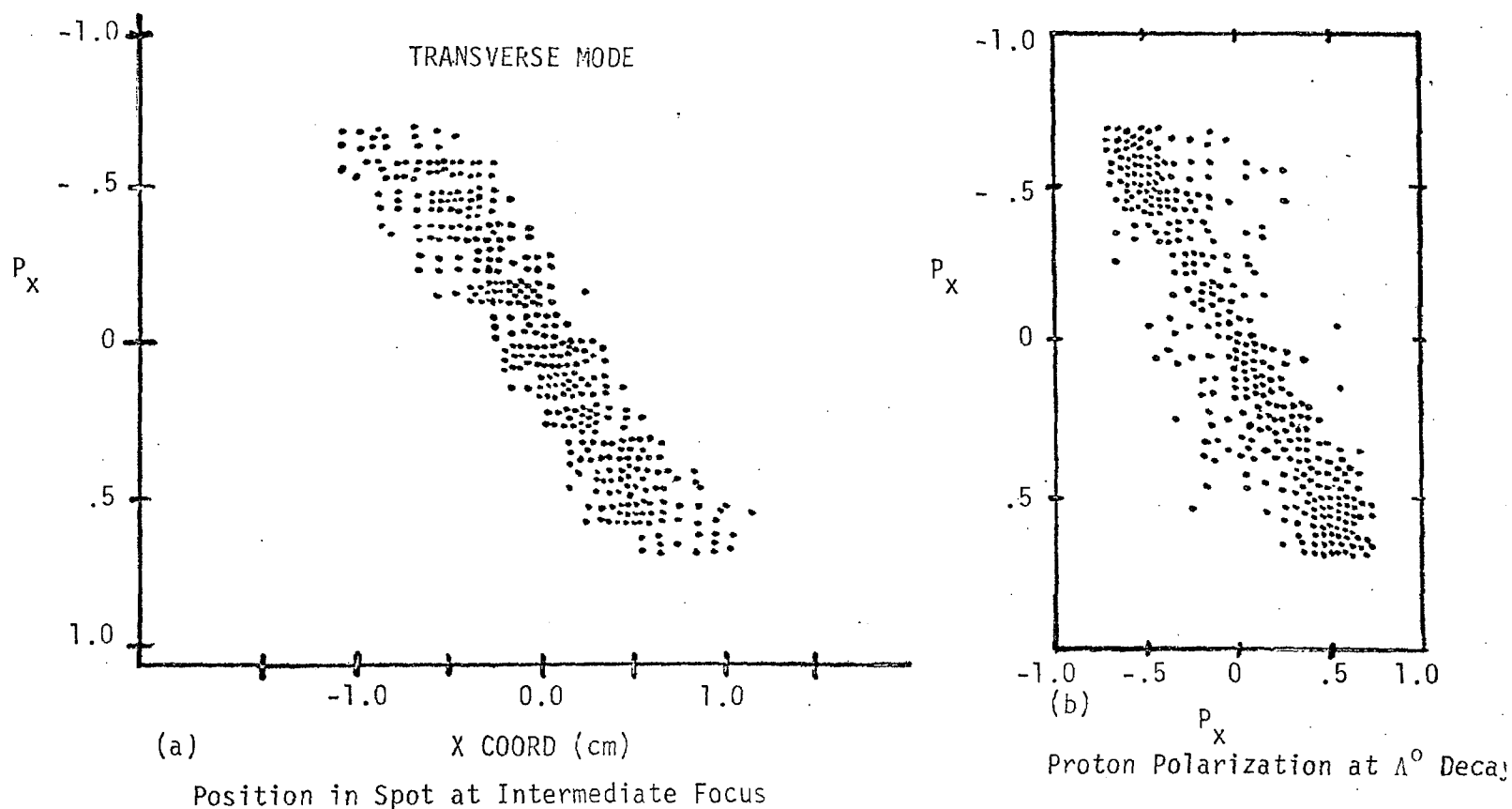


Fig. 1 Scatter plots obtained from a version of the Monte Carlo program decay turtle modified to keep track of spin precession in beam transport.

- (a) The correlation between polarization at the Λ^0 decay and position in the beam spot at the first focus which is used to select polarization in the transverse mode of operation.
- (b) Polarization at the end of the beam vs. polarization at the lambda decay. The scatter from a straight line indicates a depolarization of less than 5% with a 10% momentum bite.

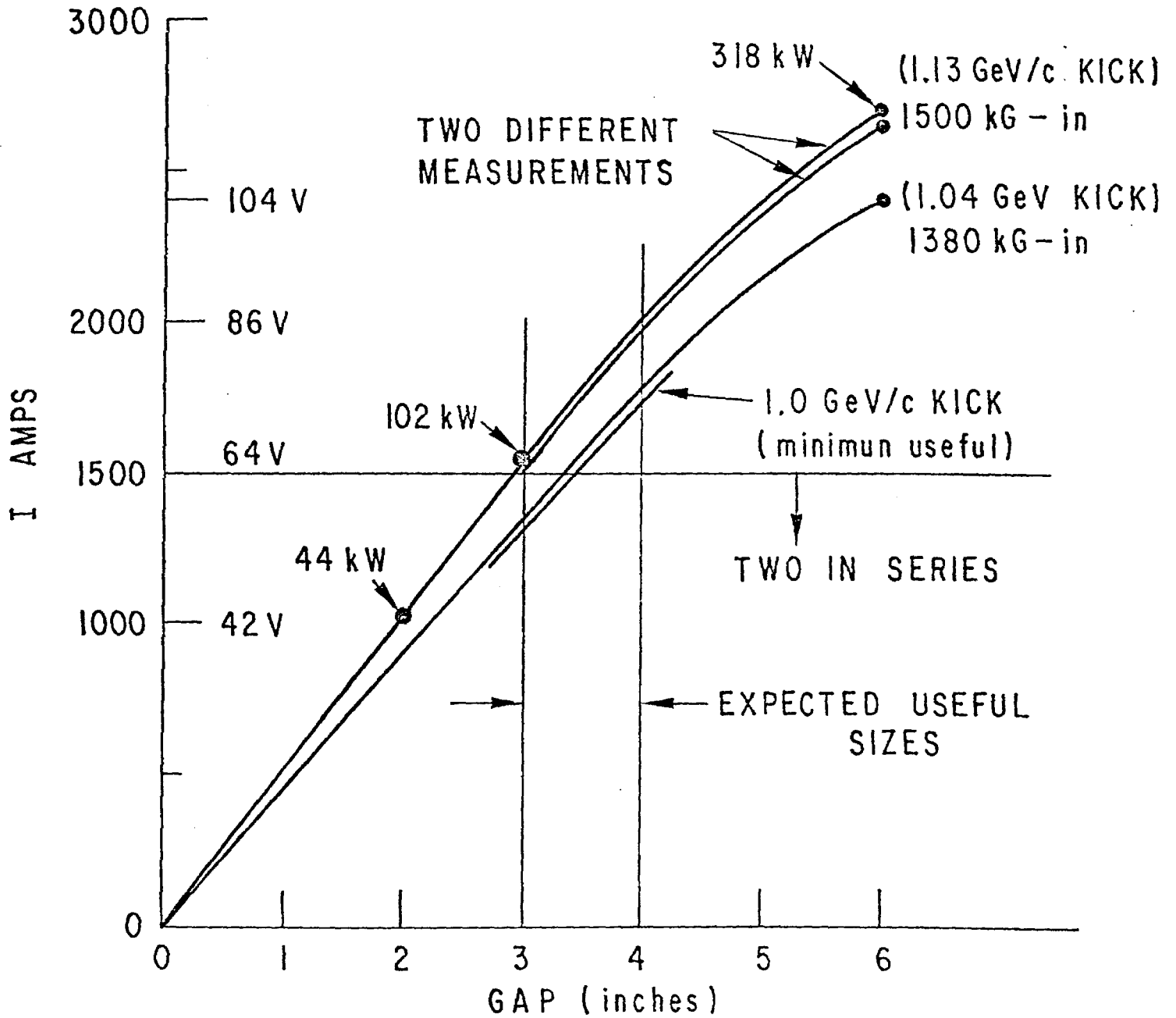


Fig. 2 Characteristics of BM-105 (18-VI-72) magnets with iron shims.

Fermilab Proposal No. 581

Scientific Spokesman:

X A. Yokosawa, ANL

FTS No.: 388-3692

CONSTRUCTION OF POLARIZED BEAMS
AND AN ENRICHED ANTIPROTON BEAM FACILITY IN THE
MESON LABORATORY AND EXPERIMENTS USING SUCH A FACILITY

I. P. Auer, E. Colton, H. Halpern, D. Hill, H. Spinka,
G. Theodosiou, D. Underwood, R. Wagner, Y. Watanabe,
and A. Yokosawa

Argonne National Laboratory, Argonne, Ill.

A. Michalowicz, D. Perrett-Gallix, and K. Kuroda,
LAPP, Annecy, France

G. Shapiro, Lawrence Berkeley Laboratory, University of
California, Berkeley, California

H. E. Miettinen, T. A. Mulera, G. S. Mutchler, G. C. Phillips,
and J. B. Roberts, Rice University, Houston, Texas

R. Birsa, F. Bradamante, M. Budini, M. Giorgi, A. Penzo,
P. Schiavon, and A. Vascotto, INFN. Sezione di Trieste,
Trieste, Italy

January 27, 1978

ABSTRACT

Lambda and anti-lambda production at Fermilab energies is so abundant that an enriched antiproton, polarized proton and polarized antiproton beams with reasonable intensity can be constructed for the use of counter physics. We particularly emphasize the completion of necessary digging and modification of the target train during the mesopause period.

We propose to construct such a facility and to study the substructure of hadrons through the spin effects at high energy. Physics motivation and proposed experiments are described. We propose measurements of total cross-section difference and of high- x_F low- p_\perp inclusive pion production using a polarized beam and a polarized target.

CONTENTS

	Page
I. Introduction	1
II. Enriched Antiprotons, Polarized p and \bar{p} in the Meson Laboratory	4
Polarized Protons from Λ Decay	
Target Train, Sweeping Magnet, Collimator, and Beam Dumping	
Polarized-Beam Transport	
Beam Polarimeter	
Necessary Equipment and Modifications	
III. Description of Proposed Experiments	
<u>Part A</u> Experiments to measure $\Delta\sigma_L^{\text{Tot}}$ in p-p scattering up to 340 GeV/c.	11
Experimental Setup	
Polarized Beam and Target	
Scintillation-Counter Hodoscopes	
Setup Requirements	
Trigger Requirements and Data Collection	
Trigger Logic and Electronics Requirements	
$\Delta\sigma_L$ Measurement	
Rates and Run Plan	
Systematic Errors	
Apparatus	
<u>Part B</u> Asymmetries in inclusive pion production with a polarized beam and target.	23
Physics Interest	

Experimental Technique

Equipment Requirements

Rates, Resolutions, and Run Plan

IV. Summary 36

V. References 37

Appendix I High-p hadron production with a toroidal
spectrometer 40

II Other possible experiments using the polarized -
beam facility 45

III Trigger logic functions 46

Figures

I. INTRODUCTION

It has been shown that spin effects are important experimentally and theoretically at high energy. Large polarizations are observed in inclusive Λ^0 production in the neutral-hyperon beam,¹ and in inclusive proton production in the internal-target experiment.² A sizeable asymmetry effect is observed at CERN in π^0 production by 24-GeV/c protons at $x \approx 0$ and high p_{\perp} .³ Unexpected energy dependence in p-p elastic polarization is observed at Fermilab energies (E-61 experiment)^{3,4} and $|t|$ -dependence near the dip region is remarkable.⁴ More importantly, the study of spin effects in the scattering of quarks could be crucial for further development of current theoretical ideas regarding the constituent nature of hadrons.^{7,8}

An attempt has been made to obtain information about the spin distribution of quark-partons by using a polarized-electron beam and a polarized-proton target.⁹ At Fermilab we can produce reasonably intense polarized-proton and antiproton beams for counter experiments from the decay of Λ and $\bar{\Lambda}$ respectively with polarization of ~50%.¹⁰

At ZGS energies the importance of spin effects has been well demonstrated: structures in the total cross-section difference,¹¹ large asymmetries in inclusive scattering;¹⁶ structures in asymmetry measurements at large p_{\perp} ,¹² and the connection to quark-quark scattering.¹³ At Fermilab energies, the polarized beam will be unique and useful in investigating effects of this nature at much higher energies.

The reason for the rise in the total cross section at energies above 150 GeV is not presently understood. This cross section can be described in terms of two s-channel helicity amplitudes, $\phi_1(0)$ and $\phi_3(0)$,¹⁴ as:

$$\sigma^{\text{Tot}} = (2\pi/k) \text{Im}\{\phi_1(0) + \phi_3(0)\},$$

where k is the center-of-mass momentum of the incident beam.

By studying these amplitudes separately, we could learn whether they behave similarly at increasing energy or whether the rise could be ascribed to one of them. The total cross-section difference in longitudinal spin states allows us to do just that:

$$\Delta\sigma_L^{\text{Tot}} = (4\pi/k) \text{Im}\{\phi_1(0) - \phi_3(0)\}.$$

The study of $\Delta\sigma_L^{\text{Tot}}$ at lower energies has proven to be useful in other ways. It has provided evidence for a diproton resonance¹⁵ and for an A_1 -like exchange trajectory. In addition to the measurements of $\phi_1(0)$ and $\phi_3(0)$, it is interesting to investigate $\phi_2(0)$, which can be determined by the total cross-section difference in transverse spin states:

$$\Delta\sigma_T^{\text{Tot}} = (-4\pi/k) \text{Im}\phi_2(0).$$

Measurements of inclusive pion production with a polarized beam, $p^\uparrow p \rightarrow \pi + x$, have revealed large asymmetries in these processes at ZGS energies, especially for large values of $x = p_L^*/p_{\text{max}}^*$.^{16,17} Recent experiments have shown that the particle ratios π^+/π^- and K^+/K^- at high x and low p_1 ¹⁸ are remarkably similar to those at $x = 0$ and high p_1 .¹⁹ These

results have been successfully interpreted in terms of the quark-parton model,²⁰ indicating that high-x meson production gives information about the constituent structure of the initial protons. Both theoretical arguments^{7c,21} and experimental data^{18,22} support the notion that the leading valence quark ($x \approx 1$) in the proton "remembers" the helicity of the proton. Thus, the measurement of asymmetries in the reactions $p \uparrow p \rightarrow \pi^{\pm} + x$ and $p \uparrow p \rightarrow \pi^{\pm} + x$ in the high-x region may be a direct way of probing the spin dependence of the quark-quark interaction. In addition, if sizeable asymmetries were found in the first reaction, then this process could be used for monitoring the beam polarization in other types of experiments.

We show in the Appendix I and II other possible experiments under consideration. A separate proposal is written on high- p_{\perp} asymmetry measurements using calorimeters.

II. ENRICHED ANTIPROTONS, POLARIZED p AND \bar{p}

IN THE MESON LABORATORY

Polarized Protons from Λ Decay

In the rest frame of the Λ^0 , the proton decays with a longitudinal polarization of 64%.²³ Under the transformation from the rest system to the lab system, the spin vector of the proton remains almost fixed. The polarization in the lab system can be in the longitudinal or transverse direction depending on $\theta_{cm} = 0$ or 90° respectively.

The production of polarized beams from Λ^0 decay has already been proposed by several authors.¹⁰ We find that there are many ways to optimize the intensity and polarization of polarized beams.

We propose to construct polarized beams by using the following two schemes. Details of the polarized beam design are given in a report.²⁴ We describe here the outline.

The basic idea is that polarization direction corresponds to decay direction of the protons in the Λ^0 rest frame. If we select this decay direction in the lab frame with some property of the beam line, we have selected the polarization. The best place to make this selection is at the first focus where protons with different decay angle have different focal points; those with $\theta_{cm} = 0$ are centered and those with $\theta_{cm} = 90^\circ$ are furthest from the center.

i) Transverse Scheme

A transversely-polarized beam can be selected at the first focus with a sliding collimator or two moving collimators as shown in Fig. 1. (Better, a vernier magnet may be used to move the beam spot). Polarization direction can be changed to the desired direction by the 4-magnet scheme. Spin reversal is done by either a collimator or a vernier magnet located downstream of the production target. This scheme gives high-intensity beam with variety of momenta.

ii) Longitudinal Scheme

By choosing fast protons from lambda decays, we will obtain protons primarily from forward-decaying events. The resulting proton polarization will be longitudinal. This scheme is for high momentum protons, $> 300 \text{ GeV}/c$ with $400 \text{ GeV}/c$ primary protons. Spin reversal is done by using a set of reversing magnets in such a way that there is no motion of the beam in the beam transport system or at the experiment.²⁴ The scheme uses 8 magnets of 27.4 kG-m field integral each.

iii) Predicted intensities of enriched antiproton and polarized beams are shown in Fig. 2 together with π background.

Table I: Summary of polarized beams

400-GeV/c primary protons, 10^{13} /spill, 1/2 interaction-length Be target, ± 1 mr acceptance, and $\pm 5\%$ momentum bite			
Scheme	Momentum	Intensity/pulse	Spin Reversal/ each spill
Transverse	<280 GeV/c	3×10^7	Collimator or Vernier
Longitudinal	>320 GeV/c	10^7	Eight-magnet scheme at the downstream end of the beam transport system

A universal set of spin precession magnets would be eight magnets of at least 27.4 kG-m field integral which fit into roughly 16 m and have 5-inch gaps. The power supplies could be ramped and the magnet polarities switched on a spill-to-spill basis. For most experiments this full set would not be necessary but the minimum set for any experiment is four magnets with 3-inch gaps. The spin-reversing scheme is illustrated in Fig. 3.

Target Train, Sweeping Magnet, Collimator, and Beam Dumping

We need zero-degree production angle, and the three-way split beam presently planned by Meson-lab physicists is well suited to our purpose. A dipole magnet to be used for sweeping is shown in Fig. 4 where the beam positions of M-1, M-2, M-3, and M-6 are also indicated. The sweeping

magnets can be drilled or cut to allow simultaneous use of the M-1, M-6, and M-3 lines with beam splitting in Meson lab. The second of the two sweeping magnets is used to sweep away hadronic shower particles that leak into the collimator opening, so that they will not get into the beam line. Collimators and beam dump are shown in Fig. 5. Collimators used at high intensity should be made of aluminum so that the hadronic shower will be spread out sufficiently to allow adequate heat dissipation. The beam should be dumped far from the coils of the sweeping magnet.

We should be compatible with other uses of the M-2 and M-3 lines in a time sharing manner. Specifically, the high-intensity K^0 experiment in M-3 and a fraction of the primary ($\sim 10^{10}$) being transported directly through our sweeping system and down the M-2 line. A new target train should be constructed during the mesopause.

Polarized-Beam Transport

The decision to plan this beam for the M-3 line which has no bend is made in terms of polarization. A focusing element such as a quadrupole triplet would depolarize a high-divergence beam such as we are proposing. The first order solution is to use another identical element after a focus to compensate and return spins to their original directions. The initial focusing stage must match the final focusing stage. An odd number of foci between the first and last stage is required.

We are constrained to compensate all bends between sets of quadrupoles and further constrained to compensate all momentum dispersions between

quadrupole sets.

The schematic of the beam transport system is shown in Fig. 6. The problems arise because the beam pipe is only 12 inches in diameter and displacements of the beam of roughly a foot are needed both for neutral beam dumping and momentum selection. Alternative methods include i) the use of superconducting magnets and ii) different beam design with more depolarization.

We recommend strongly to make a bigger beam pipe in the region of momentum selection. We need 15-ft. deep, 4-ft. wide, and 600-ft. long (4,000 cubic yards) digging.

Beam Polarimeter

While the polarization of the beam can probably be calculated to better than three per cent, including correlations of polarization with position and angle, a beam polarimeter could greatly reduce the risk of taking data where the beam was not working properly. Details of this subject are discussed extensively in reference 25. Two types of polarimeters which could in principle give an absolute measurement of the beam polarization are:

- (1) Measure the p-p asymmetry, A_{pp} , from elastic scattering in the Coulomb-nuclear interference region with an

N-type polarized beam.^[10d] Soffer *et al.*^[27] have calculated A_{pp} to be $\sim 5\%$ at $-t=2 \cdot 10^{-3}$ and almost independent of energy. This calculation assumes the strong flip amplitude $\phi_5=0$ for very small $-t$. (The hadronic polarization $A_{pp} \sim \text{Im}(\phi_1 + \phi_3)\text{Re}\phi_5$ has been observed to be very small in FNAL E-61 at moderate t values. In light of the small value of $\text{Re}(\phi_1 + \phi_3)$ at FNAL energies, we believe that hadronic $A_{pp} \sim \text{Im}\phi_5\text{Re}(\phi_1 + \phi_3)$ will be very small in the Coulomb scattering region.

The rates are quite high in the Coulomb region, and with an $A_{pp} \sim 5\%$, this should be good mechanism beam polarization measurement. The inclusive pion spectrometer (Figure 12) could be used as this polarimeter. The Čerenkov counters and hodoscopes could be used to help discriminate against inelastic events and the hodoscopes spread further apart to allow a measurement of the scattering angle to $\lesssim 1$ mr. The θ_{rms} for multiple Coulomb scattering in the LH_2 is an order of magnitude less, and thus should not jeopardize the measurement. Sample MWPC data would be used for a cleaner measurement off line. Assuming useful $\Delta\phi = \pm 45^\circ$ and $\Delta t \approx .001 \rightarrow .01$, there are 2.5×10^5 events per 200 pulses, giving $\Delta p_{\text{Beam}} = \pm .06$ for $\langle A_{pp} \rangle = .04$.

(2) The process $pA \rightarrow p\pi^0 A$ can be related via the Primakoff effect to low energy $\gamma p \rightarrow \pi^0 p$, which has large polarization asymmetries. The effective γp kinetic energy is typically 500 MeV, yielding asymmetries $\sim 40\%$ at certain scattering angles. (25,26)

Both longitudinal and transverse polarization of the beam can be analyzed using this effect, if the asymmetries in $\vec{\gamma}p \rightarrow \pi^0 p$ and $\vec{\gamma}p \rightarrow \pi^0 p$ are known at the appropriate low energies. The inclusive pion spectrometer (Figure 12) with the addition of a hodoscope of γ detectors at the end can be used for this sort of polarimeter.

The total cross section, for Coulomb dissociation, is ~ 20 mb, so the rates are quite adequate. 10^7 protons/pulse incident on a 3mm Pb target gives about 100 events/burst in the region of useful asymmetry region for $M_{p\pi} \sim 1300$ Mev, for example, thus giving $\Delta p_B \sim .03$ in about 20 minutes. These measurements require measurement of the $p\pi^0$ lab angles to .03 mR for $\pm 5^\circ$ angular resolution in the equivalent low energy γp c.m. This method should give a more certain measurement but requires a much more elaborate polarimeter.

A third type of polarimeter is discussed in the proposed experiment part B.

NECESSARY EQUIPMENT AND MODIFICATIONS

- i) Modifications to Meson lab: target train and M-3 line (See Ref. 24, p. 46 and p. 47)
- ii) High-field quadrupoles (See Ref. 24, p. 49)
- iii) Spin-precession magnets (See Ref. 24, p. 50)
- iv) We need 4000-cubic yards digging as discussed in the section of Beam Transport. According to the Architectural Service, this can be accomplished within a month with \$45 to \$50 K.

III. DESCRIPTION OF PROPOSED EXPERIMENTS

PART A EXPERIMENTS TO MEASURE $\Delta\sigma_L^{\text{Tot}}$ IN p-p SCATTERING UP TO 340 GeV/c.

We propose to measure the pp total cross-section difference of pure longitudinal spin-states, $\Delta\sigma_L^{\text{Tot}} (\sigma_{\rightarrow\rightarrow} - \sigma_{\leftarrow\leftarrow})$, in the polarized beam line at FNAL. Measurements will be made at six different momenta between 100 and 340 GeV/c, where the cross-section rises by about 1 mb unit. (38.5 to 39.5)

This experiment will be a standard transmission experiment with the detectors specially designed for a high-divergence beam.

EXPERIMENTAL SETUP:

The layout of the experimental setup is shown in Fig. 7. A polarized proton beam, in the M-3 beam line, entering from the left, passes through a threshold Cherenkov counter (C_1), set to reject π^+ 's, then through 4 scintillator-hodoscope planes (HX1, HY1, HX2, HY2) and finally interacts with a polarized proton target. The unscattered beam and forward scattered particles pass through 6 scintillator-hodoscopes (HX3, HY3, HX4, HY4, HX5, HY5).

The anticoincidence counters A define the useful beam and the counter-hodoscopes IC help in the identification of inelastic events. The detectors downstream of the target are positioned on rails so that their distances from the target can be adjusted depending on the incident proton momentum. At $p_{\text{lab}} = 200 \text{ GeV}$, $Z_5 = 18 \text{ m}$.

POLARIZED BEAM

Momentum bite: $\Delta p/p = \pm 5\%$ (rms).

Angular divergence: $\Delta\theta_b = 1$ mradian (rms).

Intensity: $I = 5 \cdot 10^5$ protons/spill.

Degree of Polarization: $P_B = 40 - 50\%$

POLARIZED TARGET.

It will consist of NH_3 molecules, of which the 3 hydrogen atoms can only be polarized. We list its characteristics:

Free-hydrogen polarization: $P_H = 80\%$

Target Density: $\rho_{\text{NH}_3} = .56 \text{ gr/cm}^3$.

Length: $L_t = 10\text{-}20 \text{ cm.}$

Diameter: $D_t = 2.5 \text{ cm.}$

SCINTILLATION-COUNTER HODOSCOPES.

Schematic diagrams for the HX1 and HY1 planes are shown in Fig. 8.

Each X-and Y-plane (i) consists of an array of N_i scintillation-counters

$5\text{mm (thick)} \times W_i \text{ mm (wide)}$

Both planes are placed parallel to each other and the center beam line passes perpendicularly through their centers. Whenever a beam-or forward scattered particle passes through a hodoscope-pair, it is almost always counted by only one X and one Y scintillation-counter. The light from both ends of each counter is fed via two fiberglass lightguides to the corresponding

photomultiplier device.

Some hodoscope characteristics are shown in the following table.

TABLE II: SCINTILLATOR-HODOSCOPIES

i	N_i	Counter Width W_i (mm)	Hodoscope Width $N_i W_i$ (mm)	Target to- Hodoscope Distance* Z_i (m)
1	20	1.0	20	-9.0
2	20	1.5	30	-0.2
3	20	1.5	30	1.0
4	30	1.5	45	9.0
5	45	1.5	68	18.0
* $P_{lab} = 200$ GeV.				

SETUP REQUIREMENTS.

For the design of this setup and hodoscope system, the following considerations were taken into account.

- i) It is possible that spills of opposite proton spins will have different π^+ -contamination. This necessitates the use of a threshold Cherenkov-counter to reject them.
- ii) The counter width size is mainly determined from efficiency and counting rate requirements as well as mechanical construction

feasibility:

$$1 \text{ mm} \leq W \leq 1.5 \text{ mm}$$

- iii) It would be desirable to have a beam spot at the target with a diameter slightly smaller than the target diameter ($D_b \leq 2.5 \text{ cm}$).
- iv) We require a t-resolution (4-vector momentum transfer):

$$\delta t \simeq (1.5 - 2.5) \cdot 10^{-3} \text{ GeV}^2.$$

For $p_{\text{lab}} = 200 \text{ GeV}$, this corresponds to a polar angle-resolution

$$\delta \theta \simeq (.20 - .26) \text{ mradians.}$$

- v) To maintain the same t-resolution, independent of the incident proton momentum, for each scintillator-hodoscope, one must maintain a target-hodoscope distance proportional to p_{lab} .

$$Z_{\text{hod}} \sim p_{\text{lab}}.$$

- vi) By requiring the beam divergence to be smaller ($\Delta \theta < 1 \text{ mrad}$) one could move the target further downstream and keep the size of the beam spot at the target the same.

In addition, one can get better t-or θ -resolution by moving the downstream hodoscopes further away from the target without increasing the number of scintillation-counters. Or, one can increase the counter widths and maintain the same angular resolution.

- vii) Since our sample of forward scattering events contains a small fraction of inelastics, care must be taken not to introduce biases in our extrapolation to $\Delta \sigma(t = 0)$.

TRIGGER REQUIREMENTS AND DATA COLLECTION

The two pairs of beam hodoscopes (see fig. 7) will be used to define the direction of incident protons.

The beam hodoscope logic will reject ambiguous or multi-particle incident tracks. In addition, the Cherenkov counter upstream (of the beam hodoscopes) will veto charged pions present in the beam. The anticoincidence counters A will be used to insure that only beam particles that potentially pass through the whole length of the target are in the trigger.

The primary function of downstream hodoscopes is to define the angles and positions of the out going particles. The presence of the three pairs of hodoscopes will provide sufficient redundancy to permit the continuous monitoring of the individual hodoscope elements. The comparison of the hodoscope hit patterns upstream and downstream of the target will provide an additional check on the continuity of the beam and scattered particle-tracks through the target.

The electronic hardware will provide sufficient flexibility to either reject multi-particle events entirely, thus selecting elastic or low multiplicity events, or to identify the leading particle track (more precisely the track with the minimum scattering angle.)

To simplify the logic we plan to process the signals generated by the X and Y arrays separately. This method lends itself more naturally to the use of the projected angles θ_x and θ_y and not to the polar angle θ . ($\theta^2 \equiv \theta_x^2 + \theta_y^2$) From the incident and outgoing angles (projected) the scattered angles will

be calculated by hardware. After each event the appropriate scalers associated with the incident and outgoing angles and positions will be incremented. At this stage we use the hardware to combine θ_x , θ_y and increment the scaler corresponding to the polar angle θ . The θ -distributions of opposite incident-proton spin-directions will serve to eliminate elastic scattering background.

These as well as the other scalers will be read into an on-line computer at least once for each spill. In addition, magnet currents, target polarization and hodoscope hit-patterns will periodically be sampled and read into the computer in order to monitor various experimental parameters such as beam profiles and phase space.

We would like to emphasize that since this is a scaler experiment and since beam polarization flips every alternate spin, it is relatively easy to obtain $\Delta\sigma_L$ values on-line.

TRIGGER LOGIC AND ELECTRONICS REQUIREMENTS

To measure a total cross-section, we must count all incident tracks within the live time of the apparatus. A transmitted particle is defined by the following 5 requirements.

T_0 = Neither the incident, nor the most forward track should be a pion.

T_1 = One and only one incident track in each x and y-plane.

T_2 = The incident track must lie within the range of the angular beam-divergence, and pass through the target.

T_3 = Only one outgoing scattering track in H4 or H5 or both.

T_4 = The most forward scattering track must match with the incident track at the target within the spatial resolution of the hodoscope-system.

We scale all beam tracks, outgoing tracks, and their matrix-coincidences. We scale separately coincidences with only 1 hit in H3 and coincidences with multiple hits in H3 and/or hits in IC1 and IC2.

The high rate of about $5 \cdot 10^6$ particles/spill in each hodoscope, poses rather stringent constraints on the electronic logic's time resolution and speed. We estimate that we need approximately a speed of 30 - 100 nsec.

To be able to distinguish particles from different RF-buckets, we need a maximum of 15 nsec in time resolution.

We plan to use standard electronic logic with matrices to perform all the required functions. In Table IIa we list the electronic circuitry to be used for most of these functions.

TABLE IIa:

FUNCTION	ELECTRONIC CIRCUIT
N_i	Digital Adder
$\sum X_i \leq 1$	Analog Linear Add
Minimum (A, B, C, ...)	Matrix + "And"
θ_x^2, θ_y^2	Matrix
Δx	Matrix

In Fig. 9 we sketch the implementation of some of the above functions.

In the appendix we express these requirements in terms of logic functions, to be hardwired in the electronic circuitry.

$\Delta\sigma_L$ MEASUREMENT

The amount of beam passing through the polarized-proton target is attenuated by both the free polarized protons and by the rest of the material in the target. The number of particles, N_i (corrected for efficiency), that is transmitted through the target into the i th solid angle covered by segments of the transmission hodoscope is given by:

$$N_i^{\pm} = N_0^{\pm} \exp \left[-\alpha_i - \frac{1}{A} (\sigma_i \pm P_B P_T \frac{\Delta\sigma_{L,i}}{2}) \right], \quad (1)$$

where \pm refers to the beam and target polarization oriented antiparallel (+) or parallel (-), N_0 is the number of incident beam particles, α_i is an attenuation constant for everything in the target except free hydrogen, σ_i is the integrated differential cross section from the i th solid angle subtended, $A = (N_A \rho_F L)^{-1} = 2320$ mb is the target constant for free hydrogen, N_A is Avogadro's number, $\rho_F = 0.0714$ gm/cm³ is the free-proton density, $L = 10$ cm is the target length, and $P_B = 0.5$ and $P_T = 0.8$ are the magnitude of the beam and target polarizations, respectively.

The partial cross-section difference for each counter, $\Delta\sigma_{L,i}$, is calculated from these numbers by:

$$\tanh \frac{\Delta\sigma_{L,i} P_B P_T}{2A} = - \frac{N_i^+/N_0^+ - N_i^-/N_0^-}{N_i^+/N_0^+ + N_i^-/N_0^-}. \quad (2)$$

Note that the dominant contributions to the attenuation, α_i and σ_i/A , exactly cancel in this expression. The efficiencies also cancel to first order because the beam polarization is flipped on alternate pulses.

RATES AND RUN PLAN

The accuracy of $\Delta\sigma_L$ measurement is expressed by:

$$\Delta(\Delta\sigma_L) \approx (4800/\sqrt{N_0})\text{mb.}$$

We wish to measure $\Delta\sigma_L$ to $\pm 10\mu\text{b}$. We will need $2.0 \cdot 10^{11}$ incident protons per beam momentum. Therefore we will need to take data for 100 hours per beam momentum. (Assume incident beam of $5 \cdot 10^6$ protons/spill). We will also need 100 hours for checking out the geometry of the experiment to reduce systematic errors. We need a total of 600 hours to complete $\Delta\sigma_L$ measurements. We note that for high-momentum data points a polarized beam will be produced by using the longitudinal scheme and for low-momentum points by the transverse scheme.

SYSTEMATIC ERRORS:

Experiments with polarized beams and polarized targets, in which the polarization of each is reversed frequently, have the happy property of cancelling out many kinds of systematic errors. Sources of -- for example, detector inefficiencies, or geometrical misalignments -- which change slowly with respect to the period of polarization reversal, have little effect on the value of the parameters measured by the experiment.

The systematic errors that are correlated with the beam or target polarization can be classified as multiplicative or additive. The multiplicative errors refer to those factors by which the raw asymmetry must be multiplied, or divided, to yield the final result. When the asymmetry is small, and the number of counts are so few that statistical errors dominate,

multiplicative errors may not be important.

Additive errors, which can introduce a spurious asymmetry into the data, are more serious. In the case where both beam and target are polarized, and reversed at independent intervals, each type of polarization can be used to monitor, and to cancel out, additive errors associated with the other polarization.

The following kinds of systematic error are common to most polarization experiments:

- 1) Target polarization measurement (multiplicative error associated with polarized target). The polarization of the target can be measured to an accuracy of $\pm 3\%$. The principal uncertainties lie in the calibration of the nuclear magnetic resonance system, using the (small) thermal equilibrium signal. Other uncertainties are introduced by non-linearities in the measuring system when the polarization becomes very large.
- 2) Beam polarization measurement (multiplicative factor associated with polarized beam). Several schemes have been suggested for measuring the beam polarization. The calculation based on beam kinematics is probably accurate to $\pm 3\%$.
- 3) Change in beam geometry with beam polarization (additive factor associated with beam). We control this source of error by (a) using the 8-magnet spin reversal scheme that maintains constant beam geometry, or doing polarization reversal upstream of the collimator, (b) using the incident beam telescope and matrix

coincidence to define acceptable incident beam direction, (c) comparing asymmetries observed with the two senses of target polarization.

In the total cross-section measurement there is an additional source of systematic error because, in a transmission geometry, the quantity measured is the total cross-section minus the cross-section for elastic scattering into the solid angle unresolvable by the detector (about .1 milrad in this design). The latter cross-section ranges from less than a millibarn up to several millibarns as the beam momentum increases.

If we assume that the angular dependence of the elastic cross-section is similar in the two spin states, this becomes a multiplicative factor whose magnitude can be estimated using the diagnostic data from those scattering events sampled by the computer.

APPARATUS

- 1) Use of one of the existing Argonne polarized proton targets.
- 2) Threshold Cherenkov upstream to reject incident pions.
- 3) Threshold Cherenkov downstream to reject events in which fast pions are produced.
- 4) Ten scintillator hodoscopes, five horizontal and five vertical whose characteristics are given in Table II.
- 5) Fast hard-wired matrix coincidence logic, with 15 ns time resolution, to perform the following functions for each event triggering the experiment.
 - a) Veto any event in which more than one scintillator has a count in any of the upstream hodoscopes.
 - b) Define trajectories that will intersect the polarized target.
 - c) Measure $(x, y)^{(in)}$ and $(x, y)^{(out)}$ - coordinates and (θ_x, θ_y) angles of these trajectories.
 - d) Calculate $\theta^2 = \theta_x^2 + \theta_y^2$.
 - e) Measure number of hits in each hodoscope. $(N^{(i)})$.
- 6) Fast scalars, gated for live-time (plus some ungated ones) to count:
 - a) Incident protons.
 - b) Events from x- and y-hodoscopes.
 - c) Events from the matrix coincidence logic.
- 7) Monitor telescope.
- 8) On-line computer to perform the following functions:
 - a) Control and measure target polarization.
 - b) Record all scalars and monitors, once per spill.
 - c) Various on-line diagnostics.

Part B: ASYMMETRIES IN INCLUSIVE PION PRODUCTION
 WITH A POLARIZED BEAM AND TARGET

ABSTRACT

We propose to measure asymmetries in inclusive production of high momentum pions in the reactions

- 1) $p \uparrow p \rightarrow \pi^{\pm} + \text{anything}$, using a transversely polarized beam and a liquid hydrogen target, and
- 2) $p \uparrow p \rightarrow \pi^{\pm} + \text{anything}$, using a longitudinally polarized beam and a longitudinally polarized target.

The measurements would be made using the polarized proton beam proposed by the M-3 Beam Workshop, and a single arm spectrometer consisting of an analyzing magnet, proportional chambers and gas threshold Čerenkov counters. The kinematic range covered by the experiments would be $p_T \leq 1.0$ GeV/c and $x = p_L^*/p_{\text{max}}^* \approx 0.5 \rightarrow 0.9$. If sizeable asymmetries are found in reaction (1), then the proposed apparatus could be used as a beam polarimeter for further experiments: modified versions of the same apparatus could be used as possible polarimeters utilizing electromagnetic effects.

PHYSICS INTEREST

Measurements of inclusive pion production in p-p collisions with a polarized beam, $p \uparrow p \rightarrow \pi^\pm + \text{anything}$, have revealed sizeable asymmetries in these processes at $p_{\text{lab}} = 6$ and 12 GeV/c. [16,17] These asymmetries seem to be energy independent, they increase with both increasing p_T and increasing x ($=p_L^*/p_{\text{max}}^*$) of the scattered pion, and reach large values (30-40%) for $x \geq 0.7$ (Figure 10). The presence of these large effects in inclusive reactions was rather unexpected, since it was thought that contributions from different inelastic channels would tend to cancel out, resulting in small asymmetries. At the present time there is no clear theoretical understanding of the origin of these effects.

In order to study the spin dependence of inclusive pion production at Fermilab energies, we propose to measure asymmetries in the processes

$$p \uparrow p \rightarrow \pi^\pm + \text{anything} \quad (1)$$

$$p \uparrow p \uparrow \rightarrow \pi^\pm + \text{anything} \quad (2)$$

with special emphasis on the high x region. The first experiment would utilize a transversely polarized beam, and thus we would measure the asymmetry

$$A_n(s, p_T, x) = \frac{E \frac{d^3\sigma_{\uparrow}}{dp^3} - E \frac{d^3\sigma_{\downarrow}}{dp^3}}{E \frac{d^3\sigma_{\uparrow}}{dp^3} + E \frac{d^3\sigma_{\downarrow}}{dp^3}}, \quad (3)$$

where $E \frac{d^3\sigma}{dp^3}$ is the invariant cross-section for pion production and \uparrow, \downarrow refer to the transversity of the incoming proton. The second experiment would employ a longitudinally polarized

beam and a longitudinally polarized target, and we would measure

$$A_{\ell\ell}(s, p_T, x) = \frac{E d^3\sigma_{++}/dp^3 - E d^3\sigma_{+-}/dp^3}{E d^3\sigma_{++}/dp^3 + E d^3\sigma_{+-}/dp^3}, \quad (4)$$

where the ++ and +- refer to the helicities of the initial protons. Presently there are no data on these parameters at Fermilab energies, and no data at all on $A_{\ell\ell}$. Furthermore, current theoretical models give very little guidance as to what to expect. Hence, it would be particularly valuable to obtain experimental information on these asymmetries, to be tested against further theoretical developments.

However, we believe that the study of these processes may yield direct information about the constituent structure of the proton and about the spin dependence of the constituent-constituent interaction. This possibility arises from the fact that recently there has been considerable success in explaining certain features of high x meson production in p - p collisions in terms of the quark-parton model. [20] It has been generally thought that the description of low p_T phenomena within the framework of this model is very involved since all the constituents must be included in the considerations simultaneously. This is in marked contrast with high p_T processes, in which the high p_T hadrons or "jets" presumably are fragments of a single quark scattered through a hard collision. However, recent data of Johnson *et al.* [18] show that the particle ratios π^+/π^- and K^+/K^- at high x and low p_T are remarkably similar to those at $x=0$ and high p_T (Antreasyan *et al.* [19]), as shown in Figure 11.

This independence of p_T seems to indicate that the relevant variable for describing meson production is the radial scaling variable $x_R = E^*/E_{\text{max}}^*$ [18] and that there may be a connection between high p_T production and low p_T , high x production.

Ochs [28] has noticed that the π^+/π^- ratio vs. x_R closely resembles the $u(x)/d(x)$ ratio, where $u(x)$ and $d(x)$ are the number of up and down quarks of fractional momentum x in a proton as determined by deep inelastic lepton scattering experiments. This observation suggests that the π^\pm production cross-sections in p-p collisions are determined by the u and d valence quark distributions in the proton, and in particular that the u quark in a fast π^+ should be one of the original u quarks in the incident proton (similar arguments hold for the d quark in π^- production). Hence, low p_T , high x single pion production gives information about the constituent structure of the initial protons.

In addition, there are theoretical reasons to believe that the leading valence quark ($x \sim 1$) in the proton carries the helicity of the proton. [21,6c] This assumption implies that the u/d ratio approaches 5 as $x \rightarrow 1$, [21] which in turn leads to the π^+/π^- ratio approaching 5 as $x_R \rightarrow 1$, in agreement with the data of Johnson *et al.* There are also data from deep inelastic scattering of longitudinally polarized electrons on longitudinally polarized protons [22] supporting the notion that quarks "remember" the helicity of the proton even at moderate values of x . Thus it may be that the alignment of the spin of the proton and the spin of the leading valence quark is a general phenomenon and this in fact is our main motivation for emphasizing the high x region.

In conclusion, we believe that measurements of the asymmetries of fast pions produced in inclusive processes (1) and (2) may be a very direct way of probing the spin dependence of the quark-quark interaction. These studies may also shed light on the question of whether the high momentum pions result from quark fragmentation through gluon emission^[29] or whether they are produced through the quark recombination process as has been recently suggested.^[20,30] Finally we wish to point out that if sizeable ($>10\%$) asymmetries were found in reaction (1) then this discovery would have an immediate application in that the proposed apparatus could be used as a simple and convenient beam polarimeter for other types of experiments.

EXPERIMENTAL TECHNIQUE

The proposed layout of the experimental apparatus is shown in Figure 12.

The transversely or longitudinally polarized proton beam is incident upon either a 100 cm long liquid hydrogen target or a longitudinally oriented polarized proton target. Since the beam originates from Λ decay, its divergence will be large ($\sim 1\text{ mrad}$). To obtain good resolution in p_T , the angle of each incoming particle is measured by the two x-y hodoscopes H1 and H2. The other hodoscopes H3 and H4 will be used in the trigger. These hodoscopes will have a spatial resolution of 1.5 mm and will be spaced 15 m apart.

The production angles of charged particles emerging from the target are measured in the multiwire proportional chambers

(MWPC) labeled P1 and P2. Their angles, after magnetic analysis, are again measured in MWPCs P3-P5. The MWPCs are standard Rice University proportional chambers with "fast" (40 nsec strobe) readout electronics so that rates 1 MHz/2 mm can be tolerated. For some parts of the experiment, especially "hot" sections can be deadened. Most of the needed MWPCs already exist and, in fact have been tested and utilized in medium and high energy physics experiments. Fast readout electronics are being constructed for all planes.

The analyzing magnet shown is a standard BM109 (24VIII72) or BM105 (18VI72) bending magnet. Such a magnet should be readily available at FNAL or one could be borrowed from Argonne.

For π^- production, particle identification is simple due to the opposite curvature of pions and protons in the field of the BM109. We plan to trigger only on π^- produced to beam left; thus, at P_5 π^- are separated from the beam by >1 m. Simply placing a scintillation counter (labeled C_π) as shown should provide a clean trigger for π^- . The π^- trigger will be tightened further by requiring the two threshold Čerenkov counters in coincidence. We expect to be able to make reliable estimates of π^- asymmetries on line.

For π^+ production, particle identification is much more difficult, especially at very high values of x . We plan to use the two gas threshold Čerenkov counters, labeled $\hat{C}1$ and $\hat{C}2$, in coincidence to suppress background from proton induced δ -rays

from the beam and the copious inelastically scattered protons ($p/\pi^+ \approx 10^4$ at $x=.9$). Each counter should discriminate against protons at a level $<10^{-2}$ giving a total suppression of $10^{-4} \rightarrow 10^{-5}$ of spurious proton triggers. We expect singles rates $\sim 10^5/\text{sec}$ for each counter, but multiple coincidence trigger requirements should eliminate this problem. The \hat{C} threshold setting along with the bend of the BM109 should strongly suppress background due to lower x pions ($p_{\text{lab}} \approx 70 \text{ GeV}/c$). These counters are standard pieces of FNAL equipment such as were used in E-61. It is our understanding that the bodies of the E-61 counters still exist in storage at FNAL, and we would hope to use them after rehabilitating the optics and providing our own photomultiplier tubes.

We plan to trigger the π^+ experiment by detecting deflection of scattered particles using the x-y hodoscopes H1-H4 and a hard-wired coincidence matrix to further suppress spurious beam induced triggers. The hodoscopes have 2 mm spatial resolution and each pair H1-H2, H3-H4 provides a lever arm of approximately 20 m. A deflection in particle trajectory of at least 0.2 mrad will be required to trigger the experiment corresponding to a cutoff $p_T \gtrsim .05 \text{ GeV}/c$. Although this requirement introduces a bias against legitimate events with a very small angle particle, we believe it is necessary for distinguishing very high x , small p_T π^+ from protons, and that in fact, this small p_T cutoff will negligibly bias the physics results. We have had experience

in previous experiments with fine grained hodoscopes and with coincidence matrix electronics. We expect to improve our spatial resolution by a factor of approximately 2 and upgrade the complexity of our matrix electronics. There should be $\lesssim 10^4$ trigger candidates/burst, so that a clean decision can be made by the matrix electronics with little deadtime.

The trigger for π^+ will therefore consist of deflection through an angle of greater than 0.2 mrad. in coincidence with a count in both Čerenkov counters. For π^- the trigger will consist of the required bend in the BM109, i.e., a count in the C_π counter and the coincidence of $\hat{C}1$ and $\hat{C}2$. This trigger can be further tightened by hodoscope requirements if necessary. For the single spin measurements with a liquid hydrogen target, an appropriate amount of target empty running will be included. From our experience at the ZGS, we expect the target empty background to be $\lesssim 20\%$.

In the case of a longitudinally polarized beam incident on a longitudinally oriented polarized target, all single spin hadronic asymmetries must vanish due to conservation of parity. Any observed asymmetries must then be due to spin-spin effects involving scattering off of the free protons (only the free protons are polarized) in the target. Thus, the problem in inelastic measurements using a transversely polarized target of contamination due to asymmetries from scattering from carbon and other bound nucleons is avoided for measurements involving longitudinal spin orientations.

Spurious asymmetries due to long term drifts in beam position, spot size, intensity or spill structure will be averaged away by reversal of the sign of the beam polarization on alternate accelerator pulses. Additional signal averaging will be provided during polarized target running by periodic reversal of the spin direction of the target polarization.

This apparatus can be used to extend these measurements to higher values of p_T simply by shifting the downstream elements in the apparatus by one meter transverse to the beam direction. At these higher values of p_T discrimination of π^+ from protons becomes less difficult due to the greater angular separation of the π^+ s from the beam protons.

EQUIPMENT REQUIREMENTS

We will need the following equipment:

1. Use of the M3 polarized proton beam operated in both the transverse and longitudinal modes.
2. A BM109 or BM105 bending magnet and power supply or the arrangement of a loan of such equipment from Argonne.
3. A 100 cm long liquid hydrogen target
4. Two threshold Čerenkov counters of the type used in E-61.
5. Use of one of the existing Argonne polarized proton targets.

The trigger and monitor counters, proportional chambers, cabling, and electronics trailer (which includes a PDP-11 computer, tape drives, discs, fast and slow logic and scalers) will be furnished by Rice. We require only AC power hook-up, beam line controls, and timing signals from accelerator control.

RATES, RESOLUTION, AND RUN PLAN

A summary of the expected rates and run time required to execute the initial parts of the experiment is shown in Table 3. The parameterizations of the inclusive scattering data by Anderson *et al.* [31] and Johnson *et al.*, [18] have been used for these rate estimates. With the initially expected intensity and beam polarization $I_0 = 10^7$ /pulse and $p_B = .4$, we should be able to measure asymmetries for $x = .6 \rightarrow .9$ in bins of .05 in five bins of p_T for $p_T < .5$ with an accuracy of $\Delta A \sim .025$ in the running time indicated. We will also explore the region $.5 \lesssim p_T \lesssim 1.0$, since the π^+ asymmetries here were largest at ZGS energies. We also request a tune up period which may be parasitic with low intensity beam on target; however, rates in the MWPCs and \hat{C} erenkov counters should be tested at $I_0 \approx 10^7$ /burst during the final stages of tune up.

The rates expected in a polarized beam-polarized target experiment at low p_T are listed in the last line of the table. We hope to execute this experiment some time after the initial polarized beam turn on, even if single spin asymmetries prove uninteresting.

We expect to use a BM105 or a BM109 shimmed to a 6" gap as the spectrometer magnet, giving a 1.2 GeV/c transverse deflection. The angular resolution of the upstream hodoscopes H1 and H2 determine the resolution $\Delta p_T \approx .03$ GeV/c, and the MWPCs give $\Delta x \approx \pm .02$. Our resolution should enable measurement of the asymmetries in sufficiently small bins to determine their x and p_T dependence. Discrimination against spurious proton triggers and lower energy pions should ensure clean measurements of π^- asymmetries up to $x=.90$, and π^+ asymmetries up to $x=.8 \rightarrow .9$.

We hope to tune and debug the apparatus during initial tune-up of the M3 beam line soon after the Mesopause. We then plan to quickly explore the high x , low p_T region for possible large single spin asymmetries. If these are found, the apparatus could then be used as a relative polarimeter for further beam tune-up. After the polarized beam is in stable operation, we then propose to explore the higher p_T pion production asymmetries. We believe that the measurements with a polarized target are especially compelling, and request an additional 200 hours as an initial run, since averaging out systematic errors may prove time consuming. A summary of running time requests are as follows:

Tune-up (mostly parasitic)	200 hours	
Low p_T : H_2	100 hours]] 300 hours
Higher p_T scan: H_2	200 hours]	
Polarized beam-polarized target run, low p_T	200 hours	

The systematic errors incurred with a polarized beam-polarized target measurement will be studied in such measurements soon to be carried out at the ZGS. We hope to attain an accuracy of $\Delta A \sim \pm 0.03$ in the measurements at Argonne.

If substantial asymmetries ($\sim 0.2-0.3$) are found in one spin measurements, a polarimeter which measures $\Delta P_B/P_B = 0.05$ in ~ 20 minutes can be effected with the same spectrometer. [25]

TABLE 3 RUNNING TIME ESTIMATES

Reaction	Simultaneously Recorded Range		$I_o(ppp)$	Target	ΔA in 5 bins of p_T for $\Delta x = .05$	Beam Time (hrs) Assume 180 useful pulses/hr on average		TOTAL (Est.)
	p_T	x				π^+	π^-	
$p+p \rightarrow \pi x$.1 \rightarrow .5	.6 \rightarrow .9	10^7	1 m LH_2	.01/ p_B	13	70	100 hrs.
$p+p \rightarrow \pi x$.5 \rightarrow 1.0	.6 \rightarrow .85	10^7	1 m LH_2	.01/ p_B	25	140	200 hrs.
$p+p \rightarrow \pi x$.1 \rightarrow .5	.6 \rightarrow .9	10^7	10 cm NH_3 , 80% polarized, 20% free H	.02/ p_B	20	105	150 hrs

IV. SUMMARY

The construction of a beam for polarized protons and anti-protons will provide a unique facility for study of some of the outstanding problems in hadron physics. In particular, the substructure and interactions of hadrons can be studied through spin effects at high energy.

We are submitting two separate proposals. In this proposal, we include measurements of the pp total cross-section difference in the region where the rise in cross-section is observed, and low- p_{\perp} large-x hadron-production process using a polarized beam and a polarized target. The second proposal concerns measurement of the asymmetry in high- p_{\perp} events.

In this proposal, we request the following machine time:

Part A, $\Delta\sigma_L$ measurements including polarized-beam tuning - 600 hours. This experiment will be a standard transmission experiment with the detectors specially designed for a high-divergence beam.

Part B, Asymmetries in inclusive pion production - 600 hours.

Equipment requirements are

- (i) a BM109 or 105 bending magnet,
- (ii) liquid hydrogen and polarized targets,
- (iii) threshold Cherenkov counters,
- (iv) scintillation-counter hodoscopes, and
- (v) multiwire proportional chambers.

REFERENCES

1. G. Bunce et al., Phys. Rev. Lett. 36, 1113 (1976).
2. M. Corcoran et al., Indiana University preprint IUHEE no. 9.
3. Private communications, L. Dick and K. Kuroda.
4. I. P. Auer et al., Phys. Rev. Lett. 39, 313 (1977).
5. I. P. Auer et al., to be published.
6. Proceedings of the Symposium on Experiments Using Enriched Antiproton, Polarized Proton, and Polarized Antiproton Beams at Fermilab Energies, edited by A. Yokosawa, ANL-HEP-CP-77-45 (1977).
7. For instance, see theoretical talks presented in Ref. 6 by a) C. K. Chen, p. 38; b) E. Fischbach, p. 65; c) R. D. Field, p. 88.
8. F. E. Close and D. Sivers, Phys. Rev. Lett. 39, 1116 (1977).
9. M. J. Alguard et al., Phys. Rev. Lett. 37, 1261 (1976).
10. Earlier work on this subject includes:
 - a) O. E. Overseth, NAL 1969 Summer Study Report, SS-118, Vol. I.
 - b) O. E. Overseth and J. Sandweiss, NAL 1969 Summer Study Report, SS-120, Vol. I.
 - c) P. Dalpiaz, J. A. Jansen, and G. Coignet, CERN/ECFA/72/4, Vol. I, p. 284.
 - d) CERN proposal SPSC/p. 87, July 1977.
11. For instance, see I. P. Auer et al., Phys. Lett. 70B, 475 (1977).
12. J. R. O'Fallon et al., Phys. Rev. Lett. 39, 733 (1977).
13. C. K. Chen, to be published.

14. s-channel helicity amplitudes: $\langle ++|++ \rangle = \phi_1$, $\langle --|++ \rangle = \phi_2$, and $\langle +-|+- \rangle = \phi_3$.
15. H. Hidaka et al., Phys. Lett. 70B, 479 (1977).
16. R. D. Klem et al., Phys. Rev. Lett. 36, 929 (1976).
17. J. B. Roberts, "Measurement of Asymmetries in Inclusive Proton-Proton Scattering," in AIP Conference Proceedings No. 35, M. L. Marshak, Editor, Argonne (1976).
18. J. R. Johnson et al., FERMILAB-Pub-77/98-EXP (October 1977).
19. D. Antreasyan et al., Phys. Rev. Lett. 38, 112 (1977) and 38, 115 (1977).
20. K. P. Das and R. C. Hwa, Phys. Lett. 68B, 549 (1977).
21. G. R. Farrar and D. R. Jackson, Phys. Rev. Lett. 35, 1416 (1975).
22. P. Cooper, Ref. 6, p. 126.
23. J. W. Cronin and O. E. Overseth, Phys. Rev. 129, 1795 (1963);
O. E. Overseth et al., Phys. Rev. Lett. 19, 391 (1967).
24. D. Underwood et al., A Polarized Beam for the M-3 line, December 1977.
25. J. B. Roberts, "Polarimeters: A Summary" (included with the proposal).
26. D. Underwood, ANL-HEP-PR-77-56.
27. E. Leader and J. Soffer, private communication.
28. W. Ochs, Nucl. Phys. B118, 397 (1977).
29. R. D. Field and R. P. Feynman, Phys. Rev. D15, 2590 (1977).
30. D. W. Duke and F. E. Taylor, FERMILAB-Pub-77/95-THY (October 1977).
31. R. L. Anderson et al., Phys. Rev. Lett. 37, 1111 (1976).
32. See. C. Sorensen's talk presented in Ref. 6, p. 210.
33. C. K. Chen, Phys. Rev. D16, 1576 (1977).

34. E. Fischbach and G. W. Look, Phys. Rev. D13, 752 (1976), D16, (1976); L. L. Frankfurt and V. B. Kopeliovich, Nucl. Phys. B103, 360 (1976); J. Missimer, L. Wolfenstein and J. Gunion, Nucl. Phys. B111, 20 (1976); E. M. Henley and F. R. Krejs, Phys. Rev. D11, 605 (1975); L. L. Frankfurt, JETP Lett. 12, 379 (1970); Sov. Phys. JETP 34, 23 (1972); M. Dobovoy, P. Langacker, and M. Suzuki, Phys. Rev. D4, 1474 (1971); N. N. Nikolaev, Sov. J. Nucl. Phys. 17, 62 (1973); K. H. Craig, Nucl. Phys. B109, 156 (1976).
35. T. T. Chou and C. N. Yang, Nucl. Phys. B107, 1 (1976); F. E. Low, Phys. Rev. D12, 163 (1975).

APPENDIX I

HIGH- P_T HADRON PRODUCTION WITH A TOROIDAL SPECTROMETERPHYSICS INTEREST

Hadron production and jet production at high- P_T seem to be two efficient ways for probing quark-quark interactions at short distances. The role of spin-forces in the dynamics of the elementary constituents of the nucleon is emphasized to some extent in the Introduction. We regard this part of physics as one to which very important contributions can come from polarized proton-proton (antiproton) experiments. To this end, we have submitted a separate proposal to study asymmetries of inclusive and jet-like products in high- P_T p-p interactions using large acceptance calorimeters. Here we would like to discuss our interest in the very interesting possibility of using a toroidal spectrometer to study inclusive-charged hadron production at high- P_T .

DETECTOR REQUIREMENTS

The limited luminosity, the low high- P_T inclusive rates, and high low- P_T background due to the sharp fall-off of the cross-section with P_T ($\sim P_T^{-8}$) impose the following stringent requirements on such an experiment:

- (a) Large ϕ -acceptance.
- (b) Maximum possible target length and beam intensity available.
- (c) High signal (high- P_T)/noise (low- P_T) ratio.
- (d) Good momentum resolution.

Up to now, all high- P_T inclusive experiments have had a very limited ϕ -acceptance ($\leq \pi/20$). We have made a preliminary Monte-Carlo study of a toroidal spectrometer design as well as two more conventional large aperture spectrometers.

The results indicate that the toroid

- (a) Is more than 3 orders of magnitude better in signal-to-noise ratio ($2 - 3 \cdot 10^3$ vs. ~ 1).
- (b) Is about 5 times better in ϕ -acceptance (85% vs. 15-20%)
- (c) It can accept simultaneously a large range of $P_T > 2$ GeV and $\chi_F \simeq 0$ inclusives with high acceptance.

DESCRIPTION OF THE SPECTROMETER AND ITS PROPERTIES

Fig. 13 shows some views of our current magnet design. The field inside the toroid has cylindrical symmetry and varies as $\sim 1/r$ (r = radius).

Fig. 14 shows the experimental set up. The beam axis coincides with the toroid axis.

The bending of each particle produced at the target and entering the magnet happens on the production plane containing the beam-toroid axis. The particle trajectory is always perpendicular to the field lines and so the field is fully utilized. The inner cylinder of the toroid of $\simeq 10$ cm radius allows the beam and the forward-going low- P_T products of multiparticle events to pass unaffected by the field. The field can be set so that positive particles bend outwards and negative ones inwards, getting trapped around the beam axis. This and the dependence of the angle of bend on the particle momentum provide this spectrometer with charge and kinematic selectivity in (χ_F, P_T) .

With such a field configuration, the low-energy ($\chi_F \leq 0$, low- P_T) particles can be swept with high efficiency away from the MWPC and DC-planes (Drift-Chamber) shown in Fig. 14. This should allow the detector to tolerate easily the rates from a 20 cm NH_3 target and a beam intensity $> 10^7$ protons/spill in an optimized setup configuration.

TRIGGER

At S_0 , S_1 , S_2 of Fig. 14, three scintillation-counter hodoscopes, finely segmented and azimuthally symmetric, define the production plane of each inclusive product as well as its x_F and P_T -range. Thus, they can provide a very tight, triple coincidence, coplanar trigger, essentially free from non-coplanar background and a suppression in the geometrical acceptance of

$$\frac{\text{signal } (P_T > 2 \text{ GeV})}{\text{noise } (P_T > 0.5 \text{ GeV})} > 10^3 .$$

Fig. 15 shows the shape of these hodoscopes and the wire configuration of MWPC and DC-planes placed after the magnet to find particle tracks and facilitate their kinematic analysis.

The part of the detector corresponding to those particles that are swept away from the beam-toroid axis has the maximum sensitivity.

Therefore, by simply switching the magnet current polarity, one could study π^+ and π^- separately at that part of the detector.

By placing a segmented Cherenkov-counter, shown in Fig. 14, behind the S_2 -hodoscope, a π^+ vs. proton discrimination will be possible. By placing a π^0 detector further downstream, one could trigger simultaneously on π^0 -inclusive production, essentially free from low-energy background.

INCLUSIVE RATES AND TRIGGERS

Inclusive rates for this experiment have been calculated using the data of Antreysan et al⁽¹⁹⁾ as well as $A_N(ppt)$, $A_{LL}(p^{\dagger}p^{\dagger})$ errors, listed in Table I along with the conditions assumed.

TABLE I

P_T (GeV)	$\sigma^{inv}(\pi^{++})$ (cm ²)	$\langle p_{Tjet} \rangle^{inc}$ (GeV)	$\delta A_{LL}(p^{\dagger}p^{\dagger})$	$\delta A_N(ppt)$
3.0	2.1×10^{-32}	3.6	<.01	<.01
4.0	7.3×10^{-34}	4.8	.03	<.01
4.5	1.0×10^{-34}	5.5	.07	.01
5.0	1.5×10^{-35}	6.1	.13	.02

$I = 3 \cdot 10^7$ protons/spill, $L_{NH_3} = 20$ cm, 1 month running (700 hours)

$$\Delta\phi/2\pi = .9, \Delta p_T = .5 \text{ GeV}, \Delta x(x \sim 0) = .1$$

CONSTRUCTION FEASIBILITY AND COSTS

Preliminary calculations and discussions with a toroid specialist at ANL* indicate that its building should pose no problems in mechanical construction. For a regular Cu-coil, water cooled magnet, with a central $\int Bdl = 20$ kGm and 2.5 meters long, the following estimates have been calculated:

$$\text{Cost} = \$25 - 30 \text{ k.}$$

Time for construction, test and calibration ≈ 5 months. In addition, the highly symmetric characteristics of the device would allow simplicity and high compactness of the detector, thus keeping building, testing, maintenance costs and time consumption low.

Finally, we point out the easiness of access to the detectors and their flexibility to adapt to different experimental conditions.

*Bert Wang, private communication.

APPENDIX II

OTHER POSSIBLE EXPERIMENTS USING THE POLARIZED-PROTON BEAM FACILITY

First, we note that we can measure $\Delta\sigma_T$ with an N-type polarized target and the apparatus described in the text. This would give us an additional clue about the rise in our total cross section.

Taking advantage of the polarized-antiproton beam, we can measure $\Delta\sigma_L$ and $\Delta\sigma_T$ for pp scattering. Theoretical interests are recently discussed by C. Sorensen.²⁹

In the dilepton-production experiment, $p^\dagger p^\dagger \rightarrow (\mu^+ \mu^-) + x$, we study the mechanism of Ψ production at $m_{\mu\mu} \approx 3$ GeV and the Drell-Yan mechanism at higher mass.^{6,7} With a polarized antiproton beam, a reaction $\bar{p}^\dagger p^\dagger \rightarrow (\mu^+ \mu^-) + x$ enables us to observe the spin effect of valence-quark and anti-valence-quark interactions.²⁶ Another exciting possibility is that one can perform an experiment like $\bar{p}p \rightarrow (\text{Jet}) + x$. Then we can observe valence quark, q_v , to anti-valence quark, \bar{q}_v , interaction, while in pp scattering, we observe $q_v - \bar{q}_s$ (anti-sea quark) interaction.

Total cross section or large- p_\perp inclusive measurements using a longitudinally-polarized beam should be useful in a search for a parity-nonconserving component in the force between nucleons. The predicted asymmetry effect varies from 10^{-2} to 10^{-5} .²⁷

Finally, we note that polarized beams are useful to pursue "old physics" such as elastic-scattering amplitude measurements at small $|t|$.^{28,29}

APPENDIX IIITRIGGER LOGIC FUNCTIONS

$$T0 = \overline{C_1} \cdot \overline{C_2}$$

where C_1, C_2 are the Cherenkov-counter signals set to detect fast pions.

We define

$$X_j^{(i)} (Y_j^{(i)}) = \text{the } j\text{th-scintillator of the } HX_i (HY_i) \text{ hodoscope.}$$

Then, the above 4 requirements read as follows:

$$T1 = (\sum_{j=1}^{N_1} X_j^{(1)} = 1) \cdot (\sum_{j=1}^{N_2} X_j^{(2)} = 1) \cdot (\sum_{j=1}^{N_1} Y_j^{(1)} = 1) \cdot (\sum_{j=1}^{N_2} Y_j^{(2)} = 1)$$

where N_i = number of scintillation-counters of H_i -hodoscope.

Define
$$\Delta X^{in} = X_{j2}^{(2)} - X_{j1}^{(1)}$$

$$\Delta Y^{in} = Y_{k1}^{(2)} - Y_{k1}^{(1)}$$

$$T2 = \bar{A} \cdot (|\Delta X^{in}| \leq M^{in}) \cdot (|\Delta Y^{in}| \leq M^{in})$$

where $M^{in} \approx 10$,

a parameter defined by the beam-hodoscopes and target setup.

$$T3 = (\sum_{j=1}^{N_4} X_j^{(4)} \leq 1) \cdot (\sum_{j=1}^{N_4} Y_j^{(4)} \leq 1) \cdot (\sum_{j=1}^{N_5} X_j^{(5)} \leq 1) \cdot (\sum_{j=1}^{N_5} Y_j^{(5)} \leq 1)$$

For every hit $(X_j^{(5)}, Y_j^{(5)})$ in H5

Find
$$\Delta X_{25j}^{out} = X_j^{(2)} - X_j^{(5)}$$

$$\Delta Y_{25j}^{out} = Y_j^{(2)} - Y_j^{(5)}$$

Then, find

$$\theta_{x25} = (|2 \cdot \Delta X^{in} - \Delta X_{25j}^{out}|)$$

$$\theta_{y25} = (|2 \cdot \Delta Y^{in} - \Delta Y_{25j}^{out}|).$$

For every hit in $(X_j^{(4)}, Y_j^{(4)})$ in H_4 , find

$$\Delta X_{24j}^{\text{out}} = X^{(2)} - X_j^{(4)}$$

$$\Delta Y_{24j}^{\text{out}} = Y^{(2)} - Y_j^{(4)} .$$

Then, find

$$\theta_{x24} = (| 2 \cdot \Delta X^{\text{in}} - \Delta X_{24j}^{\text{out}} |)$$

$$\theta_{y24} = (| 2 \cdot \Delta Y^{\text{in}} - \Delta Y_{24j}^{\text{out}} |) .$$

$$T_4 = (| \theta_{x25} - \theta_{x24} | \leq MD) \cdot (| \theta_{y25} - \theta_{y24} | \leq MD)$$

where $MD \simeq 3$ mm, which is the spatial resolution upper limit of the scintillator-hodoscope system.

Finally, the transmitted particle is defined by

$$T = T_0 \cdot T_1 \cdot T_2 \cdot T_3 \cdot T_4 .$$

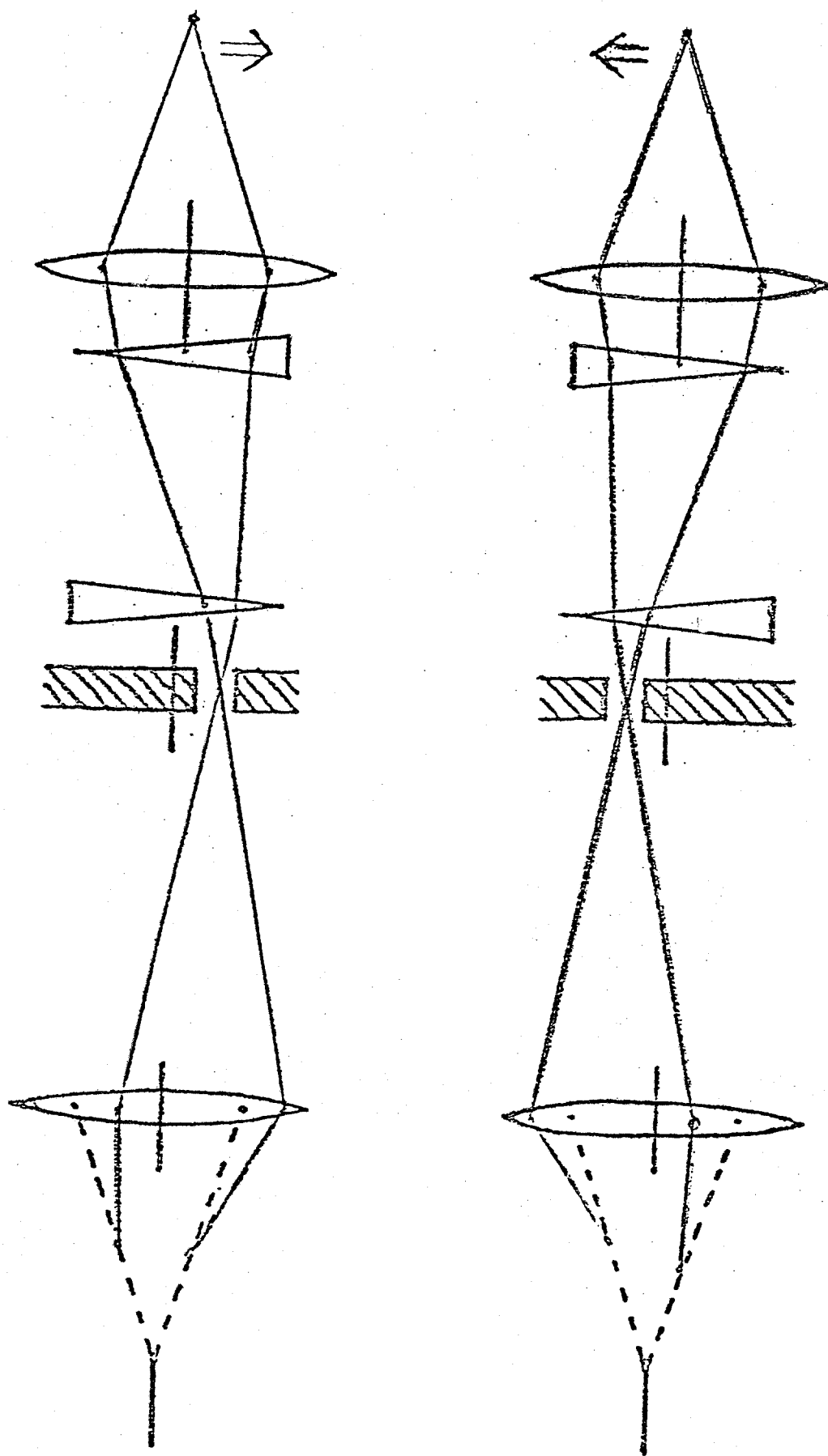


Fig. 1

Two-vernier polarization reversal.

This figure shows the verniers downstream of a moving collimator. An improved version would have one or two verniers upstream of a fixed collimator.

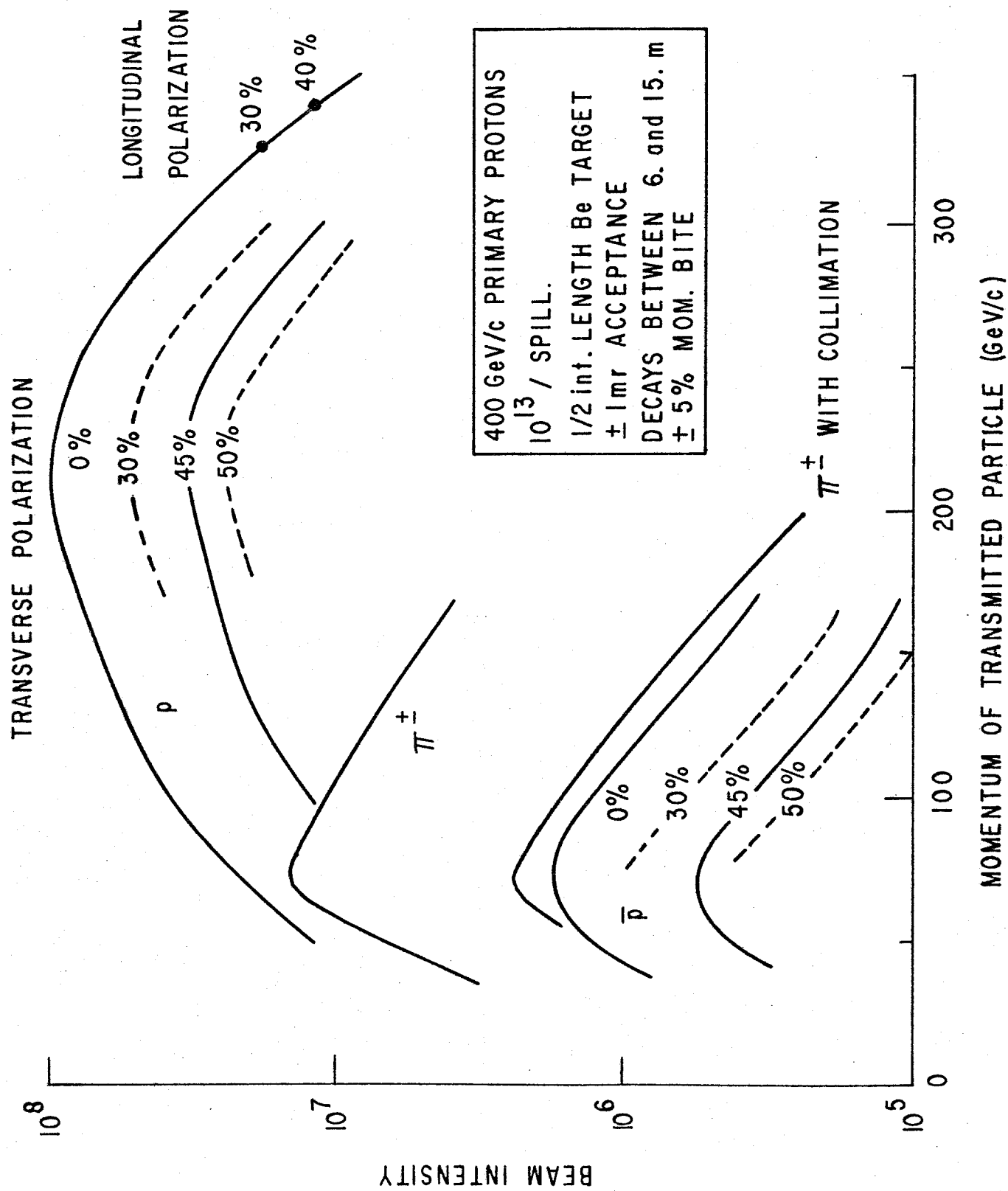
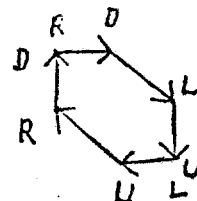
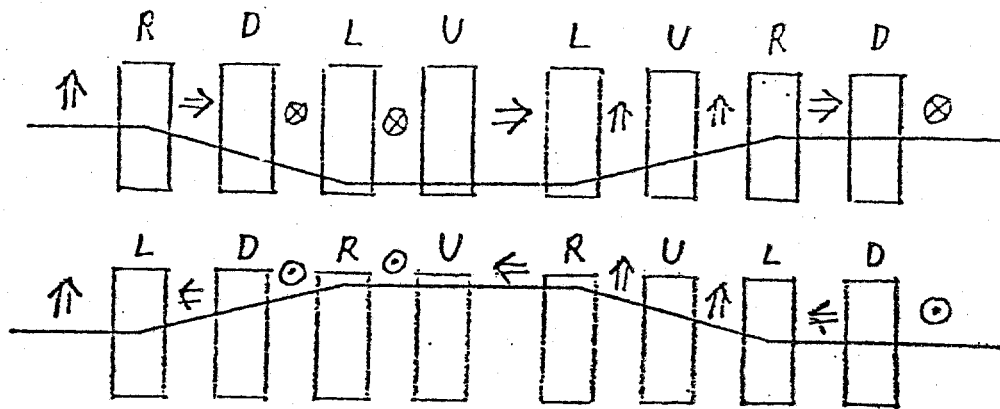
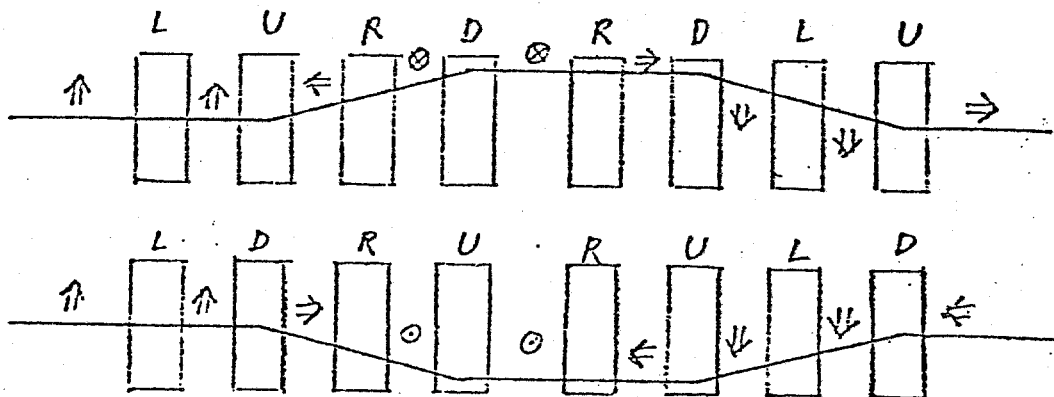


FIG. 2 Estimated polarized proton and antiproton beam-intensities.

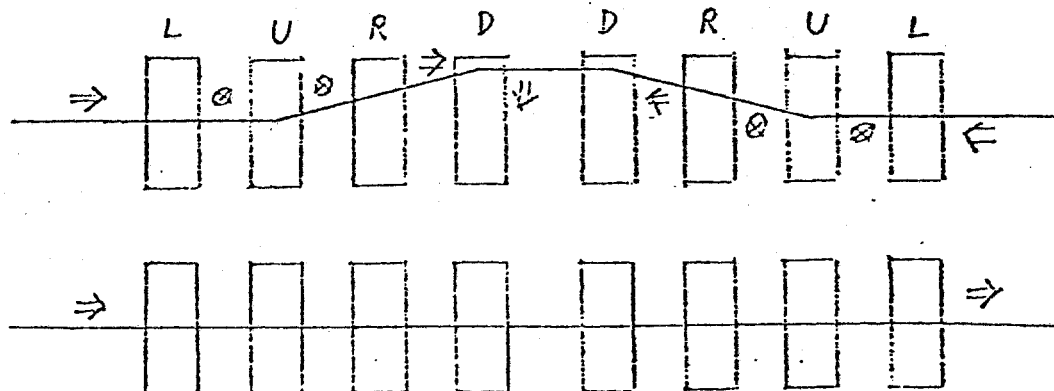
SPIN FLIPPING WITH NO NET BEAM MOTION
(Transverse) (Reverse 4 of 8 Magnets) (No verniers)



Transverse in - Transverse out

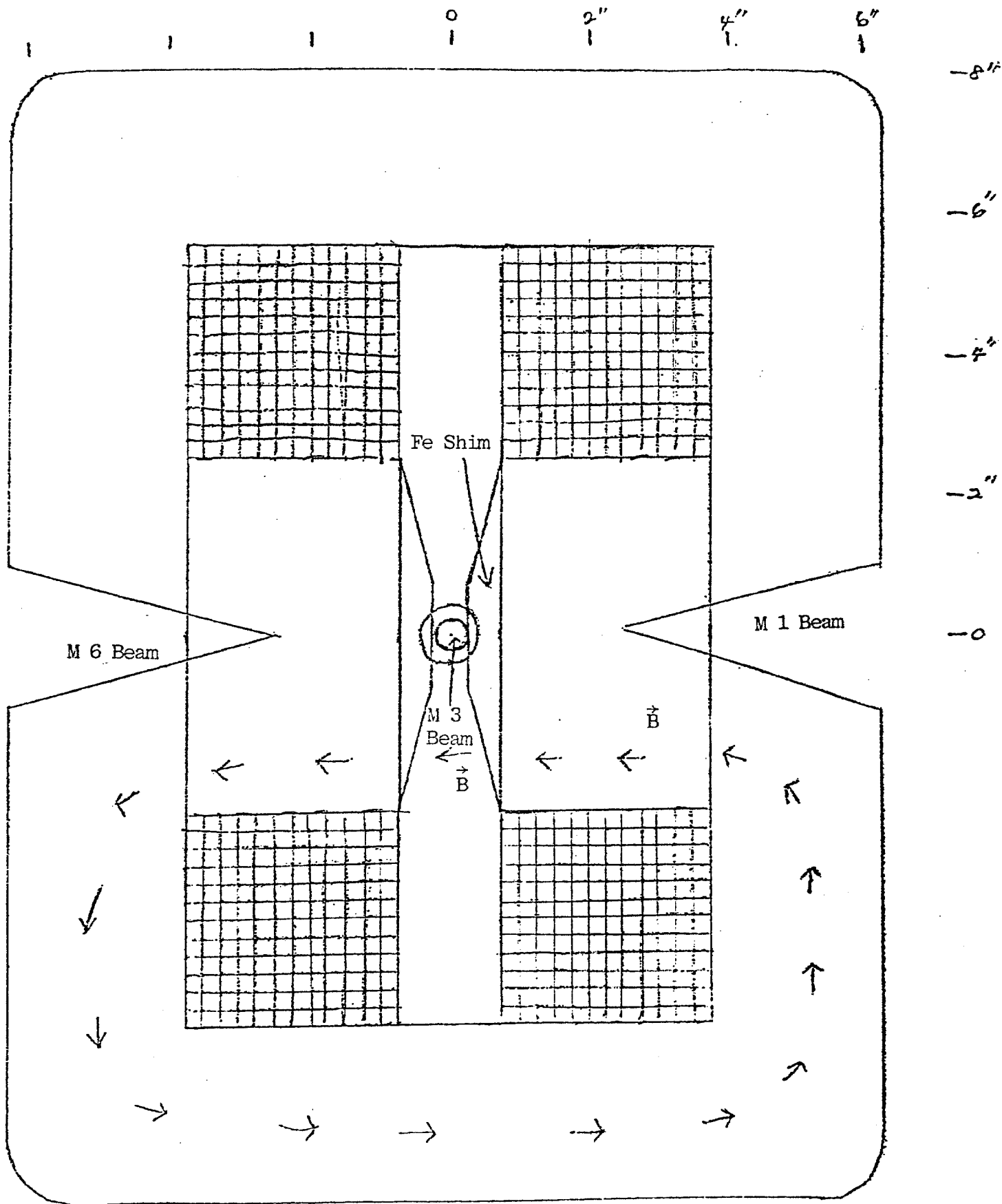


Transverse in - Longitudinal out



Longitudinal in - Longitudinal out

Fig. 3



Modified 5-1.5-1

EPB Dipole for sweeping

Fig. 4

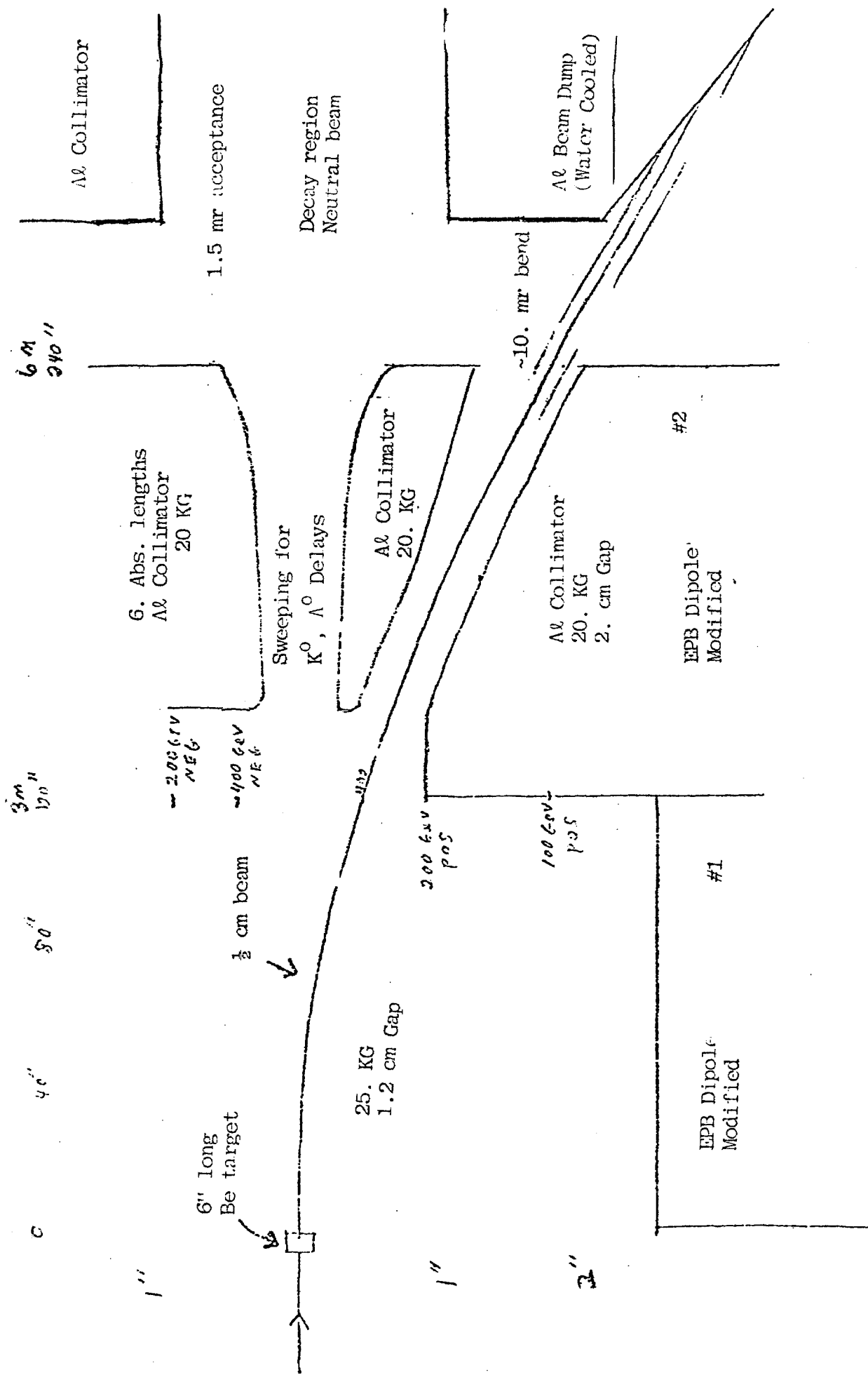


Fig. 5 Beam Sweeping for polarized beam

Transverse Scale 1:1

Longitudinal Scale 1:40

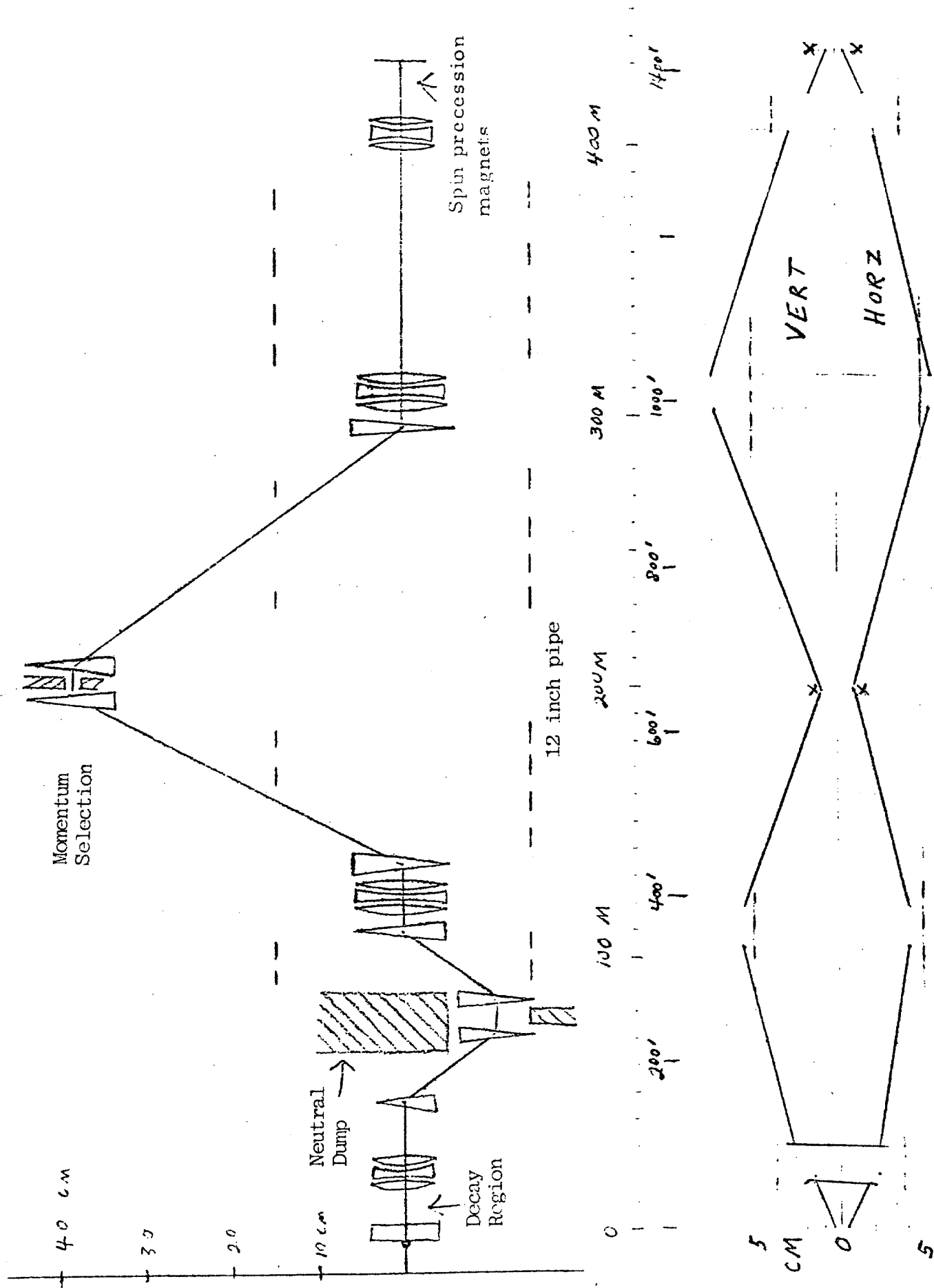


Fig. 6 Beam envelopes. The crosses (x) show the effect of a $\pm 5\%$ momentum bite.

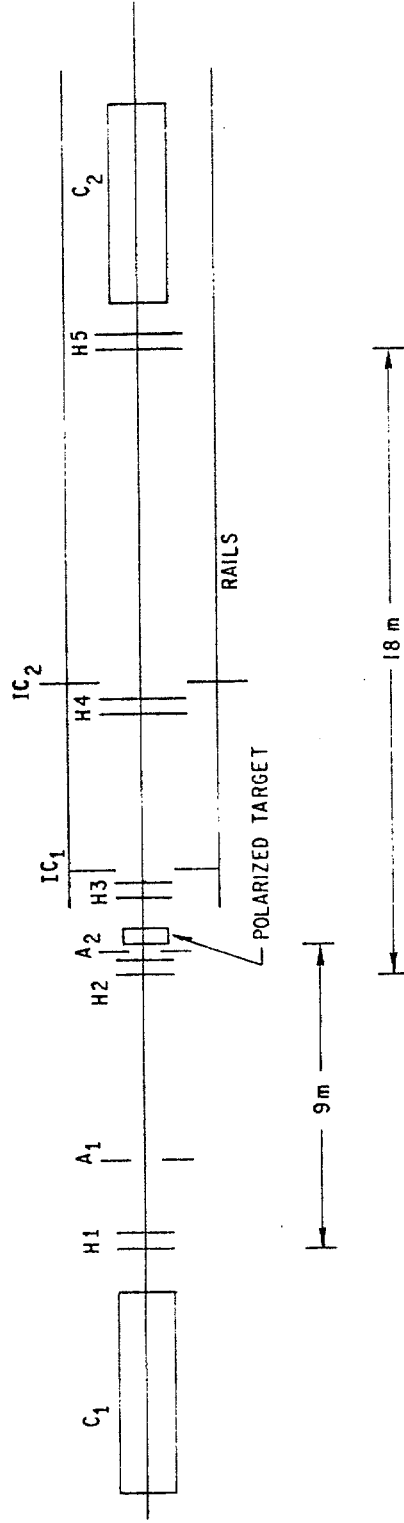


FIG. 7 Layout of total cross-section difference($\Delta\sigma_L^{\text{tot}}$) experiment at $p_{\text{lab}} = 200 \text{ GeV}/c$.

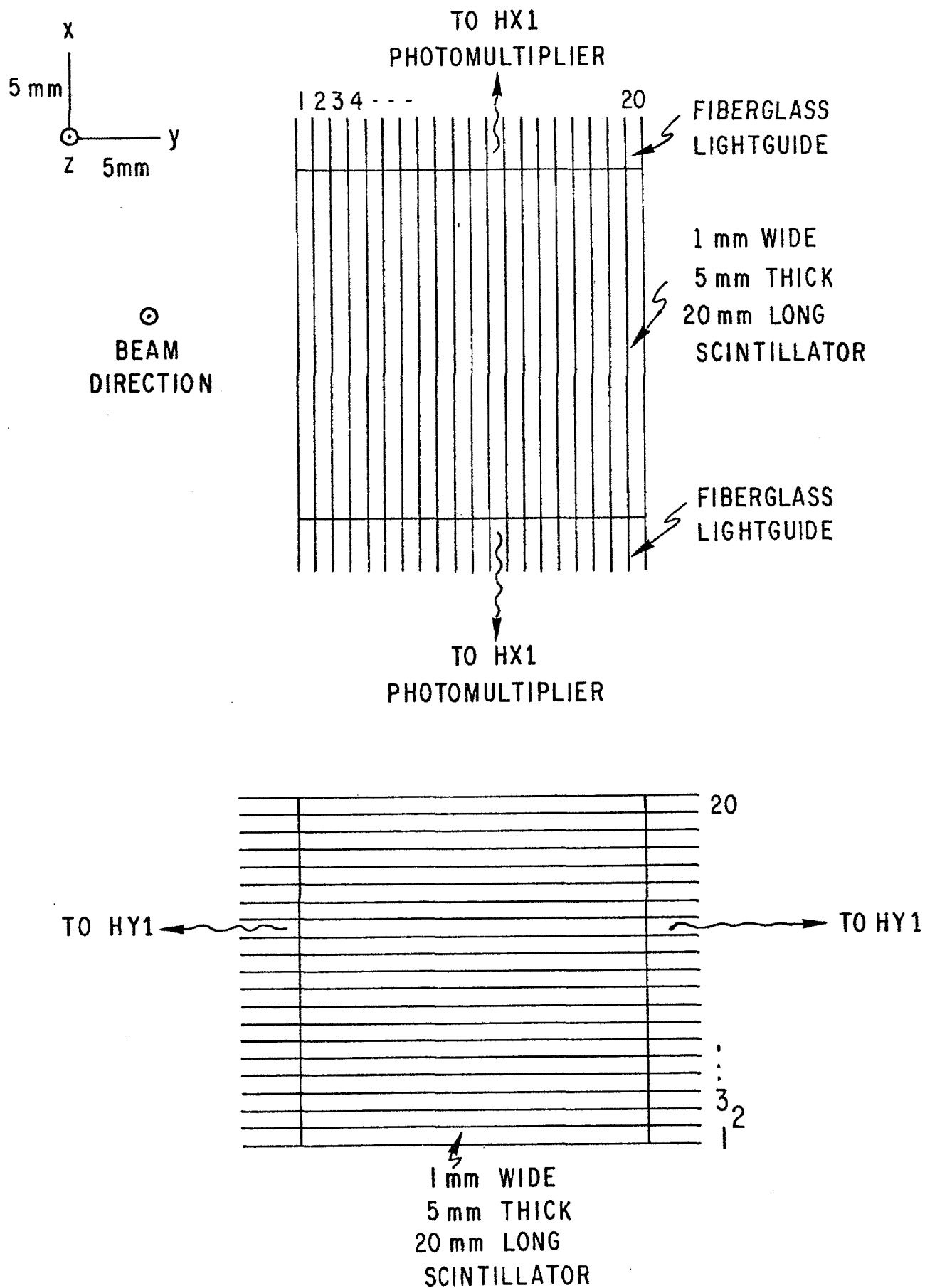
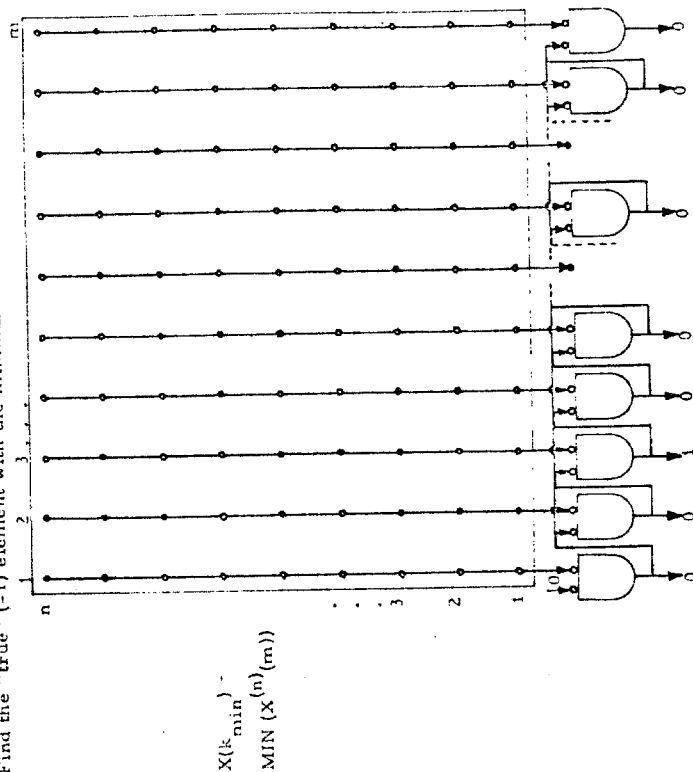


FIG.8 Scintillation-counter hodoscope layout.

$$\Delta x = x^{(i)} - x^{(j)}$$
$$\text{e.g. } X^{(3)} = (0, 0, 1, 0, 0, 1, \dots, 1, 0)$$

Find the "true" (=1) element with the minimum k-index over all arrays.



The first "1" appearing at the output suppresses all the other "1"s. Here $k_{\text{min}} = 3$. The sites of each matrix-row are inverted input points for the m elements of each array. The k th vertical line corresponds to the logical "AND" of the sites of the k th column, i.e. the k th elements of the n arrays.

Fig. 9 Electronic circuitry for hardwired logic functions.

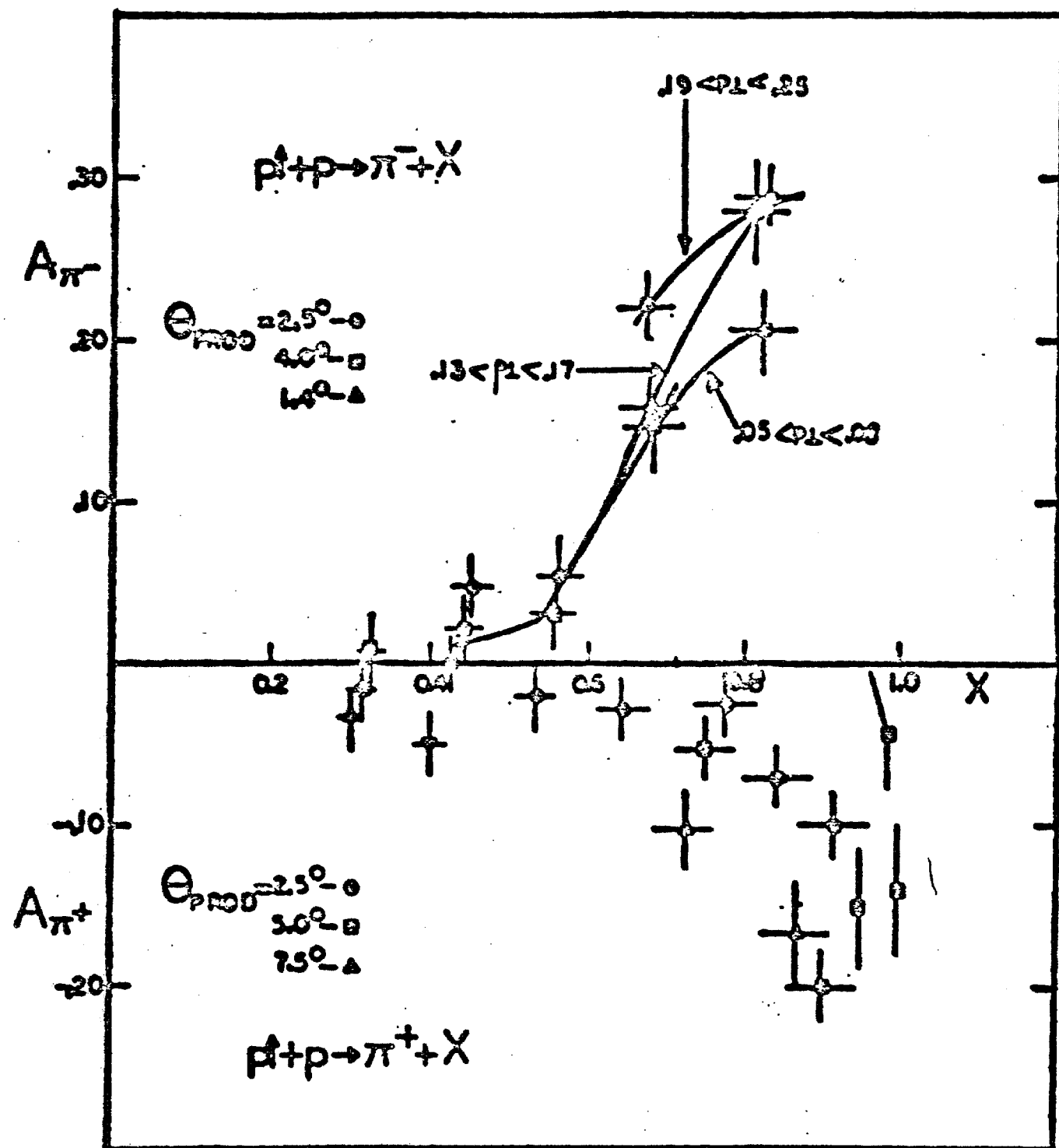


Figure 10 The asymmetry A in $p + p \rightarrow \pi^\pm + \text{anything}$ plotted against $x = p_L^*/p_{\max}^*$ at $p_{\text{lab}} = 6 \text{ GeV}/c$. Lines of approximately constant p_T are drawn for the π^- data.

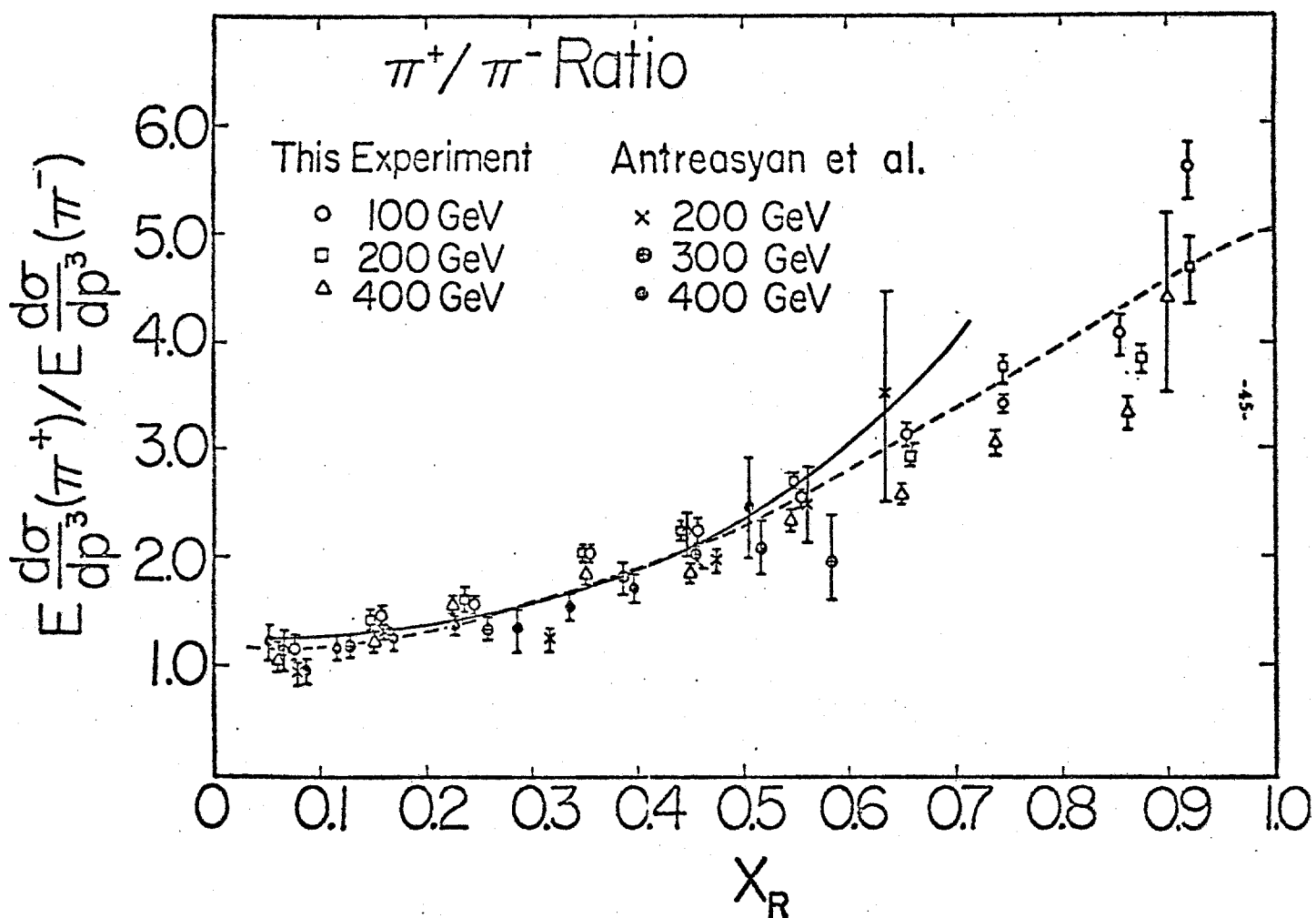


Figure 11: The π^+/π^- ratio plotted against the radial scaling variable $x_R = E^*/E_{\text{max}}^*$. The data are from Refs. [18] (Johnson *et al.*) and [19] (Antreasyan *et al.*). The smooth line is a prediction of Field and Feynman (Ref. [29]) and the dotted line is a prediction of Das and Hwa (Ref. [20]).

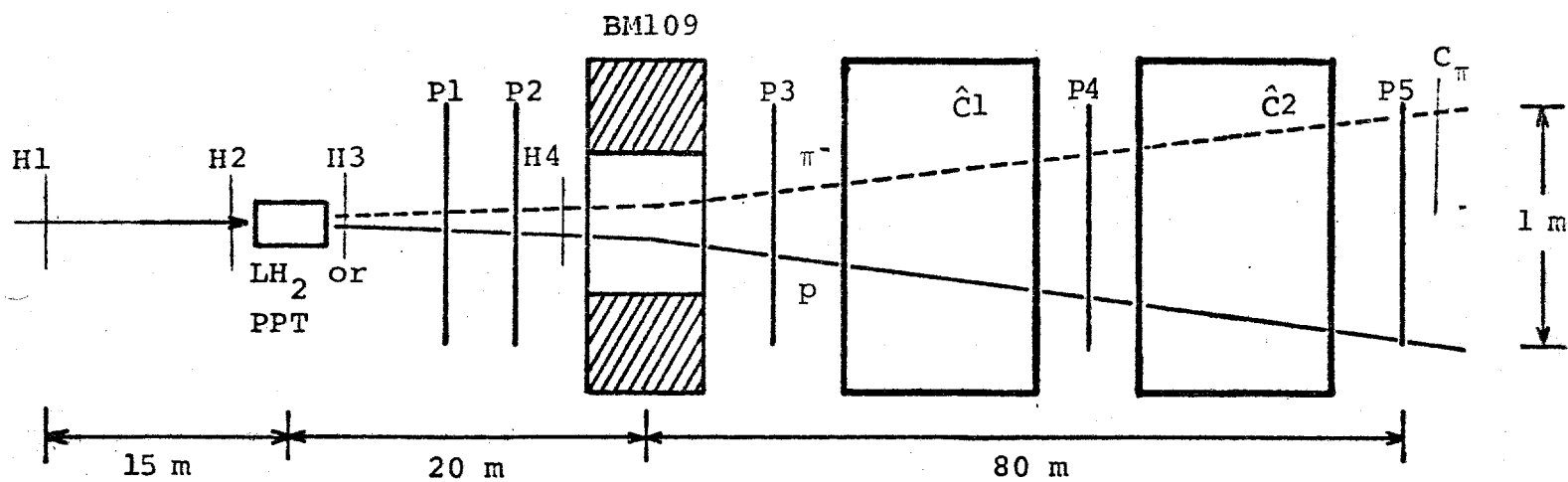
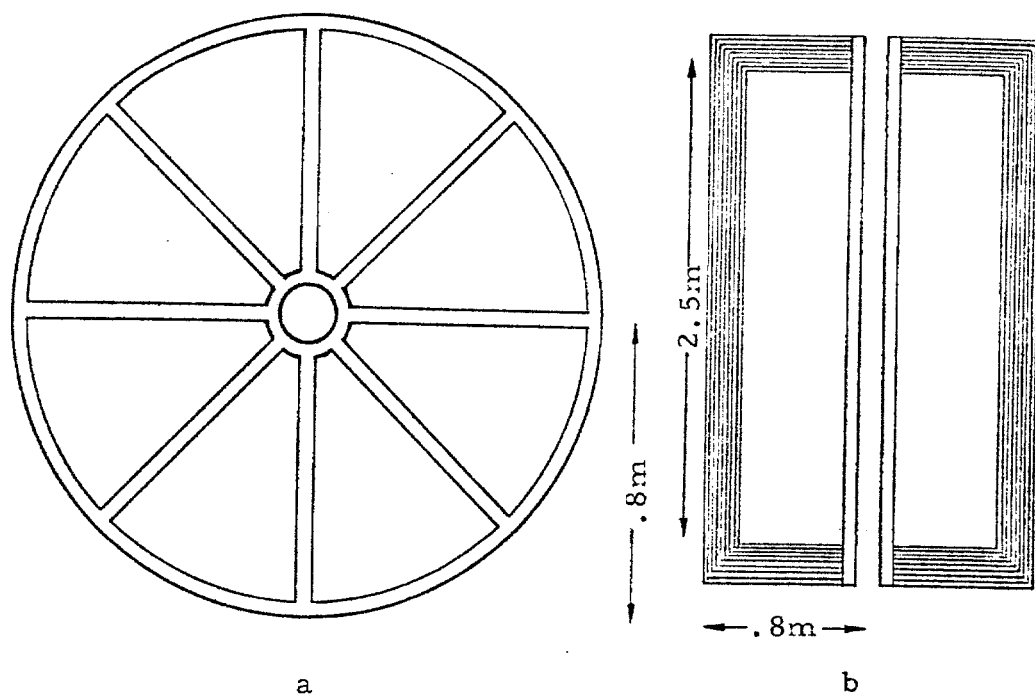


Figure 12: Proposed layout of the apparatus. H1-H4 are x-y hodoscopes, P1-P5 are multiwire proportional chambers, $\hat{C}1$ and $\hat{C}2$ are gas threshold Čerenkov counters and C_π is a scintillation counter.

ELEMENTS NOT TO SCALE



c

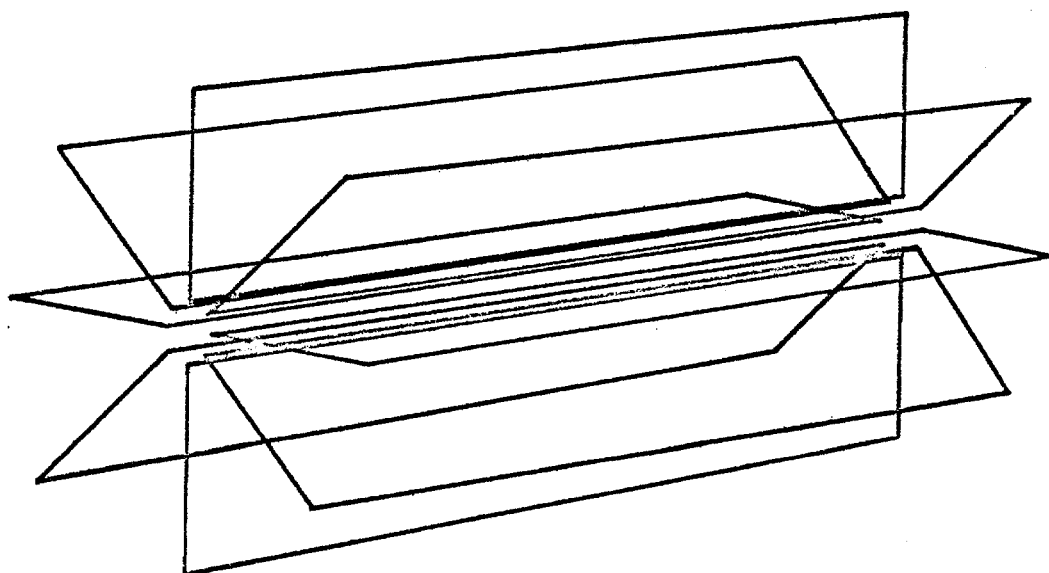


FIG.13 Toroidal-magnet design:

- a. Face-view of an 8-coils support-system with inner and outer rings,
- b. Plane-view of two coils,
- c. Overall view of the 8-coils arrangement.

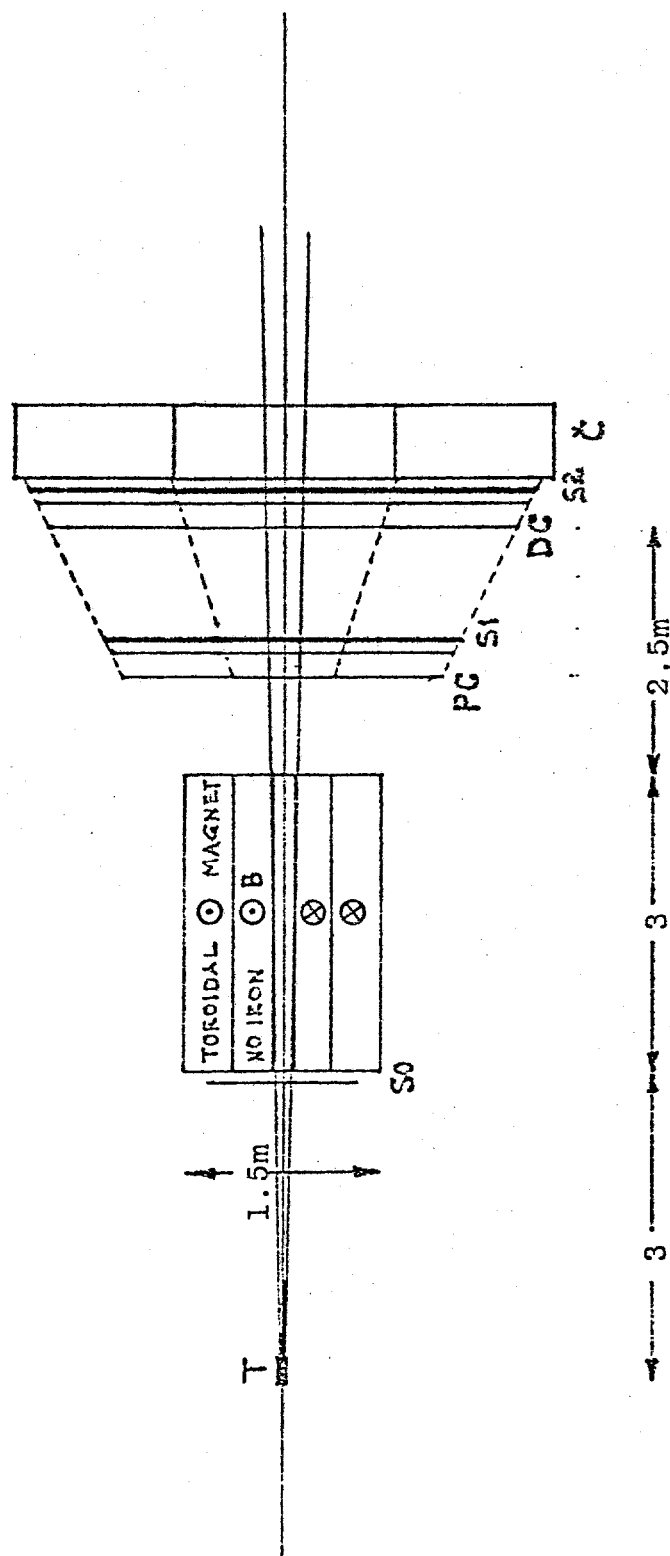


Fig. 14 Toroidal spectrometer setup for high- p_T inclusives ($pp \rightarrow \pi^\pm + \dots$)

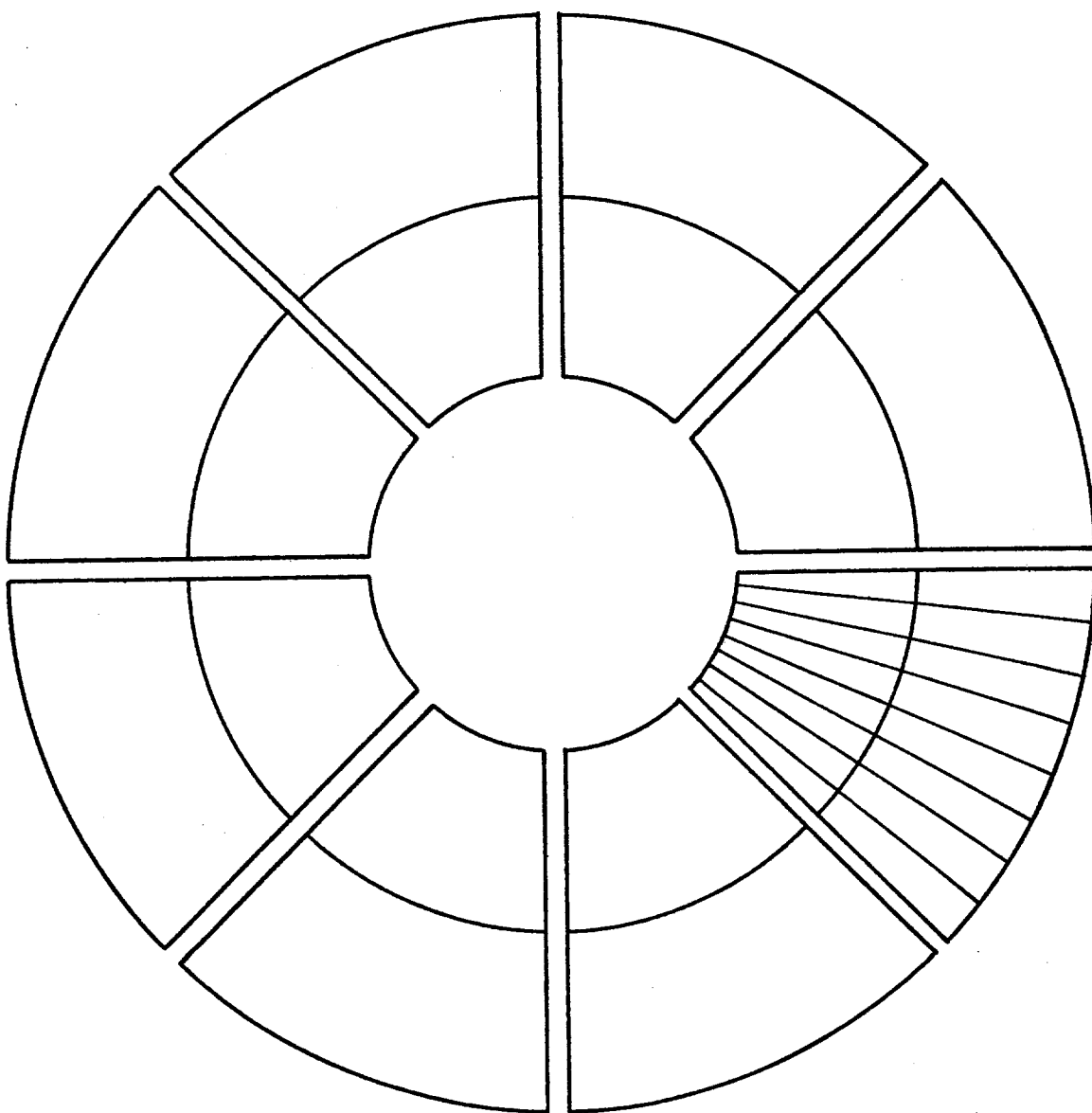


FIG. 15 Shape-sketch of the scintillation-counter hodoscopes(S_0, S_1, S_2)